Bubble Pressure Measurement and Modeling for n-Alkane + Aromatic Hydrocarbon Binary Mixtures

by

Qingchen Liu

A thesis submitted in partial fulfillment of the requirements for the degree of

Master of Science

in

CHEMICAL ENGINEERING

Department of Chemical and Materials Engineering

University of Alberta

Abstract

Commonly-used cubic equations of state (EOS) over predict the bubble point pressures (BPPs) for binary long-chain n-alkane + aromatic mixtures and frequently predict the incorrect phase diagram type. In this work, BPPs for 15 representative n-alkane + aromatic hydrocarbon binary mixtures were measured. The experimental results were compared with computed values obtained using the Peng-Robinson (PR) and Soave-Redlich-Kwong (SRK) EOS. For these cubic EOS, potential causes of the incorrect prediction of BPPs were studied. Binary interaction parameters (k_{ij}) for the PR and SRK EOS were regressed from experimental vapor-liquid equilibrium (VLE) data. It was found that negative k_{ij} values are required for cubic EOS in order to get accurate BPP predictions, contrary to the commonly-used positive or zero k_{ij} values for hydrocarbon mixtures. Regressed k_{ij}s trend towards larger negative values with increased size asymmetry of binary mixtures. Fitted k_{ij} values significantly improve the performance of PR and SRK EOS in predicting BPPs for highly asymmetric n-alkane + aromatic hydrocarbon binary mixtures. Experimental data were also used to validate other common thermodynamic models, including PC-SAFT, NRTL, UNIFAC and COSMO-SAC. These models were found to provide good BPP estimates for alkane + aromatic hydrocarbon mixtures without modification.

Key words: bubble point pressure, binary interaction parameter, equation of state, thermodynamic models, prediction

Acknowledgement

Table of Contents

List of Tables

List of Figures

Nomenclature

a energy parameter in cubic EOS

AAD   average absolute deviation

AAPD   average absolute percent deviation

a^{assoc} change of Helmholtz energy due to association in SAFT

a^{chain} change of Hlmholtz energy due to chain formation in SAFT

a^{disp} contribution to Helmholtz energy from dispersion forces in SAFT

a^{hs} hard-sphere Helmholtz energy in SAFT

a_{ij} cross energy parameter for mixture

API   American Petroleum Institute

a^{res} residual Helmholtz energy in SAFT

a^{seg} segment Helmholtz energy in SAFT

b co-volume term in cubic EOS

b_{ij} cross energy parameter for mixture

BPP   bubble point pressure

ε^{AB} associating energy

EOS   equation of state

FVF   formation volume factor

G^E excess Gibbs energy

GOR   gas oil ratio

k_{ij} binary interaction parameter

L   liquid

l_{ij} binary interaction parameter

LV   liquid–vapor

m characteristic constant (cubic EOS) or number of segments in the molecule (SAFT)

N   nuumber of stages (of distillation column)

N_c carbon number of n-alkanes

$n\text{-}C_i$ n-alkane with i number of carbon atoms

P   pressure

PAHs   polycyclic aromatic hydrocarbons

P_c critical pressure

R   reflux ratio or gas constant

T   temperature

T_c critical temperature

T_r reduced temperature

V_c critical volume

vdW1f   van der Waals one-fluid

VLE   vapor–liquid equilibrium

x   mole fraction

x_i liquid equilibrium mole fraction

α mean relative volatility or separation factor

ε segment energy parameter

κ^{AB} association volume

σ segment diameter

ω acentric factor

Chapter 1. Introduction

1.1 Bubble pressure—Practical importance

Experimental thermodynamic properties, including equilibrium properties such as bubble point pressure (BPP), enthalpy of mixing and density, and transport properties such as viscosity and thermal conductivity are crucial for the petroleum and petrochemical process industries, as they are commonly used to assist in the design, operation and development of various processes involved in production, transportation, refining and transformation of hydrocarbons.[1] Phase equilibrium data, such as vapor–liquid equilibrium (VLE) data, are typically required for the design of equipment or processes where two or multiple phases are present. For example, VLE data of crude oil and refined products are used for the design of pipelines, pumping stations, storage facilities and separation units.

The BPP of a liquid mixture is defined as the pressure at which the first gas bubble evolves from a corresponding liquid phase. In a phase envelope, BPPs at fixed compositions but different temperatures, form bubble point curves and define the boundary between liquid (L) and liquid–vapor (LV) phases and the critical locus, as depicted in Figure 1.1.
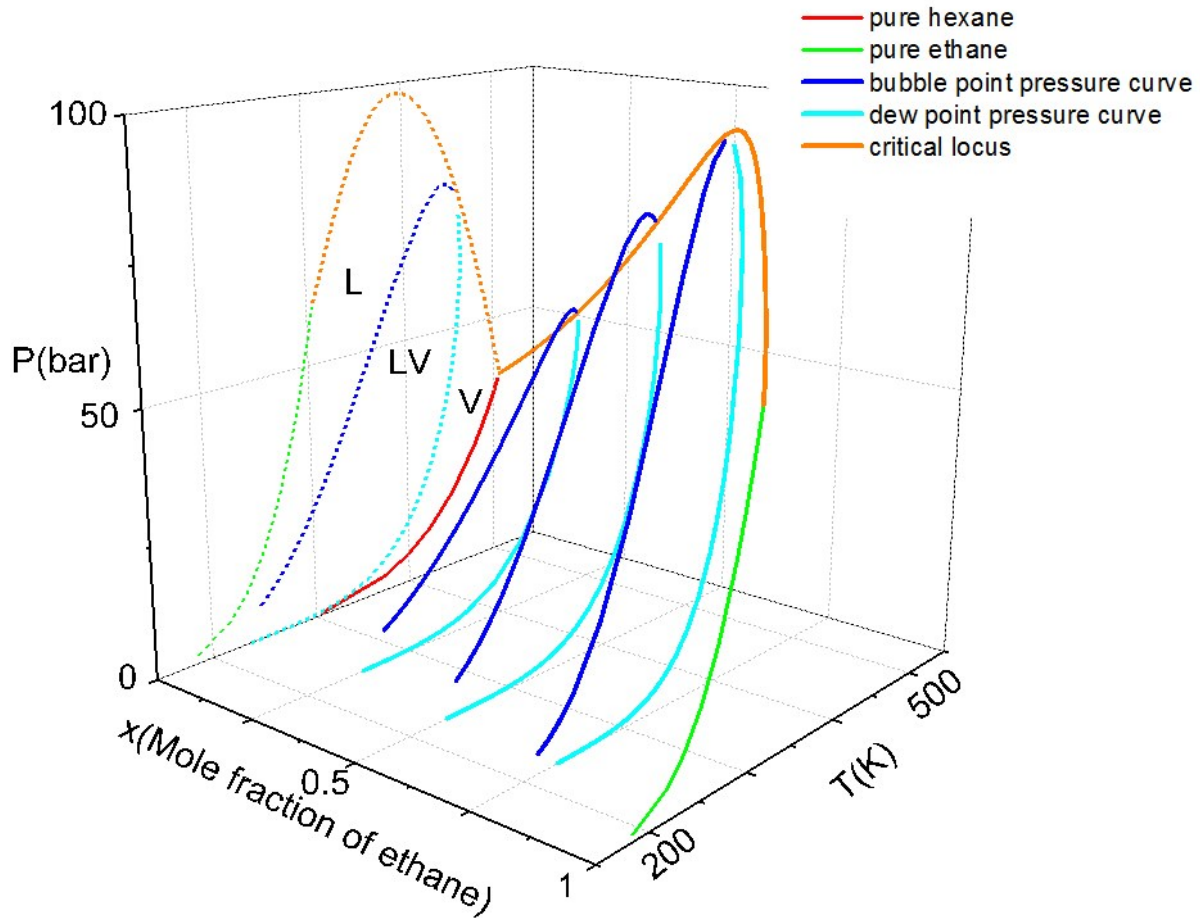
Figure 1.1 Phase diagram of ethane/hexane binary system (dash lines represent the projections of different curves on the P-T plane).

In the oil industry, the understanding of the phase behavior of hydrocarbon mixtures is paramount. Therefore, adequate knowledge of BPP is always required, as BPP is a critical component of the phase envelope and an important thermophysical property. An example could be found in upstream industry where the characteristic changes in reservoir pressure are constantly monitored and compared with BPPs of reservoir fluids for production control. In planning stages, BPP determines whether the reservoir is saturated and this information is used

to evaluate key productivity parameters such as oil formation volume factor (FVF) and solution gas oil ratio (GOR); during the production phase, the relation between reservoir pressure and BPP directly affects drive mechanisms, and ultimately affects production profiles such as liquid/gas production ratios[2].

Information regarding the BPPs of hydrocarbons, or more generally, the VLE data of hydrocarbons, is also needed in other downstream processes. For example, the operating conditions of gas pipelines are controlled based on the pressure–temperature envelope of the hydrocarbon mixture being transported to avoid condensation. VLE data of mixtures are required for the design of distillation columns, as they can be used to estimate parameters like relative volatilities. From a practical perspective, sufficient, accurate and validated VLE data permit thorough understanding of equilibrium processes, facilitating optimal process design and operation.

1.2 Thermodynamic models—The need for reliable data

Despite the importance of thermophysical property data, it is not realistic to conduct experiments for all mixtures over broad ranges of temperature, pressure and composition. In the absence of experimental data, thermodynamic models are relied upon to predict results. Many relatively accurate correlations for estimating thermophysical properties have been proposed. Equations of state (EOS) are the most commonly used ones to calculate phase behaviors of pure compounds and mixtures. In the petroleum industry, cubic EOS typically provide fast and reliable predictions. These EOS, such as Peng–Robinson[3] and Soave–Redlich–Kwong[4] EOS, derive from the van der Waals equation[5], and require only the critical properties (T_c, P_c) and acentric factor

(ω) of pure compounds as inputs. Some other thermodynamic models, such as activity coefficient models (e.g., NRTL[6], UNIFAC[7]), and models based on statistical thermodynamics theory or quantum chemistry (e.g., SAFT[8] EOS, COSMO-RS[9]) have also been developed, which have demonstrated good prediction accuracy for hydrocarbon mixtures. These models are more complex and generally require more parameters and calculation time. However, many of these alternative models have been incorporated in commercial process simulation software such as VMGSim[10] and Aspen Plus[11] to assist process simulation, design, debottlenecking and optimization calculations. These models are routinely used to predict VLE data, and to provide inputs for other thermophysical property calculations such as heat capacity and viscosity.

Although all of these models have been proven to be successful for many practical cases, they have shortcomings and limitations. They may provide numerically inaccurate or even qualitatively inaccurate predictions. Even small computed errors may propagate, causing substantial operational issues for processes. For example, in the design of a distillation column, a 5% deviation in separation factor α may lead to a doubling of the number of theoretical trays required for a separation, as illustrated in Figure 1.2[14]. Qualitative errors like incorrect phase behavior type prediction can lead to results that are far more serious (e.g., impairing process operation and safety). For example, Ahitan et al.[12] showed that cubic EOS mispredicted the phase behavior type for n-alkane + aromatic and naphthenic binary mixtures based on Van Konynenburg and Scott's classification scheme[13]. Thermodynamic models must be validated by experimental data and tuned when applied to specific cases. Reliable thermophysical property data, such as VLE data, are essential for the development and testing of well-established or newly-developed thermodynamic models.
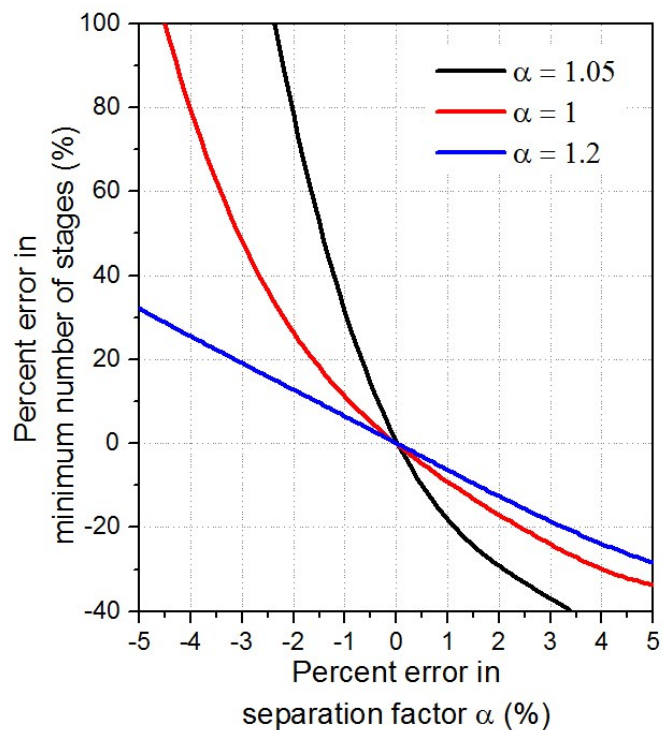
Figure 1.2 Influence of error in separation factor on the minimum number of required theoretical stages in a distillation column, adapted from the paper by Dohrn and Pfohl[14]

1.3 Mixtures of interest

It is well known that crude oils are mainly composed of paraffinic, naphthenic, and aromatic hydrocarbons.[15] A narrow boiling range may contain a wide range of compounds.[16] In the molecule-based characterization methodology, crude oils are characterized as a combination of hydrocarbon constituent molecules drawn primarily from species based on PIONA (n-paraffin, iso-paraffin, olefin, naphthenic, and aromatic) classification[17]. Irrespective of the approach adopted, representative constituent molecules provide a profile that covers molecular weights, structural segment types and segment distributions that reflect assay data (such as a distillation

curve, API gravity and Polycyclic Aromatic Hydrocarbons (PAHs)). The representative molecules are then used to model crude oils or oil fractions[18].

The growing use of representative molecule based characterization underscores the importance of phase equilibrium data for mixtures containing representative segment types. In particular, binary aliphatic–aromatic mixtures are of significant value, as VLE data of these mixtures will contribute to the understanding of the interaction between molecular segments in petroleum fractions, as well as the phase behavior of crude oil as a whole.
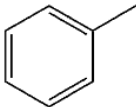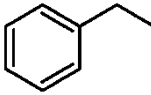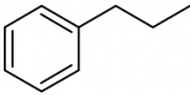
Aliphatic + aromatic mixtures appear commonly in the oil industry. For example, crude oils containing aromatics and large paraffin chains ranging from n-C_{10} up to n-C_{72} are frequently encountered in shale oil reservoirs[19]. These mixtures can cause wax deposition issues for wells and pipelines, which need to be treated carefully with dispersants. In oil refining, paraffinic + aromatic mixtures can be found in middle and heavy distillates as products from atmospheric distillation. They are also found in other processes such as catalytic reforming, blending, etc.[20] As such mixture types are widely present in crude oils, but absent from current databases, unforeseeable and potentially catastrophic issues may arise.

1.4 Objectives

Bubble point pressure data is essential for common processes in the petroleum industry. They are of particular importance to process modeling as they serve as cornerstones for the testing, development and validation of thermodynamic models. Precise descriptions of the phase behavior of complex petroleum fluids are intrinsically dependent on the knowledge of simple hydrocarbon mixtures that constitute these fluids. High-quality bubble point pressures for

representative hydrocarbon mixtures are fundamental inputs to process design, operation and simulation. The first objective of this thesis is to fill a VLE data gap in the literature for long chain n-alkane + aromatic binary mixtures. VLE data for 15 binaries comprising n-alkanes ranging from $n-C_{20}$ to $n-C_{28}$ and benzene derivatives, presented in Table 1.1, will be measured. The second objective is to use experimental VLE data to benchmark the performance of the PR, SRK and SAFT EOS. The performance of these models will be validated and modifications will be proposed to re-parameterize them for alkane + aromatic binary mixtures in general in light of the new experimental data.

Table 1.1 Selected binaries with n-alkanes and aromatics

n-Alkanes	Aromatics
$n-C_{20}$	Benzene
$n-C_{24}$	Toluene
$n-C_{28}$	Ethylbenzene
	n-Propylbenzene
	p-Xylene

1.5 References

1. Hendriks, E.; Kontogeorgis, G. M.; Dohrn, R.; de Hemptinne, J.; Economou, I. G.; Zilnik, L. F.; Vesovic, V. Industrial requirements for thermodynamics and transport properties. *Ind Eng Chem Res.* **2010**, *49*, 11131-11141.

2. Towler, B. F. Fundamental principles of reservoir engineering, vol 8, SPE textbook series. Henry L. Doherty Memorial Fund of AIME. *Society of Petroleum Engineers, Richardson* 2002.

3. Peng, D.; Robinson, D. B. A new two-constant equation of state. *Ind.Eng.Chem.Fundam* **1976**, *15*, 59-64.

4. Soave, G. Equilibrium constants from a modified Redlich-Kwong equation of state. *Chemical Engineering Science* **1972**, *27*, 1197-1203.

5. Waals, J. D.; Rowlinson, J. S. *JD van der Waals: On the continuity of the gaseous and liquid states;* North Holland: 1988; Vol. 14.

6. Renon, H.; Prausnitz, J. M. Local compositions in thermodynamic excess functions for liquid mixtures. *AIChE J.* **1968**, *14*, 135-144.

7. Fredenslund, A.; Jones, R. L.; Prausnitz, J. M. Group-contribution estimation of activity coefficients in nonideal liquid mixtures. *AIChE J.* **1975**, *21*, 1086-1099.

8. Chapman, W. G.; Gubbins, K. E.; Jackson, G.; Radosz, M. SAFT: equation-of-state solution model for associating fluids. *Fluid Phase Equilib.* **1989**, *52*, 31-38.

9. Klamt, A. Conductor-like screening model for real solvents: a new approach to the quantitative calculation of solvation phenomena. *J. Phys. Chem.* **1995**, *99*, 2224-2235.

10. VMGSim Process Simulator, Version 9.5. Virtual Materials Group Inc.: Calgary, AB 2016.

11. Aspen Plus, Version 8.8. Aspen Technology Inc.: Burlington, MA 2015.

12. Ahitan, S.; Satyro, M. A.; Shaw, J. M. Systematic misprediction of n-alkane + aromatic and naphthenic hydrocarbon phase behavior using common equations of state. *Journal of Chemical & Engineering Data* **2015**, *60*, 3300-3318.

13. Van Konynenburg, P. H.; Scott, R. L. Critical lines and phase equilibria in binary van der Waals mixtures. *Philosophical Transactions of the Royal Society of London A: Mathematical, Physical and Engineering Sciences* **1980**, *298*, 495-540.

14. Dohrn, R.; Pfohl, O. Thermophysical properties—industrial directions. *Fluid Phase Equilib.* **2002**, *194*, 15-29.

15. Speight, J. G. *The chemistry and technology of petroleum;* CRC press: 2014 .

16. Altgelt, K. H. *Composition and analysis of heavy petroleum fractions;* CRC Press: 1993.

17. Hay, G.; Loria, H.; Satyro, M. A. Thermodynamic modeling and process simulation through PIONA characterization. *Energy Fuels* **2013***, 27*, 3578-3584.

18. Molecule-based characterization methodology for correlation and prediction of properties for crude oil and petroleum fractions – an industry white paper, 2014. Aspen Technology Website. https://www.aspentech.com/Molecular_Characterization_White_Paper.pdf (accessed Dec 1, 2016)

19. Speight, J. G. *Introduction to enhanced recovery methods for heavy oil and tar sands;* Gulf Professional Publishing: 2016.

20. Gray, R. M. *Upgrading petroleum residues and heavy oils;* CRC press: 1994.

Chapter 2. Literature Review

2.1 EOS models used for hydrocarbon mixtures

Equations of state (EOS) are the principal thermodynamic model used for hydrocarbon mixtures. Numerous options, along with their related mixing rules, are available in commercial simulators for engineering calculations. Options chosen for specific applications should be selected with care. Detailed reviews concerning EOS have been reported by Anderko[1], Wei and Sadus[2], Sengers et al.[3] among others.

2.1.1 Cubic EOS

Cubic EOS are by far the most common EOS, including van der Waals (vdW)[4], Redlich–Kwong (RK)[5], Soave–Redlich–Kwong (SRK)[6], Peng–Robinson (PR)[7] equations, and Sako–Wu–Prausnitz (SWP)[8] etc. The SRK and PR equations are the most widely used models in the petroleum industry due to their simplicity and flexibility. These EOS have two parameters, an energy parameter $a(T)$ and a co-volume parameter b, which can be calculated from the critical properties (T_c, P_c) and acentric factors (ω). Cubic EOS developed from the van der Waals EOS are summarized in Table 2.1.[9]

Table 2.1 Cubic EOS[9]. *a* is cross energy term of cubic EOS. *b* is co-volume parameter. R is gas constant. T_r is reduced temperature. *m* is characteristic constant calculated from ω.

EOS	Mathematical Expression	Constants
van der Waals (vdW)	$P = \dfrac{RT}{V-b} - \dfrac{a}{V^2}$	$a = \dfrac{27}{64}\dfrac{(RTc)^2}{Pc}, b = \dfrac{1}{8}\dfrac{RTc}{Pc}$
Redlich–Kwong (RK)	$P = \dfrac{RT}{V-b} - \dfrac{a}{V(V+b)\sqrt{T}}$	$a = 0.42748\dfrac{(R^2Tc^{2.5})}{Pc}, b = 0.08664\dfrac{RTc}{Pc}$
Soave–Redlich–Kwong (SRK)	$P = \dfrac{RT}{V-b} - \dfrac{a(T)}{V(V+b)}$	$a_c = 0.42748\dfrac{(RTc)^2}{Pc}, b = 0.08664\dfrac{RTc}{Pc}$ $a(T) = a_c[1 + m(1-\sqrt{Tr})]^2$ $m = 0.48 + 1.574\,\omega - 0.176\,\omega^2$
Peng–Robinson (PR)	$P = \dfrac{RT}{V-b} - \dfrac{a(T)}{V(V+b)+b(V-b)}$	$a_c = 0.45724\dfrac{(RTc)^2}{Pc}, b = 0.0778\dfrac{RTc}{Pc}$ $a(T) = a_c[1 + m(1-\sqrt{Tr})]^2$ $m = 0.37464 + 1.54226\,\omega - 0.26992\,\omega^2$

Mixing rules are used for the energy and co-volume parameters of cubic EOS when applied to mixtures. For non-polar mixtures such as hydrocarbon mixtures, one widely employed mixing rule is the van der Waals one-fluid mixing rule (vdW1f), which assumes quadratic composition dependence for both parameters and random mixing of molecules (Equation 2.1)

$$a(T) = \sum_{i=1}^{n}\sum_{j=1}^{n} x_i x_j a_{ij}, b = \sum_{i=1}^{n}\sum_{j=1}^{n} x_i x_j b_{ij} \tag{2.1}$$

where classical combining rules are used to determine a_{ij} and b_{ij},

$$a_{ij} = \sqrt{a_i a_j}\,(1 - k_{ij})$$

(2.2)

$$b_{ij} = \frac{b_i + b_j}{2}(1 - l_{ij})$$ (2.3)

and

$$k_{ij} = k_{ji}, k_{ii} = 0.$$

l_{ij} is normally set to be 0. Thus, after substitution,

$$b = \sum_{i=1}^{n} x_i b_i$$

(2.4)

The vdW1f mixing and classical combining rules dominate for practical applications, especially for mixtures with gases and hydrocarbons.

2.1.2 Binary interaction parameter for cubic EOS and its dependency on temperature and chain length

Binary interaction parameters, k_{ij}, appears in the form of $(1-k_{ij})$ as a correction term to the geometric mean rule to estimate the cross-energy term a_{ij}. k_{ij} values are normally calculated by fitting experimental phase equilibrium data. As a regressed empirical parameter, k_{ij} can be determined from experimental VLE data such as bubble point pressures and critical point data. For example, in the original paper by Peng and Robinson[7], k_{ij} values for each binary were

obtained by minimizing deviations in predicted bubble pressure. Similar examples can be found in papers by Petersen[10], Englezos et al.[11] and Mushrif and Phoenix[12], in which other thermophysical properties were used to regress k_{ij}s.

For most non-polar mixtures, k_{ij} values are small and positive, and are frequently assumed to be zero as a default value in calculations. For some polar mixtures, non-zero values might be required in order to obtain accurate predictions. Large positive k_{ij} values have been observed for systems like alkanes + water[13], indicating low attractive forces between these types of molecules. Positive k_{ij}s are also needed for some highly asymmetric mixtures, like CO_2 + n-alkanes. For strong solvating or hydrogen bonding cases, the cross-energy term is larger than the value provided by the geometric mean rule, and negative k_{ij}s are required, e.g., for chloroform + acetone[9].

k_{ij} value can have a strong impact on bubble pressure of mixtures and hence on process design. They must be defined precisely. For instance, Peridis et al.[14] showed that small variations in k_{ij} values can change the design parameters for distillation columns significantly. The authors pointed out that the number of stages (N), reflux ratio (R) and mean relative volatility (α) are sensitive to the variation of k_{ij} values used in design calculations, as shown in Figure 2.1.
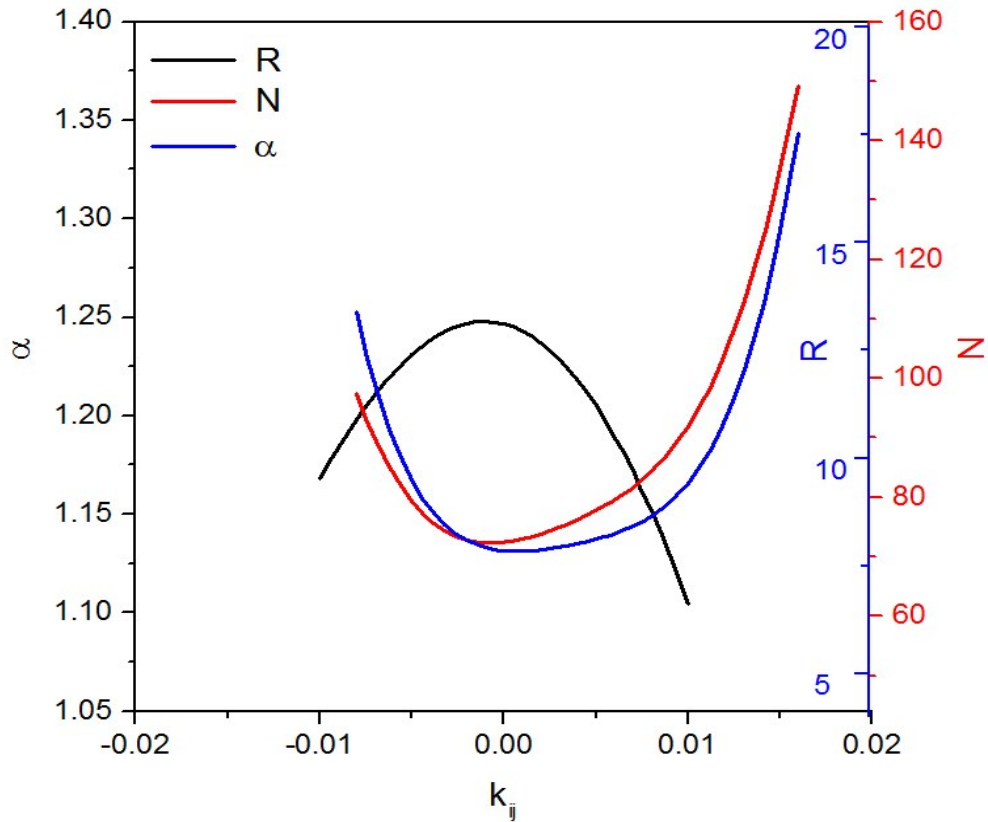
Figure 2.1 Effect of k_{ij} values on α, N, and R for the ethylbenzene-styrene system, adapted from

the work by Peridis et al. [14]

k_{ij} values variation can also impact the type of the phase behavior predicted. For example, Gegorowicz and de Loos[15] reported that the binary interaction parameters have a significant influence on the predicted LLV equilibria of asymmetric hydrocarbon mixtures. Jaubert et al.[16] illustrated that k_{ij} selection is crucial to predicting phase equilibria for simple binary mixtures like 2,2,4-trimethyl pentane + toluene, as shown in Figure 2.2. Ahitan et al.[17] have shown that negative binary interaction parameters must be used for long chain n-alkane + aromatic and naphthenic compounds in order to predict the Type I phase behavior observed experimentally for

such mixtures.
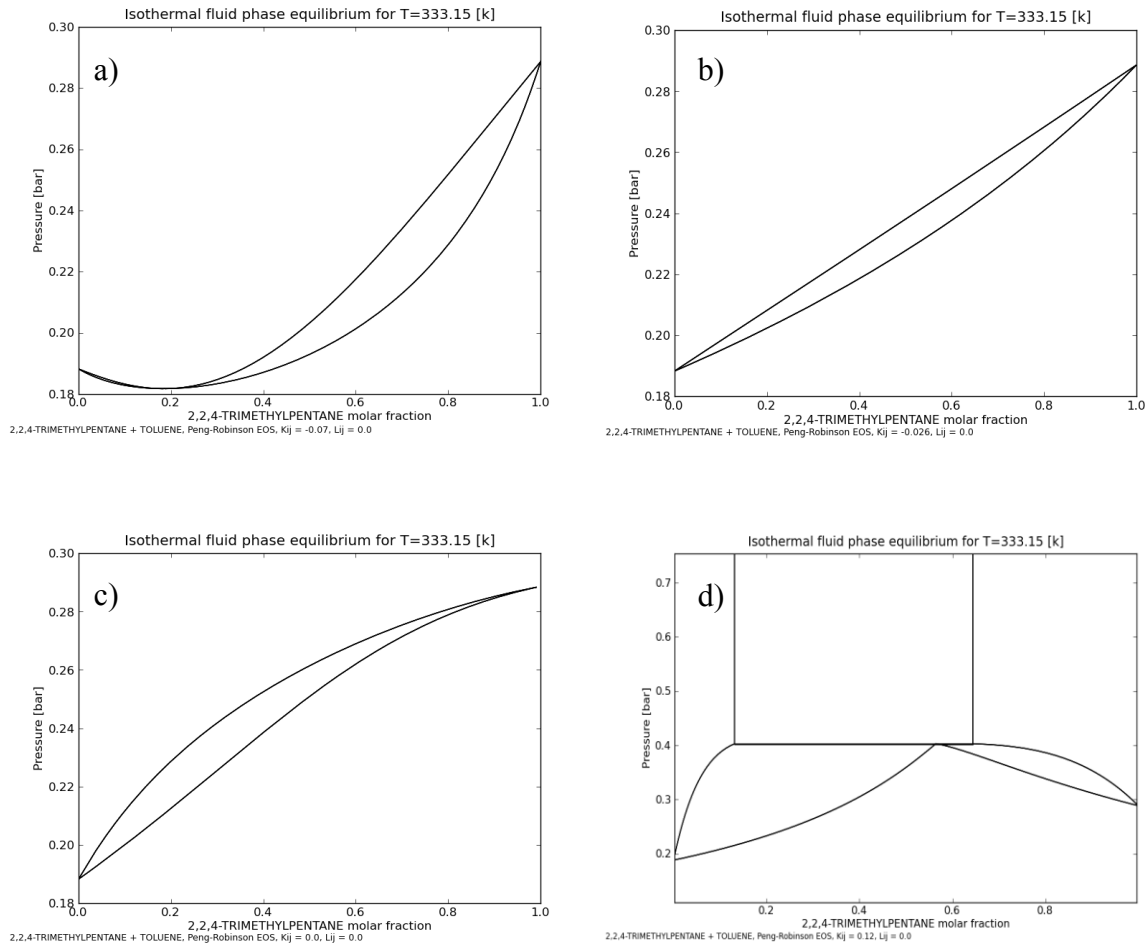
Figure 2.2 Influence of k_{ij} values on the calculated isothermal phase diagram for the 2,2,4-trimethyl pentane + toluene binary mixture at 333.15K. a) $k_{ij} = -0.07$ b) $k_{ij} = -0.026$ c) $k_{ij} = 0$ d) $k_{ij} = 0.12$, adapted from the work by Jaubert et al.[16]

Many empirical correlations for estimating binary interaction parameters have been proposed. For example, Nishiumi et al.[18] presented correlations for systems containing hydrocarbons, CO_2, N_2 and H_2S. Gao et al.[19] introduced a k_{ij} correlation for light hydrocarbons mixtures based on the critical properties of pure compounds. Kordas et al.[20] developed a generalized correlation for the CO_2 + n-alkane system with T_r of CO_2 and ω of alkanes as inputs. Stamataki and Magoulas[21]

regressed k_{ij} values for H_2S + n-alkane mixtures and obtained an expression of k_{ij} as a function of acentric factors of alkanes. Jaubert and Mutulet[22] proposed a temperature-dependent k_{ij} for the PR EOS estimated using a group contribution method. Most of these correlations predict k_{ij}s that provide better phase equilibrium predictions than the default value of zero. However, the interaction parameters calculated with these approaches sometimes provide poor results. Some of the correlations are only suitable for a limited amount of mixtures and generally cannot be extrapolated for complex or pseudo compounds. Some correlations require critical properties as inputs that are not easy to measure, such as critical volume (V_c)[23]. A detailed discussion of these correlations can be found in the paper by Coutinho et al.[24]

Some trends of the interaction parameters have been observed and correlated based on existing experimental data, and most of the analyses focus on the temperature and chain length dependency. Due to their practical importance in enhanced oil recovery, extensive research has been conducted on the k_{ij} of CO_2 + hydrocarbons systems. Kato et al.[25] generalized a k_{ij} function of temperature and ω (of alkanes) based on experimental data of CO_2 + light alkanes, and predicted a decreasing trend of k_{ij} with increasing carbon number (N_c) and a quadratic temperature dependency of k_{ij}. Similar trends for light alkanes were observed by Kordas et al.[20], yet the authors observed a decreasing trend of k_{ij} with temperature for heavier alkanes. Coutinho et al.[24] reported that the interaction parameters decrease for CO_2 + saturated hydrocarbons with increasing molecular size difference, but slightly increase for CO_2 + aromatics or CO_2 + monoalkene systems. The same authors also studied the temperature dependency of k_{ij} for these mixtures in a low temperature range, and found that the temperature effect is not very significant. Jaubert and Mutelet[22] predicted a quadratic temperature dependency for binary systems with minimum k_{ij} value located at $T_r = 0.55$, and a mixed trend for k_{ij}s with respect to hydrocarbon

size for CH_4 + n-alkanes (reversed trend observed for highly asymmetric systems with carbon number of n-alkanes higher than 14). Nevertheless, the relationship between k_{ij}s and these two factors is not universal and consistent.

As an experimentally determined parameter, the trend of k_{ij} values may vary depending on the compounds involved. Sometimes experimental data can even be at odds with predicted results from common correlations. Ahitan et al.[26] demonstrated that k_{ij}s for benzene + n-alkanes regressed from experimental data are negative and tend to decrease with increasing carbon number. This trend opposes the predicted sign and trend in k_{ij} values estimated using the correlation developed by Gao et al.[19] Similar trends were predicted for other aromatics + n-alkanes mixtures using phase stability analysis[17], but the exact values of k_{ij} remain undetermined for aromatics + long n-alkanes in the absence of experimental VLE data. Even for the same type of mixture, fitted k_{ij} based on different temperature or pressure ranges can vary significantly. Stamataki and Tassios[27] pointed out that generalized k_{ij} correlations developed for methane + alkanes mixtures cannot be extrapolated to highly asymmetric mixtures. They also showed for methane + phenanthrene mixtures, that the k_{ij} trends generalized from low-pressure VLE data fail at higher pressures. Clearly, it is necessary to revise the interaction parameters for highly asymmetric mixtures such as aromatic + long chain n-alkane binaries, as common correlations are prone to give erroneous results. More experimental data are required to pinpoint the k_{ij} values and more accurate correlations for k_{ij} values need to be developed.

2.1.3 Shortcomings for cubic EOS

Cubic EOS with classical vdW1f mixing rules predict phase equilibria for many mixtures satisfactorily. However their shortcomings and limitations are well-known. For instance, cubic EOS do not provide accurate densities even for pure n-alkanes unless volume translation is applied[28]. Cubic EOS with classical mixing rules normally exhibit reduced accuracies for polar mixtures, and frequently fail to model multiphase equilibria for polar, highly asymmetric and associating mixtures.[9,17,29,30] To mitigate these deficiencies, other than density, the most common and convenient way is to use k_{ij}s fitted to experimental data. Apart from using non-zero k_{ij} values, some other approaches have also been proposed. Many researchers including Mathias[31], Melhem et al.[32], Twu et al.[33] attempted to modify the attractive term by proposing alternative a(T) and were able to improve the performance of cubic EOS for complex mixtures. The role of l_{ij} has also been studied. Twu et al.[33] developed an asymmetric k_{ij} for cross energy parameter with two adjustable parameters k_{ij} and k_{ji}. Stamataki and Tassios[27] showed that using multiple interactions parameters (k_{ij} together with l_{ij}) is advantageous for VLE prediction near the critical region. Kontogeorgis et al.[34] studied a number of asymmetric alkane/alkane systems and found that using a single interaction parameter (l_{ij}) for the co-volume term rather than using a single k_{ij} for the energy term would provide more reasonable prediction of VLE data. These results would appear to demonstrate the superiority of l_{ij} over k_{ij} for asymmetric mixtures. However, the use of l_{ij}s has numerous drawbacks in general and their use has not been adopted broadly.

In addition, attention has been given to mixing rules based on local compositions and activity coefficient models for cubic EOS. Specifically, these mixing rules incorporate activity coefficient models into cubic EOS by equalizing the excess Gibbs energies (G^E), and have

resolved some problems caused by the classical vdW1f mixing rule. For example, Mathias and Copeman[35] applied a truncated density dependent local composition mixing rule to PR EOS and extended its application to some highly non-ideal mixtures (i.e., asymmetric and polar mixtures). Other models such as the Huron–Vidal[36] mixing rule with its modified versions MHV1[37], MHV2[38], PSRK[39] and Wong–Sandler (WS)[40] mixing rule have also been proposed. The successful application of these models on more complex mixtures, however, normally requires a database of interaction parameters regressed from extensive experimental data, which remain unavailable. For example, the initial PSRK EOS, which uses the G^E expression of UNIFAC, has been revised continually and extended to additional structural groups as data become available.[41-44] Weaknesses of these mixing rules have also been reported. For example, Boukouvalas et al.[45] found that the MHV2, PSRK, and WS mixing rules do not satisfactorily represent the phase equilibria of mixtures such as CO_2 + n-alkanes and CH_4 + n-alkanes systems. Voustas et al.[46] found that the MHV2, PSRK, and WS mixing rules yield poor VLE prediction results for asymmetric mixtures. A more detailed review on mixing rules for cubic EOS is provided by Orbey and Sandler[47]. It is worth noting that using regressed interaction parameters or complex mixing rules does not resolve the shortcomings of cubic EOS. EOS development remains an active research topic.

2.1.4 Advanced EOS based on statistical theory

The Statistical Association Fluid Theory (SAFT) was developed by Chapman et al.[48] based on Wertheim's cluster expansion of Helmholtz energy and simplification of perturbation theory[49-52]. In SAFT, hard spheres form chain segments by covalent bonds, and chain segments interact with each other through dispersion and association forces, as illustrated in Figure 2.3. SAFT EOS

19

express the residual Helmholtz energy, a^{res}, as the sum of three contributions, including a^{seg} (representing segment–segment interactions or segment energy, consisting a hard-sphere reference, a^{hs} and a dispersion contribution, a^{disp}), a^{chain} (representing covalent chain-forming bonds) and a^{assoc} (site–site specific interaction among segments):

$$a^{res} = a^{seg} + a^{chain} + a^{assoc} \tag{2.5}$$

$$\text{where } a^{seg} = a^{hs} + a^{disp} \tag{2.6}$$

Mixtures of non-associating pure compounds can be characterized by only three parameters, namely number of segments in the molecule (m), segment size (σ) and segment energy (ε). These parameters are typically estimated from vapor pressure and liquid density data. Two more parameters, denoted as association volume (κ^{AB}) and associating energy (ε^{AB}), are needed for associating systems, only.

Numerous SAFT variations exist today, such as CK–SAFT[53], PC–SAFT[54], SAFT–VR[55], and soft-SAFT[56], etc. Reviews of the development of SAFT family of EOS and modified SAFT variants can be found in many publications, such as the paper by Economou[57]. PC–SAFT is widely used. It has a parameter table for more than 500 pure compounds.[54,58]

| Hard spheres | Chain formed by covalent bonds | Association | Dispersion |
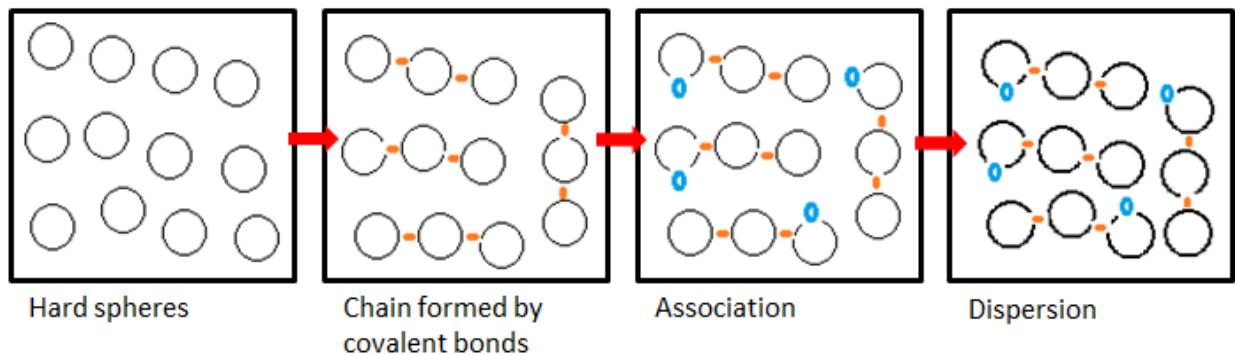
Figure 2.3 Statistical Association Fluid Theory, adapted from the work by Economou[57].

For PC–SAFT, the Lorentz–Berthelot combining rules are typically used:

$$\varepsilon_{ij} = \sqrt{\varepsilon_i \varepsilon_j}\left(1 - k_{ij}\right),\ \sigma_{ij} = \frac{\sigma_i + \sigma_j}{2} \tag{2.7}$$

Binary interaction parameters k_{ij} are introduced to correct for the dispersion energies of unlike molecules. Small positive interaction parameter values are needed in most cases to obtain excellent correlation of VLE data.[59]

2.2 Available data in literature

For binary aliphatic–aromatic mixtures available experimental VLE data have been archived: NIST TRC[60], DECHEMA[61], and DIPPR[62]. For mixtures with short n-alkanes ($N_c < 10$), there is plenty of VLE data covering a wide range of compounds, temperatures and compositions. Goral[63] reported VLE data of binaries of alkylbenzenes (benzene, toluene, ethylbenzene, and p-xylene) with a series of short alkanes (n-hexane, n-heptane, n-octane, and n-decane). For the binaries with heavier n-alkanes ($N_c > 10$), the experimental data start to become scarce. In the NIST TRC database, for benzene + n-alkanes, experimental data exist up to benzene + heptadecane [64]. Some data for benzene + n-C_{20}, n-C_{24}, n-C_{28} and n-C_{36} have only recently been reported [26]. For benzene derivatives, experimental data are scarce. For n-propylbenzene, VLE data can be found up to n-propylbenzene + n-nonane [65]. Very few VLE experimental studies for binary mixtures composed of aromatics + long chain n-alkanes are available in open literature and data for only a few conditions (compositions, temperatures and pressures) are extant. For

example, the VLE data for toluene + hexadecane has only been reported by Messow and Engel[66] at 333 and 353 K. For n-alkanes with $N_c > 20$, no experimental VLE data are available. Figure 2.4 shows the availability of VLE data for five aromatic + n-alkane binaries in the NIST database[67].
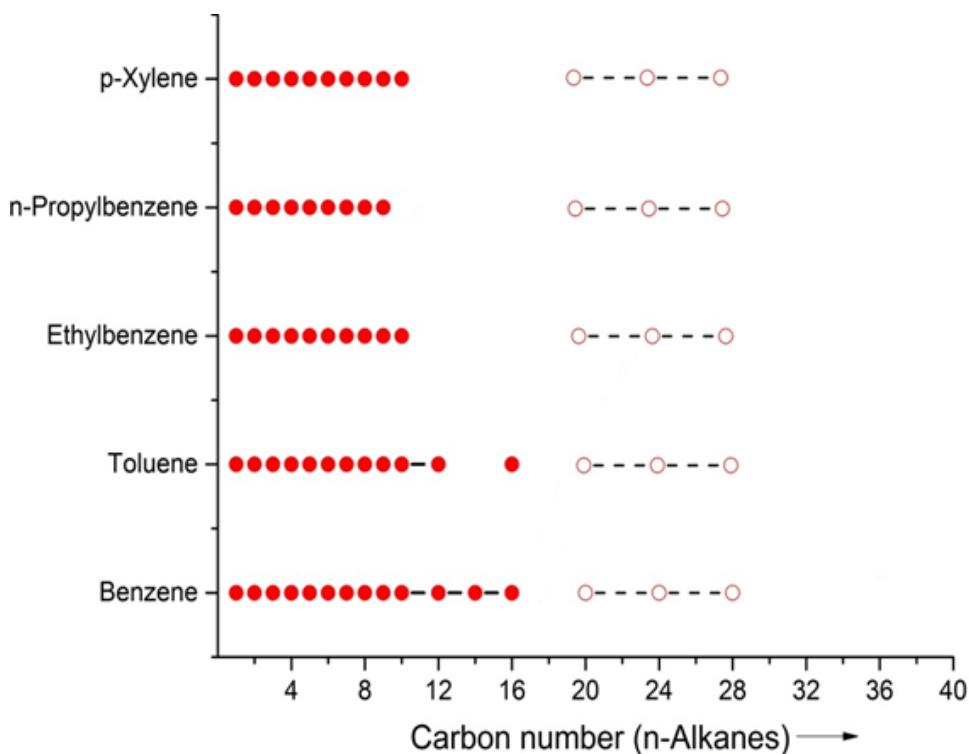
Figure 2.4 Availability of VLE data for aromatic + n-alkane binaries in NIST database.[67] Red dots indicate that there is available data in the database. Hollow circles indicate there is none.

2.3 Experimental techniques

Ambrose et al.[68] and Weir and de Loos[69] among others[70-74] reviewed techniques for determining vapor pressure. For high-pressure phase equilibria the experimental methods can be classified as analytical methods or synthetic methods, depending on whether mixture compositions are known precisely, as shown in Figure 2.5. Generally, synthetic methods allow visual observation of

phase change and do not need sampling during experiments. However, synthetic methods do not provide detailed composition information for each phase. In analytical methods phase compositions are measured using spectroscopy, refractometry or chromatography.
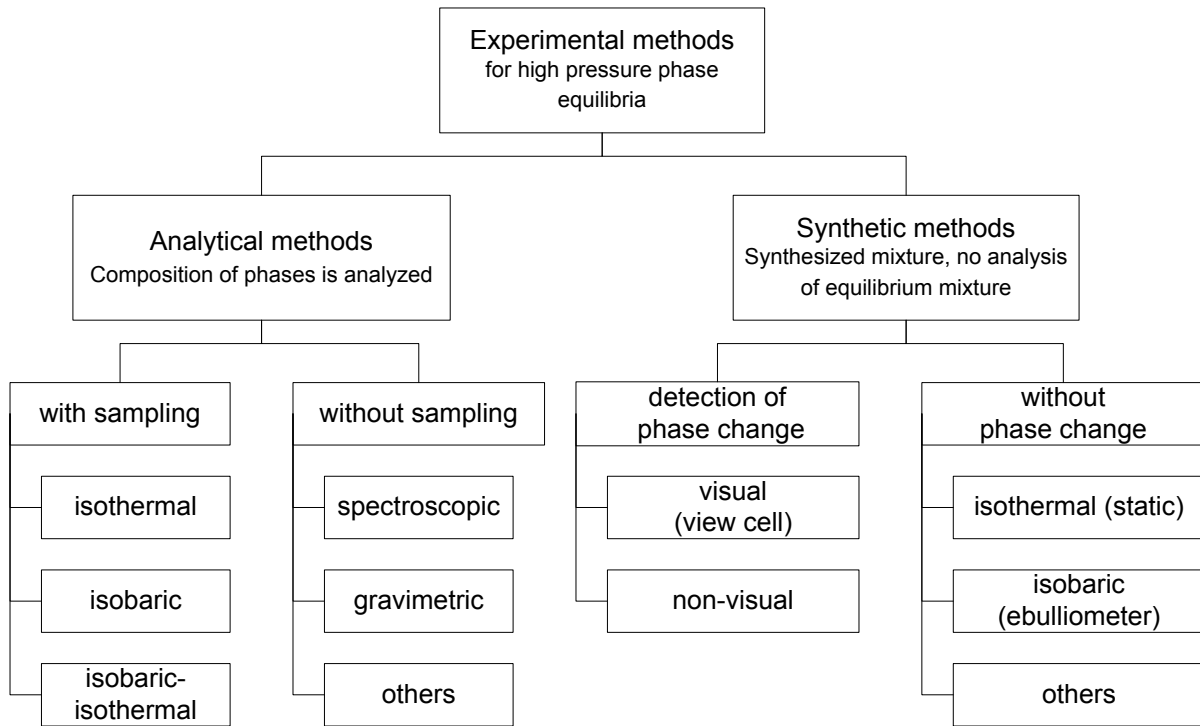
Figure 2.5 Experimental techniques for high pressure fluid phase equilibria, adapted from the work by Dohrn et al.[73]

For low pressure VLE (1 to 100 kPa), the focus of this work, experimental methods include static and dynamic methods, both of which can be conducted in a synthetic or analytical way, depending on the configuration of equipment. Static methods are commonly used and are generally more accurate. In this long established method, a degassed sample is charged into an evacuated cell and equilibrium is determined by the constancy of pressure.[75,76,77] Some modern design configurations are presented in papers by Kolbe and Gmehling[77], Morgan and

Kobayashi[78], Sako et al.[79], and Rahman and Barrufet[80].

For static cells, concerns mainly revolve around the degassing of samples and determination of equilibrium compositions (e.g., liquid equilibrium mole fraction, x_i). Degassing processes such as vacuum conditioning, distillation or multiple freezing–melting cycles (zone refining) are normally complicated and time consuming. Sampling issues can be overcome using set ups like capillary samplers, syringe pumps and special valves.

Dynamic methods normally require condensation and continuous separation of a saturated vapor phase, achieved by recirculation or continuous flow methods. Apparatus such as ebulliometry with vapor–liquid recirculation installations can be used for VLE measurement when the boiling temperatures of components are close. Special pumps (to reduce pressure variation during recirculation) and high precision temperature controls (to avoid condensation or vaporization of fluid in the recirculation loop) are needed for high-accuracy measurements. Successful designs have been reported by many authors, including Rogalski and Malanowski[81], Aim[82], de Loos et al.[83], and Stevens et al.[84] For vapor pressure under 1 kPa, gas saturation method (transpiration method)[85] or Knudsen effusion[86] can be used. Some apparatus based on a direct static method have also been proposed[87].

For this study, involving aromatics + long chain n-alkane mixtures, measurements need to be conducted in low temperature and pressure to avoid impacts of decomposition of n-alkanes. At low pressures, extracting vapor phase samples is impractical. We opted to use a synthetic direct static method and purchased a commercial unit from Grabner Instruments.

2.4 Summary of literature review

Cubic EOS with classical mixing rules and k_{ij} values fitted from VLE data typically give satisfactory phase behavior prediction of well-defined hydrocarbons. However, with default $k_{ij}s$ = 0 or $k_{ij}s$ estimated from common correlations, the risk of misprediction becomes higher. VLE of hydrocarbon mixtures with size, shape, and polarity asymmetry are areas needing careful investigation. Experimental data of binary mixtures composed of these hydrocarbons are valuable, and can assist in the characterization of complex mixtures such as heavy oil.

Extensive work has been done to improve the performance of cubic EOS. It focuses on correcting the cross energy term $a(T)$ or co-volume term b, using single or multiple interaction parameters, and complex mixing rules. EOS based on more solid theories, have been and will continue to be proposed because it is both cost and time prohibitive to generate VLE data for a wide range of mixtures. Data, particularly for families of mixtures where models perform poorly and for which data are sparse or non-existent, such as for long chain n-alkane + aromatics mixtures will remain prized, in and for themselves but also for EOS validation and testing, and for refining methods or work flows for predicting values for coefficients such as k_{ij} in the absence of data.

2.5 References

1. Anderko, A. Equation-of-state methods for the modelling of phase equilibria. *Fluid Phase Equilib.* **1990**, *61*, 145-225.

2. Wei, Y. S.; Sadus, R. J. Equations of state for the calculation of fluid-phase equilibria. *AIChE J.* **2000**, *46*, 169-196.

3. Sengers, J. V.; Kayser, R. F.; Peters, C. J.; White, H. J. *Equations of state for fluids and fluid mixtures;* Elsevier: 2000; Vol. 5.

4. Waals, J. D.; Rowlinson, J. S. *JD van der Waals: On the continuity of the gaseous and liquid states;* North Holland: 1988; Vol. 14.

5. Redlich, O.; Kwong, J. N. On the thermodynamics of solutions. V. An equation of state. Fugacities of gaseous solutions. *Chem. Rev.* **1949**, *44*, 233-244.

6. Soave, G. Equilibrium constants from a modified Redlich-Kwong equation of state. *Chemical Engineering Science* **1972**, *27*, 1197-1203.

7. Peng, D.; Robinson, D. B. A new two-constant equation of state. *Ind.Eng.Chem.Fundam* **1976**, *15*, 59-64.

8. Sako, T.; Wu, A. H.; Prausnitz, J. M. A cubic equation of state for high-pressure phase equilibria of mixtures containing polymers and volatile fluids. *J Appl Polym Sci* **1989**, *38*, 1839-1858.

9. Kontogeorgis, G. M.; Folas, G. K. *Thermodynamic models for industrial applications: from classical and advanced mixing rules to association theories;* John Wiley & Sons: 2009; .

10. Slot-Petersen, C. A systematic and consistent approach to determine binary interaction coefficients for the Peng-Robinson equation of state (includes associated papers 20308 and 20393). *SPE Reservoir Engineering* **1989**, *4*, 488-494.

11. Englezos, P.; Bygrave, G.; Kalogerakis, N. Interaction parameter estimation in cubic equations of state using binary phase equilibrium and critical point data. *Ind Eng Chem Res* **1998**, *37*, 1613-1618.

12. Mushrif, S. H.; Phoenix, A. V. Effect of Peng− Robinson binary interaction parameters on the predicted multiphase behavior of selected binary systems. *Ind Eng Chem Res* **2008**, *47*, 6280-6288.

13. Peng, D.; Robinson, D. B. Two and three phase equilibrium calculations for systems containing water. *The Canadian Journal of Chemical Engineering* **1976**, *54*, 595-599.

14. Peridis, S.; Magoulas, K.; Tassios, D. Sensitivity of distillation column design to uncertainties in Vapor–Liquid Equilibrium information. *Sep. Sci. Technol.* **1993***, 28*, 1753-1767.

15. Gregorowicz, J.; de Loos, T. W. Prediction of Liquid−Liquid−Vapor Equilibria in asymmetric hydrocarbon mixtures. *Ind Eng Chem Res* **2001***, 40*, 444-451.

16. Jaubert, J.; Vitu, S.; Mutelet, F.; Corriou, J. Extension of the PPR78 model (predictive 1978, Peng–Robinson EOS with temperature dependent k_{ij} calculated through a group contribution method) to systems containing aromatic compounds. *Fluid Phase Equilib.* **2005***, 237*, 193-211.

17. Ahitan, S.; Satyro, M. A.; Shaw, J. M. Systematic misprediction of n-alkane + aromatic and naphthenic hydrocarbon phase behavior using common equations of state. *Journal of Chemical & Engineering Data* **2015***, 60*, 3300-3318.

18. Nishiumi, H.; Arai, T.; Takeuchi, K. Generalization of the binary interaction parameter of the Peng-Robinson equation of state by component family. *Fluid Phase Equilib.* **1988***, 42*, 43-62.

19. Gao, G.; Daridon, J.; Saint-Guirons, H.; Xans, P.; Montel, F. A simple correlation to evaluate binary interaction parameters of the Peng-Robinson equation of state: binary light hydrocarbon systems. *Fluid Phase Equilib.* **1992***, 74*, 85-93.

20. Kordas, A.; Tsoutsouras, K.; Stamataki, S.; Tassios, D. A generalized correlation for the interaction coefficients of CO2—hydrocarbon binary mixtures. *Fluid Phase Equilib.* **1994***, 93*, 141-166.

21. Stamataki, S.; Magoulas, K. Prediction of phase equilibria and volumetric behavior of fluids with high concentration of hydrogen sulfide. *Oil & Gas Science and Technology* **2000***, 55*, 511-522.

22. Jaubert, J.; Mutelet, F. VLE predictions with the Peng–Robinson equation of state and temperature dependent k_{ij} calculated through a group contribution method. *Fluid Phase Equilib.* **2004***, 224*, 285-304.

23. Tsonopoulos, C.; Tan, Z. The critical constants of normal alkanes from methane to polyethylene: II. Application of the Flory theory. *Fluid Phase Equilib.* **1993***, 83*, 127-138.

24. Coutinho, J. A.; Kontogeorgis, G. M.; Stenby, E. H. Binary interaction parameters for nonpolar systems with cubic equations of state: a theoretical approach 1. CO2/hydrocarbons using SRK equation of state. *Fluid Phase Equilib.* **1994***, 102*, 31-60.

25. Kato, K.; Nagahama, K.; Hirata, M. Generalized interaction parameters for the Peng–Robinson equation of state: carbon dioxide—n-paraffin binary systems. *Fluid Phase Equilib.* **1981***, 7*, 219-231.

26. Ahitan, S.; Shaw, J. M. Quantitative comparison between predicted and experimental binary n-alkane benzene phase behaviors using cubic and PC-SAFT EOS. *Fluid Phase Equilib.* **2016**, *428*, 4-17.

27. Stamataki, S.; Tassios, D. Performance of cubic EOS at high pressures. *Revue de l'Institut Franais du Ptrole* **1998**, *53*, 367-377.

28. Péneloux, A.; Rauzy, E.; Frze, R. A consistent correction for Redlich-Kwong-Soave volumes. *Fluid Phase Equilib.* **1982**, *8*, 7-23.

29. Duarte, M. C.; Galdo, M. V.; Gomez, M. J.; Tassin, N. G.; Yanes, M. High pressure phase behavior modeling of asymmetric alkane alkane binary systems with the RKPR EOS. *Fluid Phase Equilib.* **2014**, *362*, 125-135.

30. Saber, N.; Shaw, J. M. Toward multiphase equilibrium prediction for ill-defined asymmetric hydrocarbon mixtures. *Fluid Phase Equilib.* **2009**, *285*, 73-82.

31. Mathias, P. M. A versatile phase equilibrium equation of state. *Ind. Eng. Chem. Proc. Des. Dev.* **1983**, *22*, 385-391.

32. Melhem, G. A.; Saini, R.; Goodwin, B. M. A modified Peng-Robinson equation of state. *Fluid Phase Equilib.* **1989**, *47*, 189-237.

33. Twu, C. H.; Bluck, D.; Cunningham, J. R.; Coon, J. E. A cubic equation of state with a new alpha function and a new mixing rule. *Fluid Phase Equilib.* **1991**, *69*, 33-50.

34. Kontogeorgis, G. M.; Coutsikos, P.; Harismiadis, V. I.; Fredenslund, A.; Tassios, D. P. A novel method for investigating the repulsive and attractive parts of cubic equations of state and the combining rules used with the vdW-1f theory. *Chemical engineering science* **1998**, *53*, 541-552.

35. Mathias, P. M.; Copeman, T. W. Extension of the Peng-Robinson equation of state to complex mixtures: evaluation of the various forms of the local composition concept. *Fluid Phase Equilib.* **1983**, *13*, 91-108.

36. Huron, M.; Vidal, J. New mixing rules in simple equations of state for representing vapour-liquid equilibria of strongly non-ideal mixtures. *Fluid Phase Equilib.* **1979**, *3*, 255-271.

37. Dahl, S.; Michelsen, M. L. High-pressure vapor-liquid equilibrium with a UNIFAC-based equation of state. *AIChE J.* **1990**, *36*, 1829-1836.

38. Dahl, S.; Fredenslund, A.; Rasmussen, P. The MHV2 model: a UNIFAC-based equation of state model for prediction of gas solubility and vapor-liquid equilibria at low and high pressures. *Ind Eng Chem Res* **1991**, *30*, 1936-1945.

39. Holderbaum, T.; Gmehling, J. PSRK: a group contribution equation of state based on UNIFAC. *Fluid Phase Equilib.* **1991***, 70*, 251-265.

40. Wong, D. S. H.; Sandler, S. I. A theoretically correct mixing rule for cubic equations of state. *AIChE J.* **1992***, 38*, 671-680.

41. Fischer, K.; Gmehling, J. Further development, status and results of the PSRK method for the prediction of vapor-liquid equilibria and gas solubilities. *Fluid Phase Equilib.* **1995***, 112*, 1-22.

42. Gmehling, J.; Li, J.; Fischer, K. Further development of the PSRK model for the prediction of gas solubilities and vapor-liquid-equilibria at low and high pressures II. *Fluid Phase Equilib.* **1997***, 141*, 113-127.

43. Horstmann, S.; Fischer, K.; Gmehling, J. PSRK group contribution equation of state: revision and extension III. *Fluid Phase Equilib.* **2000***, 167*, 173-186.

44. Horstmann, S.; Jabłoniec, A.; Krafczyk, J.; Fischer, K.; Gmehling, J. PSRK group contribution equation of state: comprehensive revision and extension IV, including critical constants and α-function parameters for 1000 components. *Fluid Phase Equilib.* **2005***, 227*, 157-164.

45. Boukouvalas, C.; Spiliotis, N.; Coutsikos, P.; Tzouvaras, N.; Tassios, D. Prediction of vapor-liquid equilibrium with the LCVM model: a linear combination of the Vidal and Michelsen mixing rules coupled with the original UNIF. *Fluid Phase Equilib.* **1994***, 92*, 75-106.

46. Voutsas, E. C.; Boukouvalas, C. J.; Kalospiros, N. S.; Tassios, D. P. The performance of EoS/G E models in the prediction of vapor-liquid equilibria in asymmetric systems. *Fluid Phase Equilib.* **1996***, 116*, 480-487.

47. Orbey, H.; Sandler, S. I. *Modeling vapor-liquid equilibria: cubic equations of state and their mixing rules;* Cambridge University Press: 1998; Vol. 1.

48. Chapman, W. G.; Gubbins, K. E.; Jackson, G.; Radosz, M. SAFT: equation-of-state solution model for associating fluids. *Fluid Phase Equilib.* **1989***, 52*, 31-38.

49. Wertheim, M. S. Fluids with highly directional attractive forces. I. Statistical thermodynamics. *Journal of statistical physics* **1984***, 35*, 19-34.

50. Wertheim, M. S. Fluids with highly directional attractive forces. II. Thermodynamic perturbation theory and integral equations. *Journal of statistical physics* **1984***, 35*, 35-47.

51. Wertheim, M. S. Fluids with highly directional attractive forces. III. Multiple attraction sites. *Journal of statistical physics* **1986***, 42*, 459-476.

52. Wertheim, M. S. Fluids with highly directional attractive forces. IV. Equilibrium polymerization. *Journal of statistical physics* **1986**, *42*, 477-492.

53. Huang, S. H.; Radosz, M. Equation of state for small, large, polydisperse, and associating molecules. *Ind Eng Chem Res* **1990**, *29*, 2284-2294.

54. Gross, J.; Sadowski, G. Perturbed-chain SAFT: An equation of state based on a perturbation theory for chain molecules. *Ind Eng Chem Res* **2001**, *40*, 1244-1260.

55. Gil-Villegas, A.; Galindo, A.; Whitehead, P. J.; Mills, S. J.; Jackson, G.; Burgess, A. N. Statistical associating fluid theory for chain molecules with attractive potentials of variable range. *J. Chem. Phys.* **1997**, *106*, 4168-4186.

56. Blas, F. J.; Vega, L. F. Prediction of binary and ternary diagrams using the statistical associating fluid theory (SAFT) equation of state. *Ind Eng Chem Res* **1998**, *37*, 660-674.

57. Economou, I. G. Statistical associating fluid theory: a successful model for the calculation of thermodynamic and phase equilibrium properties of complex fluid mixtures. *Ind Eng Chem Res* **2002**, *41*, 953-962.

58. Tihic, A.; Kontogeorgis, G. M.; von Solms, N.; Michelsen, M. L. Applications of the simplified perturbed-chain SAFT equation of state using an extended parameter table. *Fluid Phase Equilib.* **2006**, *248*, 29-43.

59. Gross, J.; Sadowski, G. Application of the perturbed-chain SAFT equation of state to associating systems. *Ind Eng Chem Res* **2002**, *41*, 5510-5515.

60. NIST Thermodynamics Research Center Website. http://trc.nist.gov/ (accessed Dec 20, 2016).

61. DECHEMA Gesellschaft für Chemische Technik und Biotechnologie e.V Website. http://dechema.de/ (accessed Dec 20, 2016).

62. Design Institute for Physical Property Data Website. https://www.aiche.org/dippr (accessed Dec 20, 2016).

63. Goral, M. Vapour-liquid equilibria in non-polar mixtures. III. Binary mixtures of alkylbenzenes and n-alkanes at 313.15 K. *Fluid Phase Equilib.* **1994**, *102*, 275-286.

64. Messow, U.; Schuetze, D.; Hauthal, W. Thermodynamic studies on n-paraffin solvent systems. II. Benzene (1) n-tetradecane (2), benzene (1) n-hexadecane (2), and benzene (1) n-heptadecane (2). *Chemischer Informationsdienst* **1976**, *7*.

65. Paul, H.; Krug, J.; Knapp, H. Measurements of VLE, hE and vE for binary mixtures of n-alkanes with n-alkylbenzenes. *Thermochimica acta* **1986**, *108*, 9-27.

66. Messow, U.; Engel, I. Thermodynamic studies on solvent-paraffin systems. 7. Toluene (1)-dodecane (2) and toluene (1)-hexadecane (2). *ZEITSCHRIFT FUR PHYSIKALISCHE CHEMIE-LEIPZIG* **1977**, *258*, 798-800.

67. *NIST Standard Reference Database 103b*: NIST ThermoData Engine, Version *7.1*, accessed from Aspen Plus.

68. Ambrose, D.; Ewing, M. B.; Ghiassee, N. B.; Ochoa, J. S. The ebulliometric method of vapour-pressure measurement: vapour pressures of benzene, hexafluorobenzene, and naphthalene. *The Journal of Chemical Thermodynamics* **1990**, *22*, 589-605.

69. Weir, R. D.; de Loos, T. W. *Measurement of the thermodynamic properties of multiple phases;* Gulf Professional Publishing: 2005; .

70. Fornari, R. E.; Alessi, P.; Kikic, I. High pressure fluid phase equilibria: experimental methods and systems investigated (1978–1987). *Fluid Phase Equilib.* **1990**, *57*, 1-33.

71. Dohrn, R.; Brunner, G. High-pressure fluid-phase equilibria: experimental methods and systems investigated (1988–1993). *Fluid Phase Equilib.* **1995**, *106*, 213-282.

72. Christov, M.; Dohrn, R. High-pressure fluid phase equilibria: experimental methods and systems investigated (1994–1999). *Fluid Phase Equilib.* **2002**, *202*, 153-218.

73. Dohrn, R.; Peper, S.; Fonseca, J. M. High-pressure fluid-phase equilibria: experimental methods and systems investigated (2000–2004). *Fluid Phase Equilib.* **2010**, *288*, 1-54.

74. Fonseca, J. M.; Dohrn, R.; Peper, S. High-pressure fluid-phase equilibria: experimental methods and systems investigated (2005–2008). *Fluid Phase Equilib.* **2011**, *300*, 1-69.

75. Gibbs, R. E.; Van Ness, H. C. Vapor-liquid equilibria from total-pressure measurements. A new apparatus. *Industrial & Engineering Chemistry Fundamentals* **1972**, *11*, 410-413.

76. Aim, K. Measurement of vapor-liquid equilibrium in systems with components of very different volatility by the total pressure static method. *Fluid Phase Equilib.* **1978**, *2*, 119-142.

77. Kolbe, B.; Gmehling, J. Thermodynamic properties of ethanol water. I. Vapour-liquid equilibria measurements from 90 to 150 C by the static method. *Fluid Phase Equilib.* **1985**, *23*, 213-226.

78. Morgan, D. L.; Kobayashi, R. Direct vapor pressure measurements of ten n-alkanes m the 10-C28 range. *Fluid Phase Equilib.* **1994**, *97*, 211-242.

79. Sako, T.; Sugeta, T.; Nakazawa, N.; Okubo, T.; Sato, M.; Taguchi, T.; Hiaki, T. Phase equilibrium study of extraction and concentration of furfural produced in reactor using supercritical carbon dioxide. *J. Chem. Eng. Japan* **1991**, *24*, 449-455.

80. Rahman, S.; Barrufet, M. A. A new technique for simultaneous measurement of PVT and phase equilibria properties of fluids at high temperatures and pressures. *Journal of Petroleum Science and Engineering* **1995**, *14*, 25-34.

81. Rogalski, M.; Malanowski, S. Ebulliometers modified for the accurate determination of vapour—liquid equilibrium. *Fluid Phase Equilib.* **1980**, *5*, 97-112.

82. Aim, K. A modified ebulliometric method for high-boiling substances: vapour pressures of 2-chlorobenzonitrile and 4-chlorobenzonitrile at temperatures from 380 K to 490 K. *The Journal of Chemical Thermodynamics* **1994**, *26*, 977-986.

83. de Loos, T. W.; Van der Kooi, Hedzer J; Ott, P. L. Vapor-liquid critical curve of the system ethane 2-methylpropane. *J. Chem. Eng. Data* **1986**, *31*, 166-168.

84. Stevens, R.; Shen, X. M.; De Loos, T. W.; de Swaan Arons, J. A new apparatus to measure the vapour-liquid equilibria of low-volatility compounds with near-critical carbon dioxide. Experimental and modelling results for carbon dioxide n-butanol, 2-butanol, 2-butyl acetate and vinyl acetate systems. *The Journal of Supercritical Fluids* **1997**, *11*, 1-14.

85. Macknick, A. B.; Prausnitz, J. M. Vapor pressures of high-molecular-weight hydrocarbons. *J.Chem.Eng.Data;(United States)* **1979**, *24*.

86. Knudsen, M. Die Molekularströmung der Gase durch Offnungen und die Effusion. *Annalen der Physik* **1909**, *333*, 999-1016.

87. Růžička, K.; Fulem, M.; Růžička, V. Vapor pressure of organic compounds. Measurement and correlation, 2008.http://old.vscht.cz/fch/Kvetoslav.Ruzicka/ICTP_VaporPressureGroup.pdf. (accessed January 15, 2017)

Chapter 3. Experimental

3.1 Materials

The materials, listed in Table 3.1, have purities exceeding 99% and were used in this work without further purification. Water sorption from air is the principal concern regarding BPP measurements, because aromatic compounds in particular are hydroscopic. If saturated with water at 298 K, the increase in apparent bubble pressure is approximately 2 kPa. At 323 K the impact is 12 kPa and at 343 K the impact is 31 kPa. Uncorrected deviations from reference data rarely exceeded +/- 1 kPa, even at high temperature. Thus the mole fraction of water in the aromatics is much lower than the saturated value and was ignored. Trace organic impurities have even smaller impacts on BPP measurements and can be ignored relative to the cited measurement uncertainty.

Table 3.1 Materials information

Materials	Supplier	Purity (%)
Benzene	Sigma-Aldrich	99.8%
Toluene	Fischer Chemical	99.8%
Ethylbenzene	Sigma-Aldrich	99.8%
n-Propylbenzene	Sigma-Aldrich	98%
p-Xylene	Sigma-Aldrich	99%
Eicosane	Sigma	99%
Tetracosane	Alfa Aesar	99%
Octacosane	Alfa Aesar	99%

3.2 Equipment

The equipment used for bubble pressure measurements, based on the static method, is a MINIVAP VPXpert-L from Grabner Instruments. The equipment has a measuring cell with an internal volume of 5 mL, which can be varied with an adjustable piston at the top of the cell. Samples are introduced into the measuring cell through the Luer inlet by varying the piston position. The equipment has an operating temperature range of 0 to 120 ºC and a vapor pressure measurement range of 0 to 100 kPa. The pressure is measured using a precision pressure transducer, integrated into the piston (Figure 3.1). The temperature of the measuring cell is controlled with a thermoelectric module and measured with a PT100 RTD sensor with an accuracy of ± 0.1 K. A schematic diagram of the measuring cell is shown in Figure 3.1.
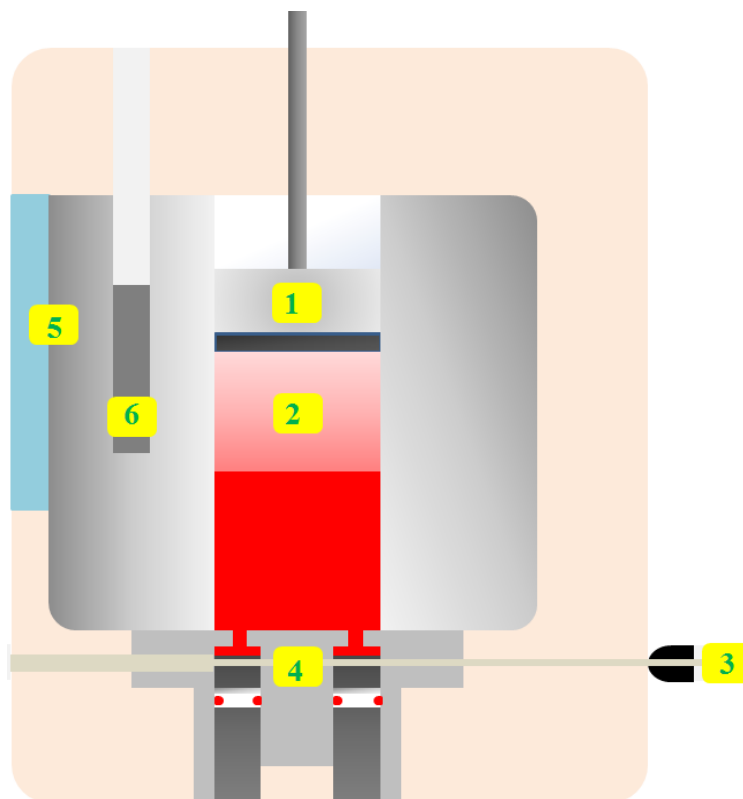
Figure 3.1 Cross-section view of the measuring cell: 1) pressure transducer 2) measuring chamber 3) Luer sample inlet 4) sample inlet valve 5) thermoelectric module 6) PT100 RTD sensor, adapted from the operation manual.[1]

3.3 Mixture preparation

Binary mixtures were prepared gravimetrically in 22 mL glass vials at room temperature by mixing solid n-alkanes with liquid aromatics. The n-alkanes were first added to the vial, and then the aromatics were transferred into the vial using a syringe. Component masses of the order of 10 grams were determined using a Mettler-Toledo MS603S balance with an accuracy of ±0.001g. The sealed glass vials containing samples were then preheated in a vacuum oven at 80 $^{\circ}$C until the solids melted. The samples were kept in the oven at a temperature above the eutectic temperature of the mixture and were quickly transferred into the measuring cell before each measurement to avoid solidification in the tubing during injection.

3.4 Mixture measurement

Prior to each experiment, the measuring chamber is rinsed, automatically with 2.5 mL of sample in order to displace air from the dead volume inside the cell. After rinsing, the piston moves to the lowest position directly above the valve, then it moves up to draw in 1 mL of sample into the measuring cell. The inlet valve is then closed. The piston then moves upward to increase the internal volume of the cell to 1.7 mL. Then the temperature of the measuring cell is increased to the starting value. A pressure reading is recorded once the system reaches equilibrium, which is determined by a pressure change of less than 0.1 kPa/min. Following that, the piston performs a second (2.5 mL) and third expansion (5 mL) and a total of three pressure readings are taken at the three piston positions at the same temperature. Based on these three readings, the actual vapor pressure of the mixture, P_{actual}, and the pressure exerted by dissolved air, P_{air}, are calculated using the following equations. In these equations, P_{total} represent the total pressure. V

represent the volume of the measuring cell. Subscript i represent the values corresponding to the ith expansion.

$$P_{totali} = P_{actual} + P_{airi}(i = 1,2,3) \tag{3.1}$$

$$P_{air1}V_1 = P_{air2}V_2 = P_{air3}V_3 \tag{3.2}$$

$$P_{actual} = P_{total3} - P_{air3} = P_{total3} - \frac{(P_{total1}-P_{total3})(P_{total2}-P_{total3})}{\frac{V_3-V_1}{V_2-V_1}(P_{total1}-P_{total2})-(P_{total1}-P_{total3})} \tag{3.3}$$

Each experiment was repeated three times. The vapor space in the measuring cell is very small, only a trace mole fraction of the mixture is vaporized.

3.5 Uncertainty analysis and validation

The sources of uncertainty include measurement uncertainties (temperature, pressure, volume), uncertainty in sample preparation (mass determination), transfer of sample into the measuring cell (composition), and air remaining in the liquid. The measurement results were validated against VLE data from the NIST database[2], for pure benzene, toluene and ethylbenzene, and three mixtures of heptane + octane, toluene + heptane and toluene + octane. These experimental data are reported in Table 3.2. For all these compounds and mixtures the experimental data were found to have an average absolute deviation (AAD) of 0.52 kPa and an average absolute percent deviation (AAPD) of 4.0 % relative to the reference data. The deviation, percent deviation, AAD and AAPD of experimental pressure values are calculated from equations 3.5 to 3.7, respectively, where P_{exp} is the experimental value (this work) and P_{ref} is the reference pressure measurement. A correction function (equation 3.8), with a sum of deviations equaling 0, was

used to eliminate systematic bias. The calibration curve is shown in Figure 3.2. With this correlation, the experimental validation data from this work have an AAD of 0.46 kPa and an AAPD of 3.0 % relative to the reference data. Pressure deviations of most of the experimental points (72 out of 77 points, 94%) fall within the range of ±1 kPa of reference data. The maximum deviation observed is −1.64 kPa. The deviations and percent deviations of corrected pressures are shown in Figure 3.3 and Figure 3.4, respectively.

$$Deviation = \frac{P_{exp} - P_{ref}}{P_{ref}} \tag{3.4}$$

$$Percent\ Deviation = \frac{P_{exp} - P_{ref}}{P_{ref}} \times 100\% \tag{3.5}$$

$$AAD = \frac{\sum |Deviation|}{number\ of\ data\ points} \tag{3.6}$$

$$AAPD = \frac{\sum |Percent\ Deviation|}{number\ of\ data\ points} \tag{3.7}$$

$$P_{corrected} = 0.990541 P_{exp} + 0.485818 kPa \tag{3.8}$$
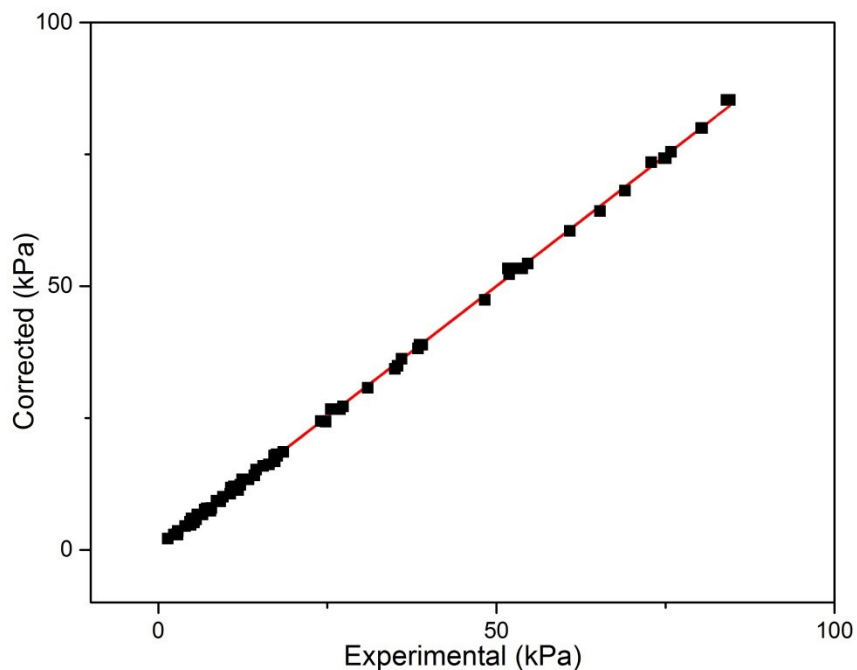
Figure 3.2 Unbiased BPP Calibration curve (——) used to eliminate systematic bias and

reference data (black squares).

Table 3.2 Experimental vapor pressures for method validation

Sample	Temperature (K) ± 0.1K	Experimental (kPa)	Corrected (kPa)	Reference data[2] (kPa)	Deviation (kPa)	Percent Deviation (%)
Benzene	293.15	9.57	9.97	10.03	−0.06	−0.65
	303.15	15.53	15.87	15.92	−0.05	−0.32
	313.15	24.07	24.33	24.39	−0.06	−0.25
	323.15	35.95	36.10	36.21	−0.11	−0.32
	333.15	51.87	51.87	52.25	−0.38	−0.74
	343.15	72.88	72.68	73.52	−0.84	−1.15
Toluene	293.15	2.72	3.18	2.92	0.26	8.91
	303.15	4.81	5.25	4.89	0.36	7.37
	313.15	7.87	8.28	7.89	0.39	4.96
	323.15	12.16	12.53	12.29	0.24	1.96
	333.15	18.51	18.82	18.54	0.28	1.51
	343.15	27.32	27.55	27.19	0.36	1.31
	353.15	39.04	39.16	38.87	0.29	0.74
	363.15	54.65	54.62	54.29	0.33	0.61

	373.15	74.79	74.57	74.25	0.32	0.43
Ethylbenzene	313.15	2.85	3.31	2.88	0.43	14.89
	323.15	4.82	5.26	4.70	0.56	11.92
	333.15	7.73	8.14	7.41	0.73	9.89
	343.15	11.81	12.18	11.31	0.87	7.73
	353.15	17.23	17.55	16.78	0.77	4.61
	363.15	24.77	25.02	24.27	0.75	3.10
	373.15	34.99	35.14	34.28	0.86	2.52
	383.15	48.27	48.30	47.39	0.91	1.92
	393.15	65.31	65.18	64.26	0.92	1.43
Toluene (0.623 mol%) + Heptane	298.15	4.71	5.15	5.27	−0.12	−2.25
	303.15	6.57	6.99	6.68	0.31	4.70
	313.15	10.64	11.03	10.65	0.38	3.52
	323.15	16.38	16.71	16.19	0.52	3.22
	335.55	26.82	27.05	26.66	0.39	1.47
	343.15	35.37	35.52	34.90	0.62	1.78
	355.25	53.61	53.59	53.33	0.26	0.49
	363.15	69.01	68.84	68.12	0.72	1.06
	368.15	80.44	80.16	79.99	0.17	0.22
Toluene (0.860 mol%) + Heptane	298.15	4.00	4.45	4.47	−0.02	−0.49
	303.15	5.63	6.06	5.76	0.30	5.25
	313.15	9.18	9.58	9.15	0.43	4.69
	323.20	14.21	14.56	14.08	0.48	3.42
	339.25	26.91	27.14	26.66	0.48	1.81
	343.20	30.99	31.18	30.69	0.49	1.61
	359.20	53.82	53.80	53.33	0.47	0.88
	363.20	60.85	60.76	60.46	0.30	0.50
	372.20	80.28	80.01	79.99	0.02	0.02
Toluene (0.161 mol%) + Heptane	298.15	4.93	5.37	5.94	−0.57	−9.61
	303.15	6.85	7.27	7.60	−0.33	−4.33
	313.15	11.22	11.60	12.02	−0.42	−3.50
	323.15	17.53	17.85	18.08	−0.23	−1.27
	332.25	25.54	25.78	26.66	−0.88	−3.28
	343.15	38.62	38.74	38.90	−0.16	−0.41
	351.75	52.13	52.12	53.33	−1.21	−2.26
	363.15	75.81	75.58	75.48	0.10	0.13
Toluene (0.261 mol%) + Heptane	298.15	5.30	5.74	5.85	−0.11	−1.95
	303.15	6.99	7.41	7.45	−0.04	−0.54
	313.15	11.33	11.71	11.82	−0.11	−0.94
	323.15	17.58	17.90	17.78	−0.12	−0.67
	332.25	25.52	25.76	26.66	−0.90	−3.36

	343.15	38.42	38.54	38.16	0.38	1.00
	351.75	51.69	51.69	53.33	−1.64	−3.08
	363.15	75.04	74.82	74.24	0.58	0.78
Heptane (0.225 mol%) + Octane	293.15	1.42	1.89	2.14	−0.25	−11.57
	312.75	5.07	5.51	5.89	−0.38	−6.49
	328.15	10.73	11.11	11.77	−0.66	−5.57
Heptane (0.465 mol%) + Octane	293.15	2.33	2.79	2.84	−0.05	−1.63
	312.75	7.17	7.59	7.83	−0.24	−3.09
	328.15	14.49	14.84	15.19	−0.35	−2.31
Heptane (0.641 mol%) + Octane	293.15	2.92	3.38	3.56	−0.18	−5.11
	312.75	8.62	9.02	9.31	−0.29	−3.07
	328.15	17.15	17.47	17.85	−0.38	−2.11
Toluene (0.312 mol%) + Octane	316.55	5.81	6.24	6.67	−0.43	−6.43
	331.95	12.42	12.79	13.33	−0.54	−4.06
	349.75	25.62	25.86	26.67	−0.81	−3.02
	370.15	52.07	52.06	53.33	−1.27	−2.38
	385.75	84.04	83.73	85.33	−1.60	−1.87
Toluene (0.699 mol%) + Octane	312.45	6.23	6.66	6.67	−0.01	−0.20
	327.55	13.37	13.73	13.33	0.40	3.00
	344.55	26.28	26.52	26.67	−0.15	−0.57
	364.75	52.75	52.74	53.33	−0.59	−1.11
	380.15	84.51	84.20	85.33	−1.13	−1.33
AAD (kPa)		0.52	0.46			
AAPD (%)		4.03	2.97			
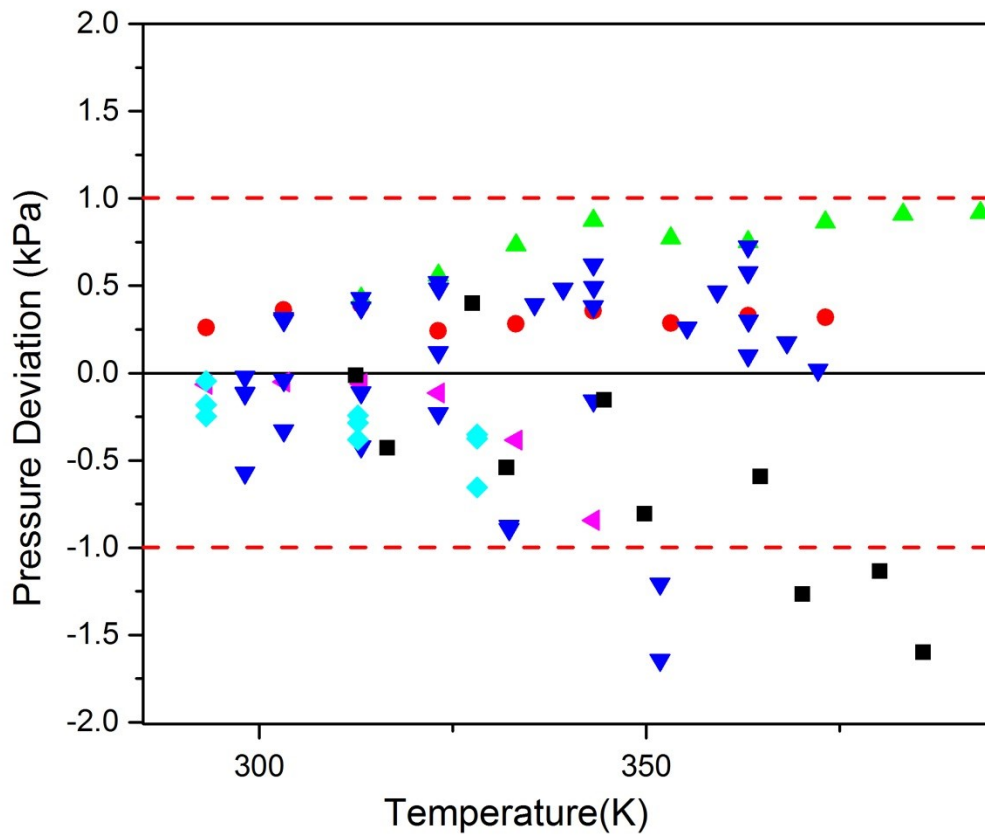
Figure 3.3 Pressure deviations after correction for: (◀)benzene, (●)toluene, (▲)ethylbenzene, (■)toluene + octane,(▼)toluene + heptane, (◆)heptane + octane.
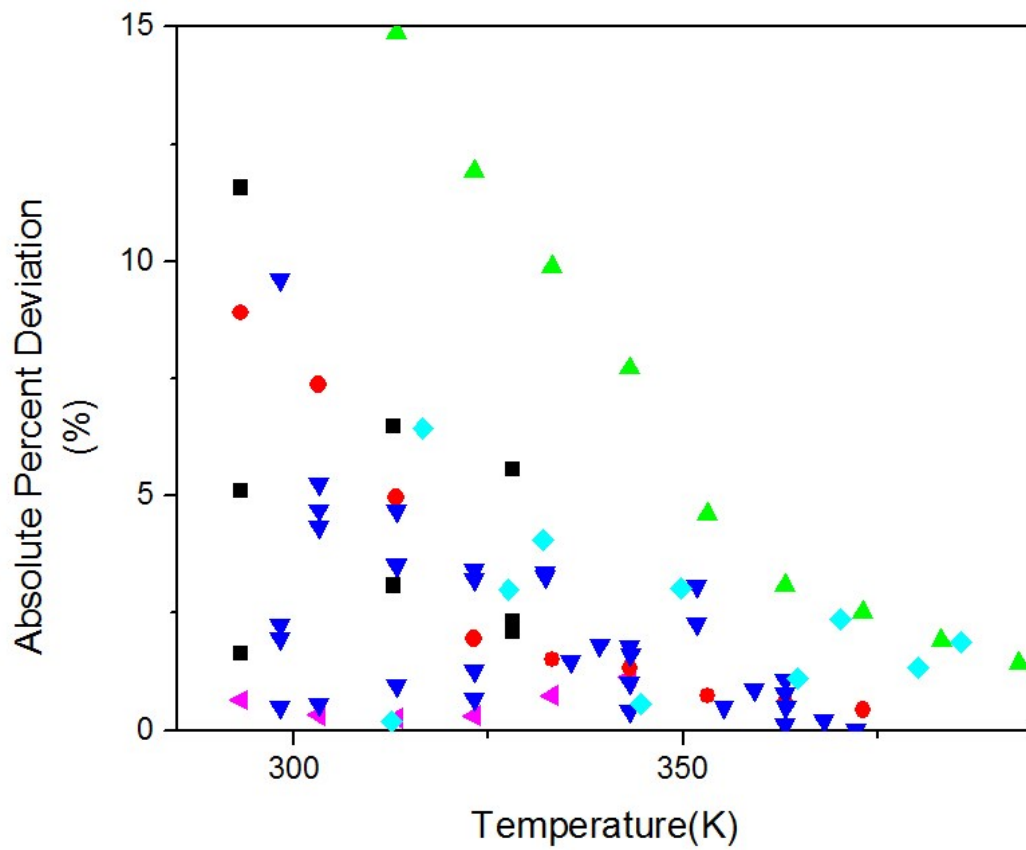
Figure 3.4 Absolute percent deviations after correction for: (◀) benzene, (●)toluene, (▲)ethylbenzene, (■)toluene + octane, (▼)toluene + heptane, (◆)heptane + octane.

3.6 References

1. Vapor Pressure Tester MINIVAP VPXpert/-L Operation Manual, 2015. Grabner Instruments.

2. *NIST Standard Reference Database 103b*: NIST ThermoData Engine, Version 7.1, accessed from Aspen Plus.

Chapter 4. Results and Discussion

4.1 Experimental data

Experimental BPPs for 15 aromatic + long chain n-alkane binary mixtures, measured in this work are presented in Table 4.1. Corrected values are obtained by applying the calibration equation (equation 3.8).

Table 4.1 Experimental BPPs obtained from this work

Temperature (K) ± 0.1 K	Mole fraction (aromatic) $x \pm 0.0001$	Experimental BPP	
		Raw	Corrected Uncertainty ± 1 kPa
Benzene + n-C$_{20}$			
313.15		5.97	6.4
323.15		8.60	9.0
333.15	0.2555	12.05	12.4
343.15		16.46	16.8
353.15		22.15	22.4
363.15		28.94	29.2
313.15		12.45	12.8
323.15		17.75	18.1
333.15	0.5083	25.17	25.4
343.15		34.59	34.7
353.15		46.57	46.6
363.15		61.31	61.2
313.15		19.21	19.5
323.15		27.87	28.1
333.15	0.7593	39.39	39.5
343.15		54.45	54.4
353.15		73.79	73.6
363.15		97.76	97.4
Toluene + n-C$_{20}$			
313.15		2.01	2.5
323.15		3.03	3.5
333.15		4.44	4.9
343.15		6.34	6.8
353.15	0.2514	8.87	9.3
363.15		12.03	12.4

373.15		16.13	16.5
383.15		20.97	21.3
393.15		27.36	27.6
313.15		4.12	4.6
323.15		6.27	6.7
333.15		9.26	9.7
343.15		13.27	13.6
353.15	0.5043	18.63	18.9
363.15		25.33	25.6
373.15		34.22	34.4
383.15		44.81	44.9
393.15		58.34	58.3
313.15		6.24	6.7
323.15		9.59	10.0
333.15		14.28	14.6
343.15		20.59	20.9
353.15	0.7526	29.07	29.3
363.15		40.02	40.1
373.15		54.24	54.2
383.15		71.69	71.5
393.15		93.81	93.5

<div align="center">Ethylbenzene + n-C₂₀</div>

323.15		1.32	1.8
333.15		2.01	2.5
343.15		2.98	3.4
353.15		4.30	4.7
363.15	0.2511	6.08	6.5
373.15		8.41	8.8
383.15		11.36	11.7
393.15		15.13	15.5
323.15		2.62	3.1
333.15		4.05	4.5
343.15		6.01	6.4
353.15		8.72	9.1
363.15	0.5015	12.39	12.8
373.15		17.25	17.6
383.15		23.42	23.7
393.15		31.29	31.5
323.15		3.86	4.3
333.15		5.97	6.4
343.15		8.97	9.4
353.15		13.15	13.5
363.15	0.7502	18.74	19.1
373.15		26.16	26.4
383.15		35.85	36.0
393.15		48.16	48.2

n-Propylbenzene + n-C$_{20}$			
333.15		0.93	1.4
343.15		1.44	1.9
353.15		2.16	2.6
363.15	0.2512	3.15	3.6
373.15		4.49	4.9
383.15		6.22	6.7
393.15		8.43	8.8
333.15		1.81	2.3
343.15		2.81	3.3
353.15		4.22	4.7
363.15	0.4999	6.21	6.6
373.15		8.89	9.3
383.15		12.43	12.8
393.15		16.96	17.3
333.15		2.60	3.1
343.15		4.04	4.5
353.15		6.14	6.6
363.15	0.75	9.07	9.5
373.15		13.06	13.4
383.15		18.44	18.8
393.15		25.32	25.6
p-Xylene + n-C$_{20}$			
323.15		1.15	1.6
333.15		1.80	2.3
343.15		2.67	3.1
353.15		3.87	4.3
363.15	0.2515	5.54	6.0
373.15		7.68	8.1
383.15		10.48	10.9
393.15		14.04	14.4
323.15		2.32	2.8
333.15		3.59	4.0
343.15		5.37	5.8
353.15		7.91	8.3
363.15	0.4991	11.21	11.6
373.15		15.72	16.1
383.15		21.46	21.8
393.15		28.81	29.0
323.15		3.44	3.9
333.15		5.34	5.8
343.15		8.07	8.5
353.15	0.7503	11.89	12.3
363.15		17.10	17.4
373.15		24.04	24.3

383.15		33.11	33.3
393.15		44.62	44.7

Benzene + n-C$_{24}$			
333.15		10.28	10.7
343.15		14.87	15.2
353.15		20.69	21.0
363.15	0.2623	27.82	28.1
373.15		36.59	36.7
383.15		47.26	47.3
393.15		59.56	59.5
333.15		23.76	24.0
343.15		33.59	33.8
353.15	0.5212	45.85	45.9
363.15		61.34	61.3
373.15		79.97	79.7
333.15		38.05	38.2
343.15	0.7637	53.47	53.5
353.15		73.04	72.9

Toluene + n-C$_{24}$			
333.15		2.30	2.8
343.15		4.21	4.7
353.15		6.68	7.1
363.15	0.2508	9.91	10.3
373.15		13.97	14.3
383.15		18.98	19.3
393.15		25.04	25.3
333.15		8.01	8.4
343.15		11.96	12.3
353.15		16.27	16.6
363.15	0.5008	23.17	23.4
373.15		31.88	32.1
383.15		42.51	42.6
393.15		55.89	55.9
333.15		13.02	13.4
343.15		19.35	19.7
353.15		27.78	28.0
363.15	0.7504	37.73	37.9
373.15		51.69	51.7
383.15		69.76	69.6
393.15		91.58	91.2

Ethylbenzene + n-C$_{24}$			
333.15		2.02	2.5
343.15		2.51	3.0
353.15		3.80	4.3

363.15	0.2557	5.54	6.0
373.15		8.26	8.7
383.15		10.42	10.8
393.15		13.47	13.8
333.15		3.46	3.9
343.15		5.41	5.8
353.15		8.07	8.5
363.15	0.5051	11.34	11.7
373.15		16.26	16.6
383.15		21.82	22.1
393.15		30.25	30.5
333.15		5.42	5.9
343.15		8.35	8.8
353.15		11.94	12.3
363.15	0.752	17.47	17.8
373.15		24.75	25.0
383.15		34.29	34.5
393.15		46.21	46.3

n-Propylbenzene + n-C$_{24}$

343.15		0.96	1.4
353.15		1.55	2.0
363.15	0.2519	2.37	2.8
373.15		3.77	4.2
383.15		5.31	5.7
393.15		7.49	7.9
343.15		2.03	2.5
353.15		3.16	3.6
363.15	0.4542	4.78	5.2
373.15		7.15	7.6
383.15		10.14	10.5
393.15		14.22	14.6
343.15		3.52	4.0
353.15		5.68	6.1
363.15	0.7593	8.45	8.9
373.15		12.54	12.9
383.15		17.72	18.0
393.15		24.71	25.0

p-Xylene + n-C$_{24}$

333.15		1.86	2.3
343.15		2.26	2.7
353.15		3.49	3.9
363.15	0.2648	5.18	5.6
373.15		7.32	7.7
383.15		10.11	10.5
393.15		13.13	13.5

333.15		3.05	3.5
343.15		4.63	5.1
353.15		7.26	7.7
363.15	0.5014	10.55	10.9
373.15		14.88	15.2
383.15		20.36	20.7
393.15		27.48	27.7
333.15		4.86	5.3
343.15		7.57	8.0
353.15		11.37	11.8
363.15	0.7509	16.49	16.8
373.15		23.33	23.6
383.15		32.14	32.3
393.15		43.65	43.7

Benzene + n-C$_{28}$

353.15		19.35	19.7
363.15		27.63	27.9
373.15	0.2885	36.52	36.7
383.15		48.36	48.4
393.15		61.12	61.1
353.15		38.98	39.1
363.15	0.5177	53.71	53.7
373.15		70.53	70.4
383.15		91.31	91.0
353.15	0.7614	66.37	66.3
363.15		90.32	90.0

Toluene + n-C$_{28}$

353.15		8.13	8.5
363.15		11.69	12.1
373.15	0.2981	16.22	16.6
383.15		21.72	22.0
393.15		28.52	28.7
353.15		15.37	15.7
363.15		21.59	21.9
373.15	0.5018	29.72	29.9
383.15		39.77	39.9
393.15		52.31	52.3
353.15		26.24	26.5
363.15		36.73	36.9
373.15	0.7598	50.34	50.4
383.15		67.55	67.4
393.15		88.96	88.6

Ethylbenzene + n-C$_{28}$

353.15	0.2584	2.91	3.4

363.15		4.46	4.9
373.15		6.63	7.1
383.15		9.30	9.7
393.15		12.61	13.0
353.15		6.96	7.4
363.15		10.28	10.7
373.15	0.5055	14.67	15.0
383.15		20.14	20.4
393.15		27.27	27.5
353.15		11.43	11.8
363.15		16.79	17.1
373.15	0.751	23.85	24.1
383.15		32.77	33.0
393.15		44.37	44.5

n-Propylbenzene + n-C$_{28}$

363.15		2.10	2.6
373.15		3.25	3.7
383.15	0.2554	4.79	5.2
393.15		6.86	7.3
353.15		3.27	3.7
363.15		5.03	5.5
373.15	0.5127	7.52	7.9
383.15		10.82	11.2
393.15		15.07	15.4
353.15		5.22	5.7
363.15		8.02	8.4
373.15	0.7525	11.83	12.2
383.15		16.89	17.2
393.15		23.64	23.9

p-Xylene + n-C$_{28}$

353.15		3.03	3.5
363.15		4.80	5.2
373.15	0.2897	7.03	7.5
383.15		9.92	10.3
393.15		13.44	13.8
353.15		6.22	6.7
363.15		9.38	9.8
373.15	0.4985	12.52	12.9
383.15		18.64	19.0
393.15		25.16	25.4
353.15		10.58	11.0
363.15		15.56	15.9
373.15		22.24	22.5
383.15	0.7536	30.79	31.0
393.15		41.79	41.9

4.2 Computed bubble pressures ($k_{ij} = 0$)

Computed BPPs for these binaries with $k_{ij} = 0$ from PR, SRK and PC–SAFT EOS are compared with experimental data in in Figure 4.1(a-o). Pure compound properties obtained from the NIST/TDE[1] database are used in VMGSim[2] to compute BPPs using both the PR and SRK EOS. The uncertainties of acentric factors (ω) were assumed to be 0, as they are not reported by the NIST/TDE database. For the PC–SAFT EOS, calculations were performed in Aspen Plus[3] using parameters reported by Gross and Sadowski[4] and Tihic et al.[5] A list of input parameters for these calculations are shown in Table 4.2 and Table 4.3.

Table 4.2 Pure compound properties for cubic EOS (from NIST/TDE database[1])

	T_c(K)	Uncertainty (K)	P_c (bar)	Uncertainty (bar)	ω
n-C$_{20}$	768.22	5.77	11.097924	0.613479	0.88151
n-C$_{24}$	799.55	5.24	8.686934	1.105986	1.0573
n-C$_{28}$	824	8	7.501554	1.373584	1.264
Benzene	562.023	0.136	48.946293	0.437887	0.20993
Toluene	591.89	0.02	41.255165	0.657753	0.26441
Ethylbenzene	617.121	0.107	36.10294	0.213088	0.30348
n-Propylbenzene	638.286	0.138	32.011135	0.421779	0.34491
p-Xylene	616.187	0.146	35.262119	0.17027	0.32317

Table 4.3 Pure compound parameters for PC–SAFT EOS

	m	σ (Å)	ε/k (K)	Reference
Benzene	2.4653	3.6478	287.35	4
Toluene	2.8149	3.7169	285.69	4
Ethylbenzene	3.0799	3.7974	287.35	4
n-Propylbenzene	3.3438	3.8438	288.13	4
p-Xylene	3.1723	3.7781	283.77	4
n-C$_{20}$	7.9849	3.9869	257.75	5

				5
n-C$_{24}$	9.4034	3.9896	254.61	
n-C$_{28}$	10.8004	4.0019	255.67	5

As illustrated in Figure 4.1(a-o), the PC–SAFT EOS tends to underestimate BPP values but provides much better approximations of experimental data than Cubic EOS. With k$_{ij}$ values set to zero, cubic EOS systematically over-predict BPPs for aromatic + long chain alkane binaries and provide poor estimates for BPPs at the tested experimental conditions. For cubic EOS, the overestimation of BPPs becomes more remarkable as the binary becomes more asymmetric (i.e., as the n-alkane chain length increases or chain substitution to the aromatic ring increases), as evidenced by the increased gap between experimental and predicted results. Detailed absolute deviations of predicted results and their percentage for PR, SRK and PC-SAFT EOS are shown in Table 4.4, Table 4.5, and Table 4.6, respectively. Clearly, Cubic EOS overestimate the repulsion effect between aromatics and long chain alkanes. Their energy and co-volume terms do not describe the interaction for these asymmetric mixtures adequately. Hence the need for custom fit interaction parameters rooted in experimental data.

Table 4.4 Experimental data vs. calculated outcomes from PR EOS with k$_{ij}$ = 0

Temperature (K) ±0.1K	Aromatic Mole Fraction $x \pm 0.0001$	Bubble Pressure (kPa)		Deviation	
		Experimental Uncertainty ± 1kPa	Calculated from PR EOS with k$_{ij}$ = 0	Absolute Deviation (kPa)	Absolute Percent Deviation (%)
		Benzene + n-C$_{20}$			
313.15		6.4	10.6	4.2	66.0
323.15		9.0	15.0	6.0	66.3
333.15		12.4	20.6	8.2	65.9

343.15	0.2555	16.8	27.7	10.9	64.6
353.15		22.4	36.4	14.0	62.7
363.15		29.2	47.1	17.9	61.5
313.15		12.8	19.6	6.8	52.9
323.15		18.1	27.8	9.7	53.6
333.15		25.4	38.5	13.1	51.6
343.15	0.5083	34.7	52.2	17.4	49.9
353.15		46.6	69.2	22.6	48.6
363.15		61.2	90.3	29.1	47.5
313.15		19.5	25.1	5.6	28.8
323.15		28.1	36.1	8.0	28.6
333.15		39.5	50.7	11.2	28.4
343.15	0.7593	54.4	69.6	15.2	27.9
353.15		73.6	93.5	19.9	27.0
363.15		97.4	123.3	25.9	26.5

Toluene + n-C$_{20}$

313.15		2.5	3.5	1.0	41.3
323.15		3.5	5.2	1.7	49.8
333.15		4.9	7.6	2.7	54.4
343.15		6.8	10.6	3.8	56.4
353.15	0.2514	9.3	14.6	5.3	57.2
363.15		12.4	19.7	7.3	58.6
373.15		16.5	26.0	9.5	57.3
383.15		21.3	33.7	12.4	58.0
393.15		27.6	42.9	15.3	55.5
313.15		4.6	6.4	1.8	39.0
323.15		6.7	9.6	2.9	42.8
333.15		9.7	13.9	4.2	43.5
343.15		13.6	19.7	6.1	45.1
353.15	0.5043	18.9	27.3	8.4	44.6
363.15		25.6	37.1	11.5	44.8
373.15		34.4	49.3	14.9	43.3
383.15		44.9	64.4	19.5	43.4
393.15		58.3	82.7	24.4	41.9
313.15		6.7	8.0	1.3	18.8
323.15		10.0	12.1	2.1	20.8
333.15		14.6	17.8	3.2	22.0
343.15		20.9	25.6	4.7	22.3
353.15	0.7526	29.3	35.8	6.5	22.3
363.15		40.1	49.2	9.1	22.6
373.15		54.2	66.1	11.9	22.0
383.15		71.5	87.4	15.9	22.2
393.15		93.5	113.5	20.0	21.4

Ethylbenzene + n-C$_{20}$

323.15		1.8	1.9	0.1	7.2
333.15		2.5	2.9	0.4	16.9

343.15		3.4	4.3	0.9	26.4
353.15		4.7	6.2	1.5	31.0
363.15	0.2511	6.5	8.6	2.1	32.5
373.15		8.8	11.8	3.0	34.0
383.15		11.7	15.8	4.1	35.3
393.15		15.5	20.9	5.4	34.5
323.15		3.1	3.5	0.4	12.5
333.15		4.5	5.3	0.8	18.2
343.15		6.4	7.9	1.5	23.1
353.15		9.1	11.4	2.3	25.0
363.15	0.5015	12.8	16.0	3.2	25.2
373.15		17.6	22.1	4.5	25.5
383.15		23.7	29.8	6.1	25.9
393.15		31.5	39.6	8.1	25.7
323.15		4.3	4.4	0.1	3.3
333.15		6.4	6.9	0.5	7.1
343.15		9.4	10.3	0.9	9.2
353.15		13.5	15.0	1.5	10.9
363.15	0.7502	19.1	21.3	2.2	11.6
373.15		26.4	29.7	3.3	12.4
383.15		36.0	40.5	4.5	12.4
393.15		48.2	54.2	6.0	12.4

<div align="center">n-Propylbenzene + n-C$_{20}$</div>

333.15		1.4	1.1	0.3	18.1
343.15		1.9	1.8	0.1	7.2
353.15		2.6	2.6	0.0	1.4
363.15	0.2512	3.6	3.8	0.2	6.6
373.15		4.9	5.5	0.6	11.3
383.15		6.7	7.6	0.9	13.1
393.15		8.8	10.3	1.5	17.3
333.15		2.3	2.1	0.2	9.2
343.15		3.3	3.2	0.1	2.0
353.15	0.4999	4.7	4.9	0.2	3.5
363.15		6.6	7.1	0.5	7.9
373.15		9.3	10.2	0.9	9.4
383.15		12.8	14.2	1.4	11.1
393.15		17.3	19.5	2.2	12.6
333.15		3.1	2.8	0.3	11.1
343.15		4.5	4.3	0.2	4.3
353.15		6.6	6.5	0.1	1.1
363.15		9.5	9.6	0.1	1.4
373.15	0.7500	13.4	13.9	0.5	3.5
383.15		18.8	19.5	0.7	3.9
393.15		25.6	26.9	1.3	5.3

<div align="center">p-Xylene + n-C$_{20}$</div>

323.15		1.6	1.6	0.0	2.0

333.15		2.3	2.5	0.2	8.6
343.15		3.1	3.7	0.6	19.8
353.15		4.3	5.4	1.1	24.9
363.15	0.2515	6.0	7.6	1.6	26.5
373.15		8.1	10.5	2.4	29.3
383.15		10.9	14.2	3.3	30.0
393.15		14.4	18.8	4.4	30.7
323.15		2.8	3.0	0.2	5.6
333.15		4.0	4.6	0.6	13.9
343.15		5.8	6.8	1.0	17.6
353.15	0.4991	8.3	9.9	1.6	19.7
363.15		11.6	14.1	2.5	21.7
373.15		16.1	19.6	3.5	21.9
383.15		21.7	26.7	4.9	22.5
393.15		29.0	35.7	6.7	23.0
323.15		3.9	3.8	0.1	1.4
333.15		5.8	6.0	0.2	3.3
343.15		8.5	9.1	0.6	6.6
353.15	0.7503	12.3	13.3	1.0	8.3
363.15		17.4	19.1	1.7	9.8
373.15		24.3	26.8	2.5	10.3
383.15		33.3	36.8	3.5	10.5
393.15		44.7	49.6	4.9	10.9

Benzene + n-C$_{24}$

333.15		10.7	23.7	13.0	121.1
343.15	0.2623	15.2	31.5	16.3	107.5
353.15		21.0	41.2	20.2	96.4
363.15		28.1	53.0	24.9	88.4
373.15		36.7	66.9	30.2	82.3
383.15		47.3	83.2	35.9	76.0
393.15		59.5	102.1	42.6	71.6
333.15	0.5212	24.0	44.2	20.2	84.1
343.15		33.8	59.4	25.6	75.7
353.15		45.9	78.3	32.4	70.5
363.15		61.3	101.3	40.0	65.2
373.15		79.7	128.9	49.2	61.8
333.15	0.7637	38.2	53.4	15.2	39.9
343.15		53.5	74.5	21.0	39.3
353.15		72.9	101.7	28.8	39.6

Toluene + n-C$_{24}$

333.15	0.2508	2.8	8.0	5.2	186.4
343.15		4.7	11.2	6.5	138.9
353.15		7.1	15.4	8.3	116.4
363.15		10.3	20.6	10.3	100.0
373.15		14.3	27.1	12.8	89.4
383.15		19.3	35.0	15.7	81.3

393.15		25.3	44.5	19.2	75.8
333.15	0.5008	8.4	14.8	6.4	76.4
343.15		12.3	20.9	8.6	70.0
353.15		16.6	28.8	12.2	73.7
363.15		23.4	38.9	15.5	66.3
373.15		32.1	51.5	19.4	60.5
383.15		42.6	67.1	24.5	57.4
393.15		55.9	85.8	29.9	53.6
333.15	0.7504	13.4	18.7	5.3	39.4
343.15		19.7	27.2	7.5	37.9
353.15		28.0	37.9	9.9	35.4
363.15		37.9	51.8	13.9	36.7
373.15		51.7	69.4	17.7	34.3
383.15		69.6	91.3	21.7	31.2
393.15		91.2	118.3	27.1	29.7
Ethylbenzene + n-C$_{24}$					
333.15	0.2557	2.5	3.3	0.8	30.8
343.15		3.0	4.8	1.8	59.3
353.15		4.3	6.8	2.5	58.3
363.15		6.0	9.5	3.5	57.9
373.15		8.7	12.9	4.2	48.3
383.15		10.8	17.2	6.4	59.5
393.15		13.8	22.6	8.8	63.7
333.15		3.9	5.9	2.0	51.1
343.15		5.8	8.7	2.9	49.6
353.15		8.5	12.5	4.0	46.5
363.15	0.5051	11.7	17.4	5.7	49.1
373.15		16.6	23.9	7.3	44.1
383.15		22.1	32.2	10.1	45.5
393.15		30.5	42.5	12.0	39.2
333.15	0.7520	5.9	7.4	1.5	26.0
343.15		8.8	11.1	2.3	25.9
353.15		12.3	16.1	3.8	30.8
363.15		17.8	22.8	5.0	28.1
373.15		25.0	31.6	6.6	26.4
383.15		34.5	42.9	8.4	24.4
393.15		46.3	57.3	11.0	23.7
n-Propylbenzene + n-C$_{24}$					
343.15	0.2519	1.4	2.0	0.6	45.0
353.15		2.0	3.0	1.0	50.4
363.15		2.8	4.3	1.5	55.0
373.15		4.2	6.1	1.9	45.7
383.15		5.7	8.4	2.7	48.0
393.15		7.9	11.4	3.5	44.4
343.15	0.4542	2.5	3.4	0.9	36.3
353.15		3.6	5.1	1.5	41.0

363.15		5.2	7.4	2.2	41.6
373.15		7.6	10.4	2.8	37.3
383.15		10.5	14.5	4.0	37.7
393.15		14.6	19.6	5.0	34.6
343.15	0.7593	4.0	4.7	0.7	18.3
353.15		6.1	7.1	1.0	17.0
363.15		8.9	10.5	1.6	17.9
373.15		12.9	15.0	2.1	16.6
383.15		18.0	21.1	3.1	17.2
393.15		25.0	29.0	4.0	15.9
p-Xylene + n-C_{24}					
333.15	0.2648	2.3	3.0	0.7	31.2
343.15		2.7	4.4	1.7	64.6
353.15		3.9	6.4	2.5	63.5
363.15		5.6	8.9	3.3	59.5
373.15		7.7	12.2	4.5	58.9
383.15		10.5	16.4	5.9	56.5
393.15		13.5	21.7	8.2	60.5
333.15	0.5014	3.5	5.2	1.7	49.4
343.15		5.1	7.8	2.7	52.2
353.15		7.7	11.2	3.5	45.6
363.15		10.9	15.8	4.9	45.1
373.15		15.2	21.8	6.6	43.5
383.15		20.7	29.5	8.8	42.4
393.15		27.7	39.1	11.4	41.2
333.15	0.7509	5.3	6.6	1.3	25.2
343.15		8.0	10.0	2.0	24.5
353.15		11.8	14.6	2.8	23.4
363.15		16.8	20.8	4.0	23.7
373.15		23.6	29.0	5.4	22.8
383.15		32.3	39.6	7.3	22.6
393.15		43.7	53.1	9.4	21.5
Benzene + n-C_{28}					
353.15	0.2885	19.7	45.9	26.2	133.1
363.15		27.9	59.0	31.1	111.3
373.15		36.7	74.5	37.8	102.9
383.15		48.4	92.7	44.3	91.5
393.15		61.1	113.7	52.6	86.1
353.15	0.5177	39.1	79.5	40.4	103.4
363.15		53.7	102.8	49.1	91.4
373.15		70.4	130.7	60.3	85.6
383.15		91.0	163.6	72.6	79.8
353.15	0.7614	66.3	102.0	35.7	53.8
363.15		90.0	136.6	46.6	51.8
Toluene + n-C_{28}					
353.15	0.2981	8.5	18.4	9.9	117.0

363.15		12.1	24.7	12.6	104.4
373.15		16.6	32.5	15.9	96.0
383.15		22.0	42.0	20.0	91.1
393.15		28.7	53.5	24.8	86.3
353.15	0.5018	15.7	29.6	13.9	88.7
363.15		21.9	39.9	18.0	82.3
373.15		29.9	52.8	22.9	76.6
383.15		39.9	68.6	28.7	72.0
393.15		52.3	87.7	35.4	67.8
353.15	0.7598	26.5	38.9	12.4	46.9
363.15		36.9	53.8	16.9	45.7
373.15		50.4	71.9	21.5	42.7
383.15		67.4	94.6	27.2	40.3
393.15		88.6	122.3	33.7	38.0

Ethylbenzene + n-C$_{28}$

353.15	0.2584	3.4	7.0	3.6	106.1
363.15		4.9	9.7	4.8	98.9
373.15		7.1	13.3	6.2	86.8
383.15		9.7	17.7	8.0	82.4
393.15		13.0	23.2	10.2	78.3
353.15		7.4	12.8	5.4	73.1
363.15	0.5055	10.7	17.9	7.2	67.5
373.15		15.0	24.5	9.5	63.6
383.15		20.4	32.9	12.5	61.5
393.15		27.5	43.4	15.9	57.9
353.15	0.7510	11.8	16.6	4.8	40.9
363.15		17.1	23.5	6.4	37.5
373.15		24.1	32.5	8.4	35.0
383.15		33.0	44.1	11.1	33.7
393.15		44.5	58.7	14.2	32.0

n-Propylbenzene + n-C$_{28}$

363.15	0.2554	2.6	4.5	1.9	72.5
373.15		3.7	6.3	2.6	70.7
383.15		5.2	8.7	3.5	67.4
393.15		7.3	11.8	4.5	61.1
353.15	0.5127	3.7	5.8	2.1	55.6
363.15		5.5	8.4	2.9	51.9
373.15		7.9	11.8	3.9	49.9
383.15		11.2	16.4	5.2	46.6
393.15		15.4	22.3	6.9	44.9
353.15	0.7525	5.7	7.3	1.6	28.9
363.15		8.4	10.8	2.4	28.2
373.15		12.2	15.4	3.2	26.3
383.15		17.2	21.6	4.4	25.4
393.15		23.9	29.6	5.7	23.8

p-Xylene + n-C$_{28}$

353.15	0.2897	3.5	7.0	3.5	101.1
363.15		5.2	9.9	4.7	89.6
373.15		7.5	13.5	6.0	80.1
383.15		10.3	18.1	7.8	76.1
393.15		13.8	23.9	10.1	73.3
353.15	0.4985	6.7	11.4	4.7	70.3
363.15		9.8	16.1	6.3	64.0
373.15		12.9	22.1	9.2	71.6
383.15		19.0	29.9	10.9	57.3
393.15		25.4	39.6	14.2	56.0
353.15	0.7536	11.0	15.0	4.0	36.5
363.15		15.9	21.4	5.5	34.5
373.15		22.5	29.8	7.3	32.3
383.15		31.0	40.6	9.6	31.0
393.15		41.9	54.4	12.5	29.8
AAD (kPa)				9.5	
AAPD (%)					44.8

Table 4.5 Experimental data vs. calculated outcomes from SRK EOS with $k_{ij} = 0$

Temperature (K) ±0.1K	Aromatic Mole Fraction $x \pm 0.0001$	Bubble Pressure(kPa)		Deviation	
		Experimental Uncertainty ± 1kPa	Calculated from PR EOS with $k_{ij} = 0$	Absolute Deviation (kPa)	Absolute Percent Deviation (%)
Benzene + n-C_{20}					
313.15		6.4	9.7	3.3	51.7
323.15		9.0	13.8	4.8	53.1
333.15		12.4	19.1	6.7	53.7
343.15	0.2555	16.8	25.8	9.0	53.5
353.15		22.4	34.2	11.8	52.5
363.15		29.2	44.4	15.2	52.0
313.15		12.8	18.1	5.3	41.2
323.15		18.1	25.8	7.7	42.8
333.15		25.4	36.0	10.6	41.9
343.15	0.5083	34.7	49.1	14.3	41.2
353.15		46.6	65.6	19.0	40.7
363.15		61.2	85.9	24.7	40.3
313.15		19.5	23.6	4.1	21.0
323.15		28.1	34.2	6.1	21.7
333.15		39.5	48.3	8.8	22.3
343.15	0.7593	54.4	66.7	12.3	22.6
353.15		73.6	90.1	16.5	22.4

363.15		97.4	119.4	22.0	22.5

Toluene + n-C$_{20}$					
313.15		2.5	3.0	0.5	18.3
323.15		3.5	4.5	1.0	27.3
333.15		4.9	6.5	1.6	32.9
343.15		6.8	9.3	2.5	36.3
353.15	0.2514	9.3	12.9	3.6	38.5
363.15		12.4	17.5	5.1	41.2
373.15		16.5	23.3	6.8	41.3
383.15		21.3	30.5	9.2	43.1
393.15		27.6	39.2	11.6	42.0
313.15		4.6	5.5	0.9	18.7
323.15		6.7	8.3	1.6	23.7
333.15		9.7	12.2	2.5	25.9
343.15		13.6	17.5	3.9	28.8
353.15	0.5043	18.9	24.5	5.6	29.7
363.15		25.6	33.6	8.0	31.1
373.15		34.4	45.0	10.6	30.8
383.15		44.9	59.2	14.3	31.9
393.15		58.3	76.6	18.3	31.5
313.15		6.7	7.1	0.4	5.4
323.15		10.0	10.9	0.9	8.5
333.15		14.6	16.2	1.6	10.8
343.15		20.9	23.5	2.6	12.3
353.15	0.7526	29.3	33.2	3.9	13.3
363.15		40.1	45.9	5.8	14.5
373.15		54.2	62.2	8.0	14.8
383.15		71.5	82.7	11.2	15.7
393.15		93.5	108.1	14.6	15.6

Ethylbenzene + n-C$_{20}$					
323.15		1.8	1.7	0.1	7.3
333.15		2.5	2.6	0.1	2.3
343.15		3.4	3.8	0.4	11.9
353.15		4.7	5.5	0.8	17.3
363.15	0.2511	6.5	7.8	1.3	19.8
373.15		8.8	10.8	2.0	22.2
383.15		11.7	14.6	2.9	24.4
393.15		15.5	19.3	3.8	24.6
323.15		3.1	3.1	0.0	1.1
333.15		4.5	4.7	0.2	5.2
343.15		6.4	7.1	0.7	10.8
353.15		9.1	10.3	1.2	13.7
363.15	0.5015	12.8	14.7	1.9	14.9
373.15		17.6	20.4	2.8	16.2
383.15		23.7	27.8	4.1	17.4
393.15		31.5	37.2	5.7	18.0

323.15		4.3	4.0	0.3	6.6
333.15		6.4	6.3	0.1	2.0
343.15		9.4	9.5	0.1	1.0
353.15		13.5	14.0	0.5	3.5
363.15	0.7502	19.1	20.1	1.0	5.0
373.15		26.4	28.1	1.7	6.5
383.15		36.0	38.6	2.6	7.3
393.15		48.2	52.0	3.8	7.9

n-Propylbenzene + n-C$_{20}$

333.15		1.4	1.0	0.4	25.8
343.15		1.9	1.6	0.3	15.0
353.15		2.6	2.4	0.2	6.3
363.15	0.2512	3.6	3.6	0.0	0.7
373.15		4.9	5.1	0.2	4.5
383.15		6.7	7.2	0.5	6.9
393.15		8.8	9.8	1.0	11.6
333.15		2.3	1.9	0.4	17.1
343.15		3.3	3.0	0.3	9.6
353.15	0.4999	4.7	4.5	0.2	3.6
363.15		6.6	6.7	0.1	1.4
373.15		9.3	9.6	0.3	3.6
383.15		12.8	13.6	0.8	5.9
393.15		17.3	18.7	1.4	7.9
333.15		3.1	2.5	0.6	18.0
343.15		4.5	4.0	0.5	10.8
353.15		6.6	6.1	0.5	6.9
363.15		9.5	9.1	0.4	3.7
373.15	0.7500	13.4	13.3	0.1	0.9
383.15		18.8	18.8	0.0	0.1
393.15		25.6	26.1	0.5	2.0

p-Xylene + n-C$_{20}$

323.15		1.6	1.5	0.1	7.7
333.15		2.3	2.3	0.0	0.7
343.15		3.1	3.4	0.3	10.5
353.15		4.3	5.0	0.7	16.3
363.15	0.2515	6.0	7.1	1.1	18.5
373.15		8.1	9.9	1.8	22.0
383.15		10.9	13.5	2.6	23.4
393.15		14.4	18.0	3.6	24.7
323.15		2.8	2.7	0.1	3.6
333.15		4.0	4.2	0.2	5.1
343.15		5.8	6.4	0.6	9.5
353.15	0.4991	8.3	9.3	1.0	12.4
363.15		11.6	13.4	1.8	15.1
373.15		16.1	18.7	2.6	16.0
383.15		21.7	25.6	3.8	17.3

393.15		29.0	34.3	5.3	18.4
323.15		3.9	3.6	0.3	8.9
333.15		5.8	5.6	0.2	3.5
343.15		8.5	8.5	0.0	0.5
353.15	0.7503	12.3	12.7	0.4	3.0
363.15		17.4	18.3	0.9	5.2
373.15		24.3	25.8	1.5	6.3
383.15		33.3	35.7	2.4	7.2
393.15		44.7	48.3	3.6	8.1

Benzene + n-C$_{24}$

333.15		10.7	21.7	11.0	103.1
343.15	0.2623	15.2	29.1	13.9	91.7
353.15		21.0	38.3	17.3	82.2
363.15		28.1	49.4	21.3	75.6
373.15		36.7	62.6	25.9	70.5
383.15		47.3	78.1	30.8	65.1
393.15		59.5	96.1	36.6	61.5
333.15	0.5212	24.0	41.0	17.0	70.9
343.15		33.8	55.4	21.6	64.0
353.15		45.9	73.4	27.5	59.9
363.15		61.3	95.4	34.1	55.6
373.15		79.7	121.9	42.2	52.9
333.15	0.7637	38.2	52.1	13.9	36.5
343.15		53.5	73.1	19.6	36.7
353.15		72.9	98.2	25.3	34.7

Toluene + n-C$_{24}$

333.15	0.2508	2.8	7.3	4.5	162.1
343.15		4.7	10.3	5.6	120.2
353.15		7.1	14.3	7.2	100.7
363.15		10.3	19.2	8.9	86.5
373.15		14.3	25.4	11.1	77.5
383.15		19.3	32.9	13.6	70.6
393.15		25.3	42.0	16.7	66.1
333.15	0.5008	8.4	13.7	5.3	63.0
343.15		12.3	19.5	7.2	58.2
353.15		16.6	27.0	10.4	62.6
363.15		23.4	36.6	13.2	56.6
373.15		32.1	48.8	16.7	51.9
383.15		42.6	63.7	21.1	49.6
393.15		55.9	81.9	26.0	46.5
333.15	0.7504	13.4	17.9	4.5	33.3
343.15		19.7	25.7	6.0	30.5
353.15		28.0	36.1	8.1	29.0
363.15		37.9	49.6	11.7	30.9
373.15		51.7	66.8	15.1	29.3
383.15		69.6	88.3	18.7	26.9

393.15		91.2	114.8	23.6	25.9

Ethylbenzene + n-C$_{24}$					
333.15	0.2557	2.5	3.0	0.5	18.8
343.15		3.0	4.4	1.4	46.0
353.15		4.3	6.3	2.0	46.2
363.15		6.0	8.8	2.8	46.7
373.15		8.7	12.1	3.4	38.6
383.15		10.8	16.2	5.4	49.9
393.15		13.8	21.3	7.5	54.6
333.15		3.9	5.4	1.5	38.6
343.15		5.8	8.0	2.2	38.4
353.15		8.5	11.6	3.1	36.5
363.15	0.5051	11.7	16.4	4.7	39.9
373.15		16.6	22.6	6.0	36.0
383.15		22.1	30.5	8.4	38.1
393.15		30.5	40.5	10.0	32.8
333.15	0.7520	5.9	6.9	1.0	17.2
343.15		8.8	10.4	1.6	18.2
353.15		12.3	15.2	2.9	23.7
363.15		17.8	21.7	3.9	22.0
373.15		25.0	30.3	5.3	21.1
383.15		34.5	41.4	6.9	19.9
393.15		46.3	55.5	9.2	19.8

n-Propylbenzene + n-C$_{24}$					
343.15	0.2519	1.4	1.8	0.4	31.8
353.15		2.0	2.8	0.8	37.9
363.15		2.8	4.0	1.2	43.3
373.15		4.2	5.7	1.5	35.6
383.15		5.7	7.9	2.2	38.7
393.15		7.9	10.7	2.8	36.0
343.15	0.4542	2.5	3.1	0.6	24.7
353.15		3.6	4.7	1.1	30.1
363.15		5.2	6.9	1.7	31.8
373.15		7.6	9.8	2.2	28.7
383.15		10.5	13.6	3.1	30.0
393.15		14.6	18.6	4.0	27.7
343.15	0.7593	4.0	4.4	0.4	9.8
353.15		6.1	6.7	0.6	9.7
363.15		8.9	9.9	1.0	11.4
373.15		12.9	14.3	1.4	11.0
383.15		18.0	20.2	2.2	12.3
393.15		25.0	27.9	2.9	11.8

p-Xylene + n-C$_{24}$					
333.15	0.2648	2.3	2.7	0.4	19.1
343.15		2.7	4.1	1.4	50.7
353.15		3.9	5.9	2.0	50.9

363.15		5.6	8.3	2.7	48.2
373.15		7.7	11.4	3.7	48.7
383.15		10.5	15.5	5.0	47.2
393.15		13.5	20.5	7.0	51.7
333.15	0.5014	3.5	4.8	1.3	36.8
343.15		5.1	7.2	2.1	40.6
353.15		7.7	10.4	2.7	35.6
363.15		10.9	14.8	3.9	36.0
373.15		15.2	20.6	5.4	35.4
383.15		20.7	28.0	7.3	35.2
393.15		27.7	37.3	9.6	34.7
333.15	0.7509	5.3	6.2	0.9	16.2
343.15		8.0	9.3	1.3	16.7
353.15		11.8	13.8	2.0	16.7
363.15		16.8	19.8	3.0	17.7
373.15		23.6	27.8	4.2	17.6
383.15		32.3	38.2	5.9	18.1
393.15		43.7	51.4	7.7	17.7
Benzene + n-C$_{28}$					
353.15	0.2885	19.7	42.6	22.9	116.2
363.15		27.9	54.9	27.0	96.8
373.15		36.7	69.6	32.9	89.6
383.15		48.4	86.8	38.4	79.4
393.15		61.1	106.8	45.7	74.8
353.15	0.5177	39.1	74.4	35.3	90.3
363.15		53.7	96.5	42.8	79.7
373.15		70.4	123.1	52.7	74.9
383.15		91.0	154.6	63.6	69.9
353.15	0.7614	66.3	100.7	34.4	51.8
363.15		90.0	132.4	42.4	47.1
Toluene + n-C$_{28}$					
353.15	0.2981	8.5	17.1	8.6	101.3
363.15		12.1	23.1	11.0	90.5
373.15		16.6	30.5	13.9	83.5
383.15		22.0	39.5	17.5	79.6
393.15		28.7	50.4	21.7	75.7
353.15	0.5018	15.7	27.7	12.0	76.3
363.15		21.9	37.5	15.6	71.3
373.15		29.9	49.8	19.9	66.6
383.15		39.9	65.0	25.1	62.9
393.15		52.3	83.4	31.1	59.5
353.15	0.7598	26.5	37.5	11.0	41.4
363.15		36.9	51.4	14.5	39.3
373.15		50.4	69.1	18.7	37.1
383.15		67.4	91.2	23.8	35.3
393.15		88.6	118.4	29.8	33.6

Ethylbenzene + n-C$_{28}$					
353.15	0.2584	3.4	6.5	3.1	90.3
363.15		4.9	9.0	4.1	84.7
373.15		7.1	12.4	5.3	74.4
383.15		9.7	16.6	6.9	71.2
393.15		13.0	21.8	8.8	68.1
353.15		7.4	11.9	4.5	61.1
363.15	0.5055	10.7	16.8	6.1	56.9
373.15		15.0	23.1	8.1	54.1
383.15		20.4	31.2	10.8	52.9
393.15		27.5	41.3	13.8	50.2
353.15	0.7510	11.8	15.7	3.9	33.0
363.15		17.1	22.3	5.2	30.7
373.15		24.1	31.1	7.0	29.1
383.15		33.0	42.4	9.4	28.5
393.15		44.5	56.7	12.2	27.5
n-Propylbenzene + n-C$_{28}$					
363.15	0.2554	2.6	4.1	1.5	59.4
373.15		3.7	5.9	2.2	58.8
383.15		5.2	8.1	2.9	56.7
393.15		7.3	11.1	3.8	51.5
353.15	0.5127	3.7	5.3	1.6	43.8
363.15		5.5	7.8	2.3	41.5
373.15		7.9	11.1	3.2	40.6
383.15		11.2	15.5	4.3	38.4
393.15		15.4	21.2	5.8	37.5
353.15	0.7525	5.7	6.9	1.2	20.6
363.15		8.4	10.2	1.8	21.0
373.15		12.2	14.6	2.4	20.0
383.15		17.2	20.6	3.4	19.9
393.15		23.9	28.5	4.6	19.1
p-Xylene + n-C$_{28}$					
353.15	0.2897	3.5	6.5	3.0	85.7
363.15		5.2	9.2	4.0	76.2
373.15		7.5	12.6	5.1	68.4
383.15		10.3	17.0	6.7	65.5
393.15		13.8	22.6	8.8	63.5
353.15	0.4985	6.7	10.6	3.9	58.5
363.15		9.8	15.1	5.3	53.6
373.15		12.9	20.9	8.0	61.7
383.15		19.0	28.3	9.3	49.0
393.15		25.4	37.7	12.3	48.3
353.15	0.7536	11.0	14.2	3.2	28.8
363.15		15.9	20.3	4.4	27.8
373.15		22.5	28.5	6.0	26.5
383.15		31.0	39.1	8.1	26.0

393.15		41.9	52.5	10.6	25.4
AAD (kPa)				7.9	
AAPD (%)					36.1

Table 4.6 Experimental data vs. calculated outcomes from PC-SAFT with $k_{ij} = 0$

Temperature (K) ±0.1K	Aromatic Mole Fraction $x \pm 0.0001$	Bubble Pressure(kPa)		Deviation	
		Experimental Uncertainty ± 1kPa	Calculated from PR EOS with $k_{ij} = 0$	Absolute Deviation (kPa)	Absolute Percent Deviation (%)
Benzene + n-C$_{20}$					
313.15		6.4	4.9	1.5	23.44
323.15		9.0	7.2	1.8	20.00
333.15		12.4	10.2	2.2	17.74
343.15	0.2555	16.8	14	2.8	16.67
353.15		22.4	19	3.4	15.18
363.15		29.2	25.2	4	13.70
313.15		12.8	10.9	1.9	14.84
323.15		18.1	15.9	2.2	12.15
333.15		25.4	22.6	2.8	11.02
343.15	0.5083	34.7	31.4	3.4	9.77
353.15		46.6	42.6	4	8.58
363.15		61.2	56.7	4.5	7.35
313.15		19.5	17.8	1.7	8.72
323.15		28.1	26.1	2	7.12
333.15		39.5	37.4	2.1	5.32
343.15	0.7593	54.4	52.2	2.2	4.04
353.15		73.6	71.4	2.2	2.99
363.15		97.4	95.5	1.9	1.95
Toluene + n-C$_{20}$					
313.15		2.5	1.7	0.8	32.00
323.15		3.5	2.6	0.9	25.71
333.15		4.9	3.8	1.1	22.45
343.15		6.8	5.6	1.2	17.65
353.15	0.2514	9.3	7.9	1.4	15.05
363.15		12.4	10.9	1.5	12.10
373.15		16.5	14.7	1.8	10.91
383.15		21.3	19.5	1.8	8.45
393.15		27.6	25.4	2.2	7.97
313.15		4.6	3.6	1	21.74
323.15		6.7	5.6	1.1	16.42
333.15		9.7	8.4	1.3	13.40
343.15		13.6	12.2	1.4	10.29

353.15	0.5043	18.9	17.3	1.6	8.47
363.15		25.6	24	1.6	6.25
373.15		34.4	32.6	1.8	5.23
383.15		44.9	43.4	1.5	3.34
393.15		58.3	56.8	1.5	2.57
313.15		6.7	5.8	0.9	13.43
323.15		10.0	9	1	10.00
333.15		14.6	13.5	1.1	7.53
343.15		20.9	19.7	1.2	5.74
353.15	0.7526	29.3	28.1	1.2	4.10
363.15		40.1	39.2	0.9	2.24
373.15		54.2	53.4	0.8	1.48
383.15		71.5	71.4	0.1	0.14
393.15		93.5	93.7	0.2	0.21

Ethylbenzene + n-C_{20}

323.15		1.8	1	0.8	44.44
333.15		2.5	1.6	0.9	36.00
343.15		3.4	2.4	1	29.41
353.15		4.7	3.6	1.1	23.40
363.15	0.2511	6.5	5.1	1.4	21.54
373.15		8.8	7.2	1.6	18.18
383.15		11.7	9.8	1.9	16.24
393.15		15.5	13.2	2.3	14.84
323.15		3.1	2.2	0.9	29.03
333.15		4.5	3.4	1.1	24.44
343.15		6.4	5.2	1.2	18.75
353.15		9.1	7.7	1.4	15.38
363.15	0.5015	12.8	11	1.8	14.06
373.15		17.6	15.5	2.1	11.93
383.15		23.7	21.3	2.4	10.13
393.15		31.5	28.7	2.8	8.89
323.15		4.3	3.4	0.9	20.93
333.15		6.4	5.4	1	15.63
343.15		9.4	8.3	1.1	11.70
353.15		13.5	12.2	1.3	9.63
363.15	0.7502	19.1	17.6	1.5	7.85
373.15		26.4	24.8	1.6	6.06
383.15		36.0	34.2	1.8	5.00
393.15		48.2	46.2	2	4.15

n-Propylbenzene + n-C_{20}

333.15		1.4	0.7	0.7	50.00
343.15		1.9	1.1	0.8	42.11
353.15		2.6	1.7	0.9	34.62
363.15	0.2512	3.6	2.5	1.1	30.56
373.15		4.9	3.6	1.3	26.53
383.15		6.7	5.2	1.5	22.39

393.15		8.8	7.1	1.7	19.32
333.15		2.3	1.5	0.8	34.78
343.15		3.3	2.3	1	30.30
353.15	0.4999	4.7	3.6	1.1	23.40
363.15		6.6	5.3	1.3	19.70
373.15		9.3	7.7	1.6	17.20
383.15		12.8	11	1.8	14.06
393.15		17.3	15.2	2.1	12.14
333.15		3.1	2.3	0.8	25.81
343.15		4.5	3.7	0.8	17.78
353.15		6.6	5.6	1	15.15
363.15		9.5	8.4	1.1	11.58
373.15	0.7500	13.4	12.2	1.2	8.96
383.15		18.8	17.4	1.4	7.45
393.15		25.6	24.1	1.5	5.86

p-Xylene + n-C_{20}

323.15		1.6	0.9	0.7	43.75
333.15		2.3	1.5	0.8	34.78
343.15		3.1	2.2	0.9	29.03
353.15		4.3	3.3	1	23.26
363.15	0.2515	6.0	4.8	1.2	20.00
373.15		8.1	6.7	1.4	17.28
383.15		10.9	9.3	1.6	14.68
393.15		14.4	12.5	1.9	13.19
323.15		2.8	2	0.8	28.57
333.15		4.0	3.1	0.9	22.50
343.15		5.8	4.8	1	17.24
353.15	0.4991	8.3	7.1	1.2	14.46
363.15		11.6	10.2	1.4	12.07
373.15		16.1	14.4	1.7	10.56
383.15		21.7	19.9	1.9	8.72
393.15		29.0	26.9	2.1	7.24
323.15		3.9	3.2	0.7	17.95
333.15		5.8	5	0.8	13.79
343.15		8.5	7.6	0.9	10.59
353.15	0.7503	12.3	11.4	0.9	7.32
363.15		17.4	16.4	1	5.75
373.15		24.3	23.3	1	4.12
383.15		33.3	32.2	1.1	3.30
393.15		44.7	43.6	1.1	2.46

Benzene + n-C_{24}

333.15		10.7	9.7	1	9.35
343.15	0.2623	15.2	13.4	1.8	11.84
353.15		21.0	18.2	2.8	13.33
363.15		28.1	24.1	4	14.23
373.15		36.7	31.3	5.4	14.71

383.15		47.3	40.1	7.2	15.22
393.15		59.5	50.6	8.9	14.96
333.15	0.5212	24.0	22.2	1.8	7.50
343.15		33.8	30.8	3	8.88
353.15		45.9	41.8	4.1	8.93
363.15		61.3	55.7	5.6	9.14
373.15		79.7	72.8	6.9	8.66
333.15	0.7637	38.2	37	1.2	3.14
343.15		53.5	51.6	1.9	3.55
353.15		72.9	70.5	2.4	3.29

Toluene + n-C$_{24}$

333.15	0.2508	2.8	3.5	0.7	25.00
343.15		4.7	5.1	0.4	8.51
353.15		7.1	7.3	0.2	2.82
363.15		10.3	10.1	0.2	1.94
373.15		14.3	13.6	0.7	4.90
383.15		19.3	18.1	1.2	6.22
393.15		25.3	23.6	1.7	6.72
333.15	0.5008	8.4	7.9	0.5	5.95
343.15		12.3	11.5	0.8	6.50
353.15		16.6	16.4	0.2	1.20
363.15		23.4	22.7	0.7	2.99
373.15		32.1	30.8	1.3	4.05
383.15		42.6	41	1.6	3.76
393.15		55.9	53.7	2.2	3.94
333.15	0.7504	13.4	13.2	0.2	1.49
343.15		19.7	19.3	0.4	2.03
353.15		28.0	27.5	0.5	1.79
363.15		37.9	38.3	0.4	1.06
373.15		51.7	52.2	0.5	0.97
383.15		69.6	69.7	0.1	0.14
393.15		91.2	91.6	0.4	0.44

Ethylbenzene + n-C$_{24}$

333.15	0.2557	2.5	1.5	1	40.00
343.15		3.0	2.3	0.7	23.33
353.15		4.3	3.4	0.9	20.93
363.15		6.0	4.8	1.2	20.00
373.15		8.7	6.8	1.9	21.84
383.15		10.8	9.3	1.5	13.89
393.15		13.8	12.5	1.3	9.42
333.15		3.9	3.3	0.6	15.38
343.15		5.8	5	0.8	13.79
353.15		8.5	7.4	1.1	12.94
363.15	0.5051	11.7	10.6	1.1	9.40
373.15		16.6	14.9	1.7	10.24
383.15		22.1	20.5	1.6	7.24

393.15		30.5	27.6	2.9	9.51
333.15	0.7520	5.9	5.3	0.6	10.17
343.15		8.8	8.1	0.7	7.95
353.15		12.3	12	0.3	2.44
363.15		17.8	17.4	0.4	2.25
373.15		25.0	24.4	0.6	2.40
383.15		34.5	33.7	0.8	2.32
393.15		46.3	45.5	0.8	1.73

n-Propylbenzene + n-C_{24}

343.15	0.2519	1.4	1	0.4	28.57
353.15		2.0	1.6	0.4	20.00
363.15		2.8	2.3	0.5	17.86
373.15		4.2	3.4	0.8	19.05
383.15		5.7	4.8	0.9	15.79
393.15		7.9	6.6	1.3	16.46
343.15	0.4542	2.5	2	0.5	20.00
353.15		3.6	3.1	0.5	13.89
363.15		5.2	4.5	0.7	13.46
373.15		7.6	6.6	1	13.16
383.15		10.5	9.3	1.2	11.43
393.15		14.6	12.9	1.7	11.64
343.15	0.7593	4.0	3.7	0.3	7.50
353.15		6.1	5.6	0.5	8.20
363.15		8.9	8.4	0.5	5.62
373.15		12.9	12.2	0.7	5.43
383.15		18.0	17.3	0.7	3.89
393.15		25.0	24.1	0.9	3.60

p-Xylene + n-C_{24}

333.15	0.2648	2.3	1.5	0.8	34.78
343.15		2.7	2.2	0.5	18.52
353.15		3.9	3.3	0.6	15.38
363.15		5.6	4.7	0.9	16.07
373.15		7.7	6.6	1.1	14.29
383.15		10.5	9.1	1.4	13.33
393.15		13.5	12.3	1.2	8.89
333.15	0.5014	3.5	3	0.5	14.29
343.15		5.1	4.6	0.5	9.80
353.15		7.7	6.8	0.9	11.69
363.15		10.9	9.8	1.1	10.09
373.15		15.2	13.9	1.3	8.55
383.15		20.7	19.1	1.6	7.73
393.15		27.7	25.9	1.8	6.50
333.15	0.7509	5.3	4.9	0.4	7.55
343.15		8.0	7.5	0.5	6.25
353.15		11.8	11.2	0.6	5.08
363.15		16.8	16.2	0.6	3.57

373.15		23.6	22.9	0.7	2.97
383.15		32.3	31.7	0.6	1.86
393.15		43.7	42.9	0.8	1.83

Benzene + n-C$_{28}$					
353.15	0.2885	19.7	18.6	1.1	5.58
363.15		27.9	24.6	3.3	11.83
373.15		36.7	32	4.7	12.81
383.15		48.4	40.9	7.5	15.50
393.15		61.1	51.5	9.6	15.71
353.15	0.5177	39.1	38.9	0.2	0.51
363.15		53.7	51.7	2	3.72
373.15		70.4	67.4	3	4.26
383.15		91.0	86.5	4.5	4.95
353.15	0.7614	66.3	68	1.7	2.56
363.15		90.0	90.9	0.9	1.00

Toluene + n-C$_{28}$					
353.15	0.2981	8.5	8.2	0.3	3.53
363.15		12.1	11.3	0.8	6.61
373.15		16.6	15.3	1.3	7.83
383.15		22.0	20.3	1.7	7.73
393.15		28.7	26.4	2.3	8.01
353.15	0.5018	15.7	15.5	0.2	1.27
363.15		21.9	21.5	0.4	1.83
373.15		29.9	29.1	0.8	2.68
383.15		39.9	38.7	1.2	3.01
393.15		52.3	50.5	1.8	3.44
353.15	0.7598	26.5	27.3	0.8	3.02
363.15		36.9	37.9	1	2.71
373.15		50.4	51.6	1.2	2.38
383.15		67.4	69	1.6	2.37
393.15		88.6	90.5	1.9	2.14

Ethylbenzene + n-C$_{28}$					
353.15	0.2584	3.4	3.2	0.2	5.88
363.15		4.9	4.6	0.3	6.12
373.15		7.1	6.4	0.7	9.86
383.15		9.7	8.7	1	10.31
393.15		13.0	11.7	1.3	10.00
353.15		7.4	7.1	0.3	4.05
363.15	0.5055	10.7	10.1	0.6	5.61
373.15		15.0	14.2	0.8	5.33
383.15		20.4	19.5	0.9	4.41
393.15		27.5	26.2	1.3	4.73
353.15	0.7510	11.8	11.8	0	0.00
363.15		17.1	17	0.1	0.58
373.15		24.1	23.9	0.2	0.83
383.15		33.0	32.9	0.1	0.30

393.15		44.5	44.4	0.1	0.22

n-Propylbenzene + n-C_{28}					
363.15	0.2554	2.6	2.2	0.4	15.38
373.15		3.7	3.2	0.5	13.51
383.15		5.2	4.6	0.6	11.54
393.15		7.3	6.3	1	13.70
353.15	0.5127	3.7	3.4	0.3	8.11
363.15		5.5	5	0.5	9.09
373.15		7.9	7.3	0.6	7.59
383.15		11.2	10.3	0.9	8.04
393.15		15.4	14.3	1.1	7.14
353.15	0.7525	5.7	5.5	0.2	3.51
363.15		8.4	8.2	0.2	2.38
373.15		12.2	11.9	0.3	2.46
383.15		17.2	16.8	0.4	2.33
393.15		23.9	23.4	0.5	2.09

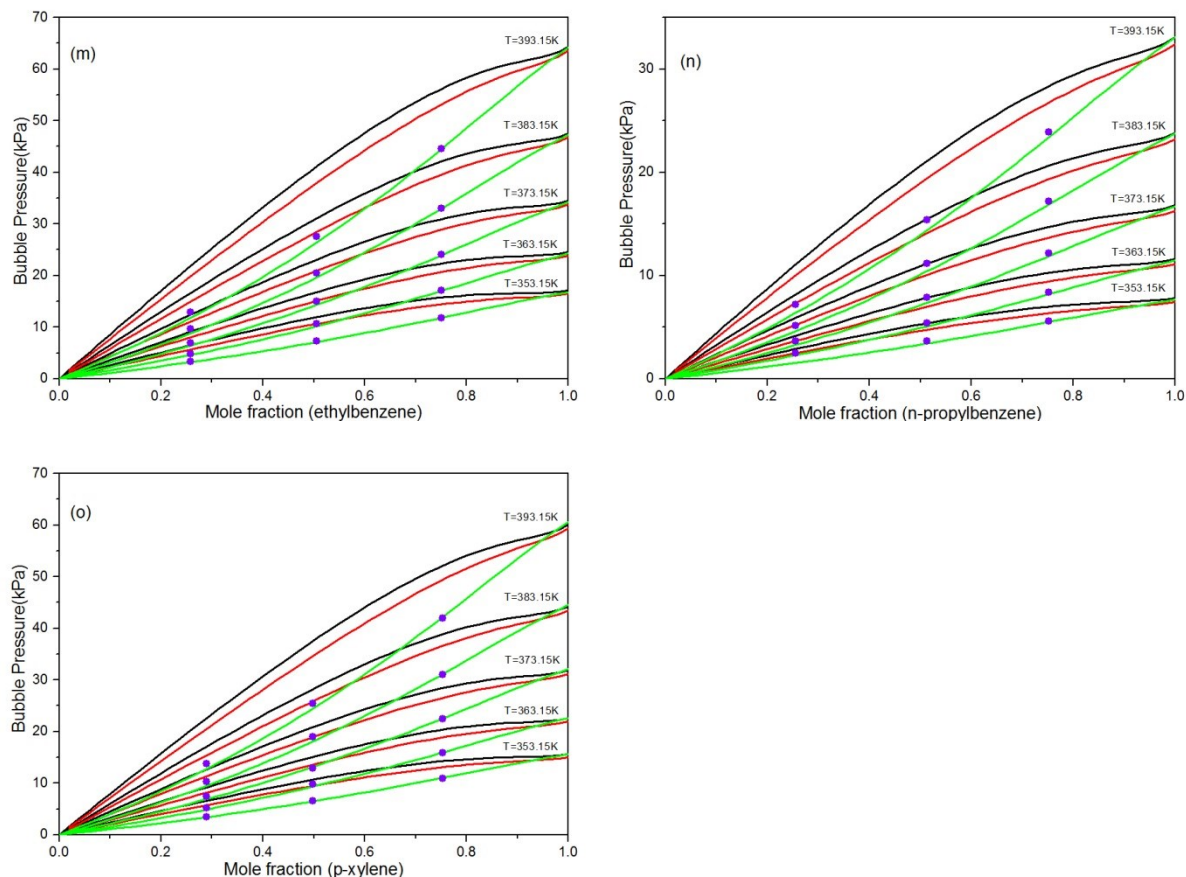| p-Xylene + n-C_{28}					
353.15	0.2897	3.5	3.4	0.1	2.86
363.15		5.2	4.9	0.3	5.77
373.15		7.5	6.8	0.7	9.33
383.15		10.3	9.4	0.9	8.74
393.15		13.8	12.7	1.1	7.97
353.15	0.4985	6.7	6.5	0.2	2.99
363.15		9.8	9.3	0.5	5.10
373.15		12.9	13.1	0.2	1.55
383.15		19.0	18	1.0	5.26
393.15		25.4	24.4	1.0	3.94
353.15	0.7536	11.0	11	0.0	0.00
363.15		15.9	15.9	0.0	0.00
373.15		22.5	22.5	0.0	0.00
383.15		31.0	31.1	0.1	0.32
393.15		41.9	42.1	0.2	0.48
AAD (kPa)				1.3	
AAPD (%)					10.97

74
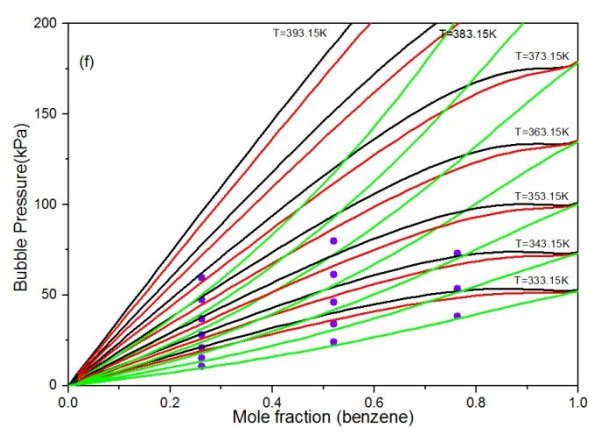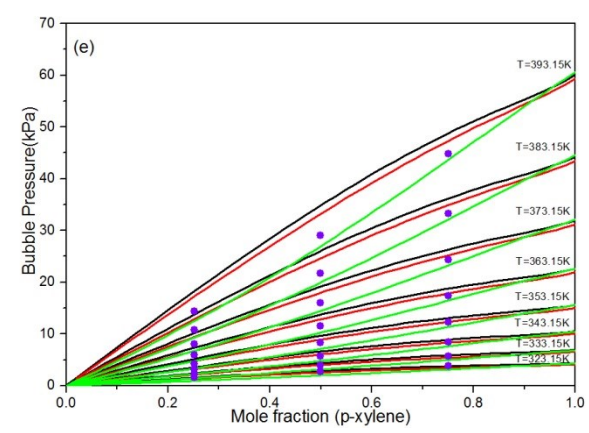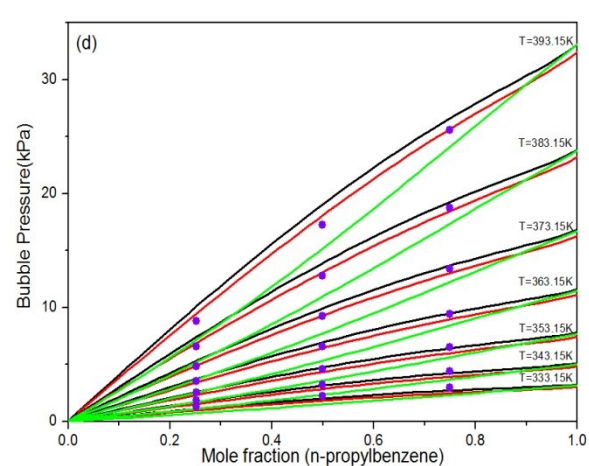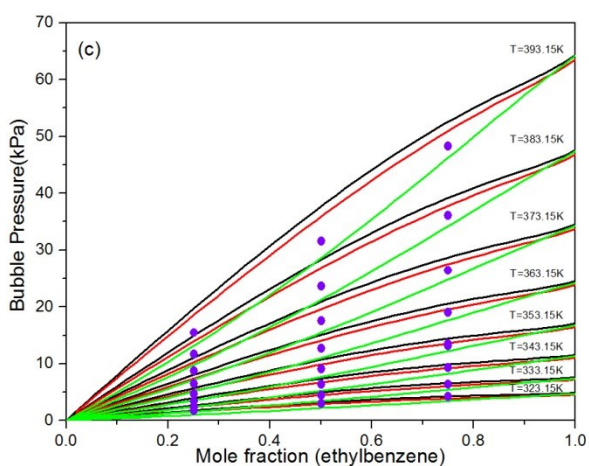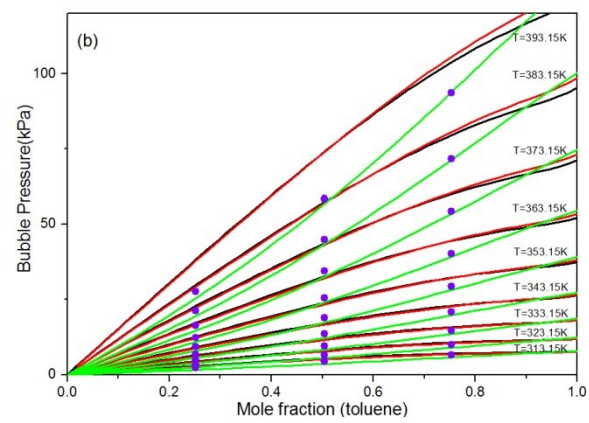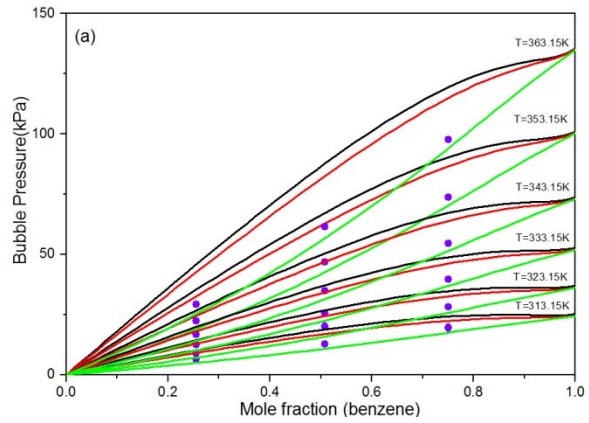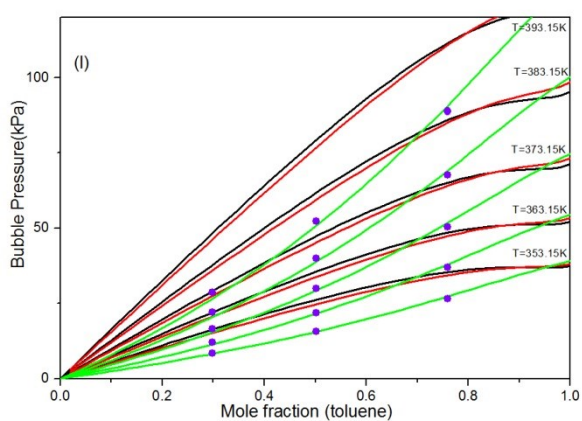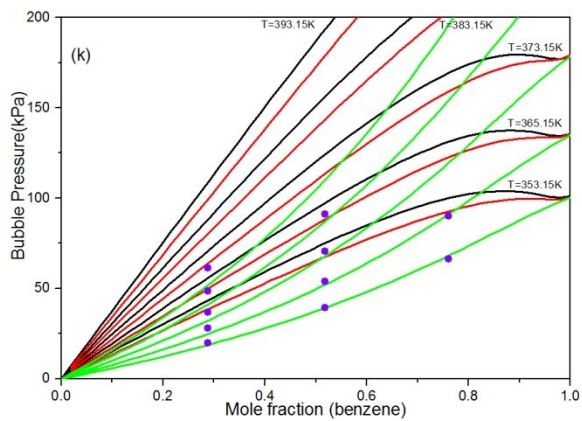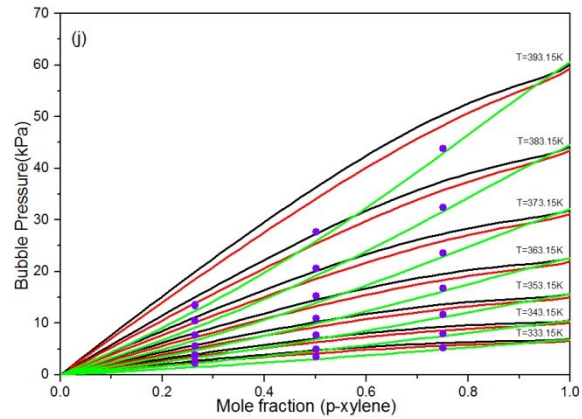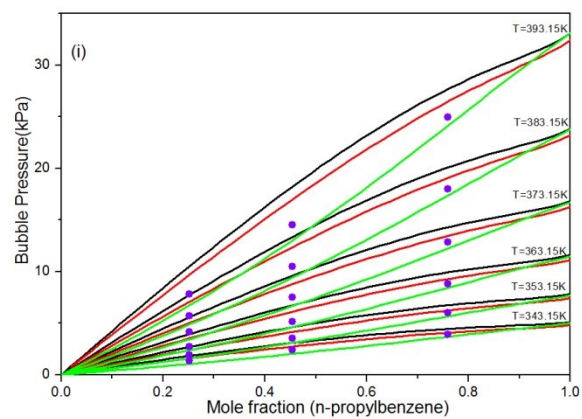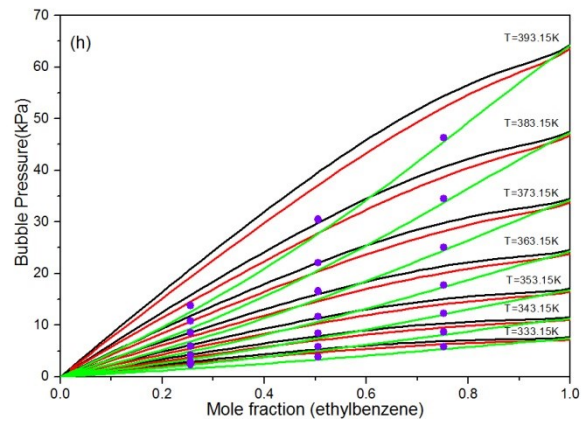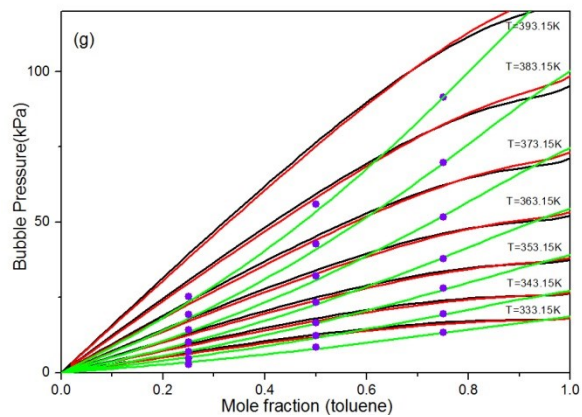
Figure 4.1 Bubble pressure–mole fraction diagram for: (a) benzene + n-C_{20}, (b) toluene + n-C_{20}, (c) ethylbenzene + n-C_{20}, (d) n-propylbenzene + n-C_{20}, (e) p-xylene + n-C_{20}, (f) benzene + n-C_{24}, (g) toluene + n-C_{24}, (h) ethylbenzene + n-C_{24}, (i) n-propylbenzene + n-C_{24}, (j) p-xylene + n-C_{24}, (k) benzene + n-C_{28}, (l) toluene + n-C_{28}, (m) ethylbenzene + n-C_{28}, (n) n-propylbenzene + n-C_{28}, (o) p-xylene + n-C_{28}. Computed results from PR, SRK, and PC-SAFT EOS with standard k_{ij}s are shown using black, red and green curves, respectively. The purple dots (⬤) are experimental data from this work.

4.3 Regressed composition and temperature independent k_{ij} values for the PR and SRK EOS

Regressed k_{ij} values for the PR and SRK EOS were obtained by fitting the computed outcomes, based on NIST critical properties for components to experimental BPPs using a least squares objective function (Equation 4.1):

$$Objective\ Function = \sum_{i}^{n}(Experimental\_BPP_i - Calculated\_BPP_i)^2 \tag{4.1}$$

k_{ij} values were regressed by minimizing the sum of squared residuals. Calculations were performed in VMGSim. Fitted composition and temperature independent k_{ij} values for the PR and SRK EOS are reported in Table 4.7. Uncertainties associated with these k_{ij} values are determined based on the range of k_{ij} values that provide BPP estimates within ± 1 kPa of all experimental measurements for a mixture. For most mixtures there was a range of k_{ij} values that met this criterion, and their mean value and range are reported. In some cases there is only a best fit value, as no single value fully met this criterion. Exceptional cases include benzene + n-C$_{20}$, toluene + n-C$_{24}$ and benzene + n-C$_{28,}$ and details are shown in section 4.4.1. For such cases, the range of best fitted k_{ij}s can be narrow (less than ± 0.001), and therefore the reported uncertainty of k_{ij} is close to 0 (e.g., benzene+n-C$_{28}$). It is noteworthy that regressed k_{ij} values are negative, which is at odds with the conventional assumption that k_{ij} should be positive or close to 0. The regressed k_{ij} values trend towards larger negative values when the size asymmetry of the binary increases.

With these temperature–independent fitted k_{ij}s, computed BPPs for the PR and SRK EOS are much improved as illustrated in Figure 4.2(a-o) and shown in detail in Tables 4.8 and 4.9 respectively, where absolute and percent deviations at each experimental condition are provided. On average, regressed values fall within experimental uncertainties. The impact of using fitted k_{ij}s on BPP prediction accuracy is further illustrated in Figure 4.3, where AAPD is plotted against n-alkane carbon number (Figure 4.3(a and c)) and by aromatic type (Figure 4.3(b and d)) for the PR and SRK EOS respectively. With k_{ij} = 0, the prediction errors of PR and SRK EOS are high, especially for highly asymmetric binaries. By contrast, fitted k_{ij} values reduce deviations significantly for both the PR and SRK EOS.

Table 4.7 Regressed temperature and composition independent k_{ij} values

Mixture	k_{ij}			
	PR EOS	Uncertainty (±)	SRK EOS	Uncertainty (±)
n-C$_{20}$ + Benzene	−0.065	0.002	−0.055	0.001
n-C$_{20}$ + Toluene	−0.052	0.001	−0.043	0.001
n-C$_{20}$ + Ethylbenzene	−0.034	0.005	−0.027	0.004
n-C$_{20}$ + n-Propylbenzene	−0.019	0.009	−0.012	0.008
n-C$_{20}$ + p-Xylene	−0.034	0.006	−0.027	0.005
n-C$_{24}$ + Benzene	−0.085	0.001	−0.076	0.001
n-C$_{24}$ + Toluene	−0.075	0.001	−0.067	0.001
n-C$_{24}$ + Ethylbenzene	−0.055	0.002	−0.048	0.003
n-C$_{24}$ + n-Propylbenzene	−0.041	0.009	−0.035	0.010
n-C$_{24}$ + p-Xylene	−0.054	0.005	−0.048	0.005
n-C$_{28}$ + Benzene	−0.100	0.000	−0.092	0.000
n-C$_{28}$ + Toluene	−0.084	0.002	−0.077	0.003
n-C$_{28}$ + Ethylbenzene	−0.069	0.005	−0.062	0.006
n-C$_{28}$ + n-Propylbenzene	−0.053	0.009	−0.046	0.009
n-C$_{28}$ + p-Xylene	−0.067	0.004	−0.061	0.004
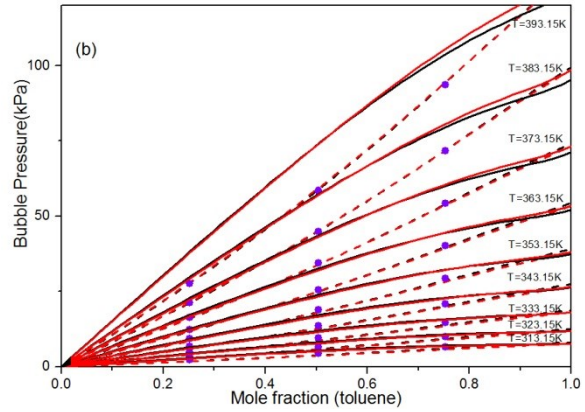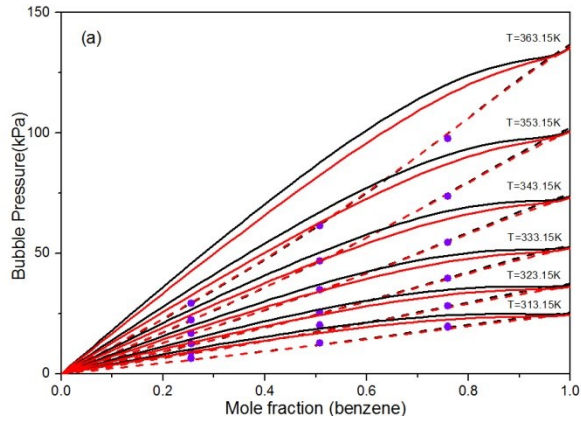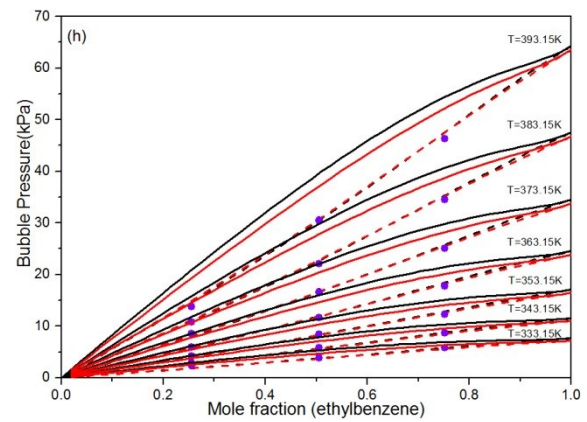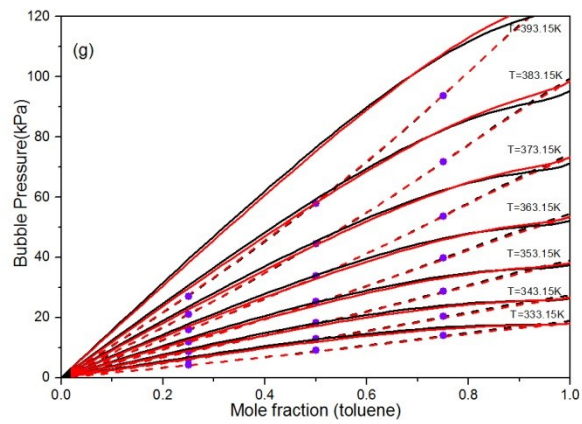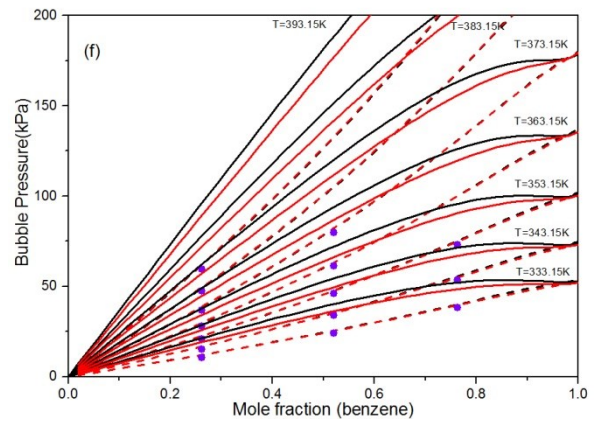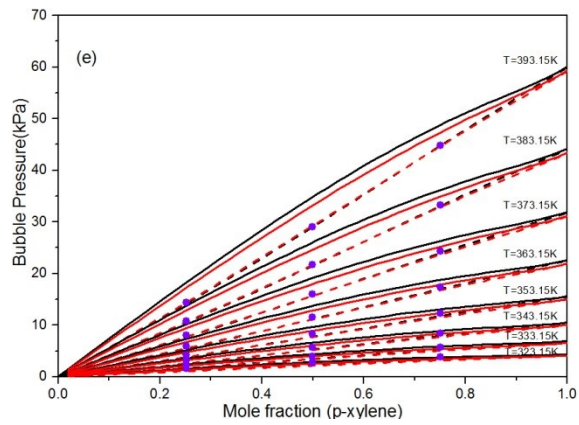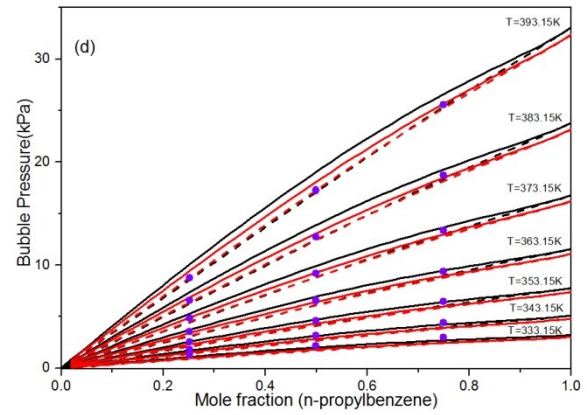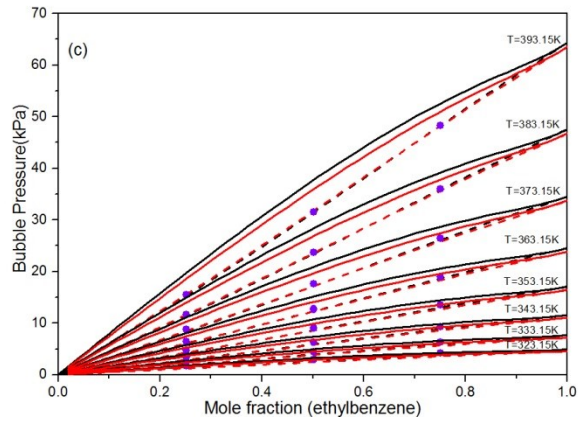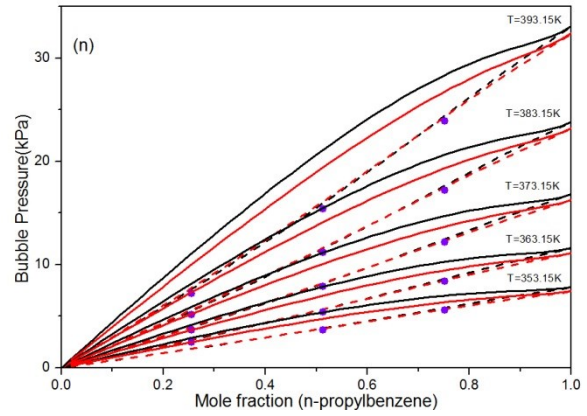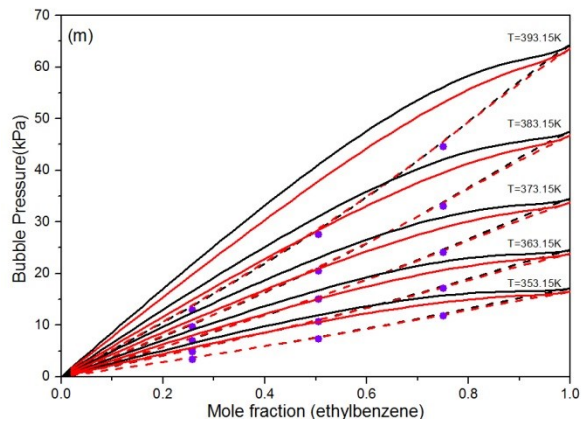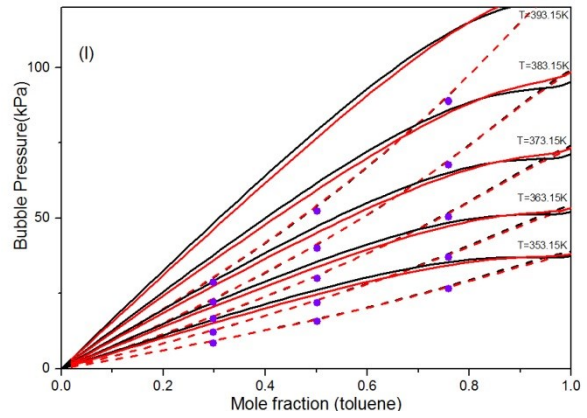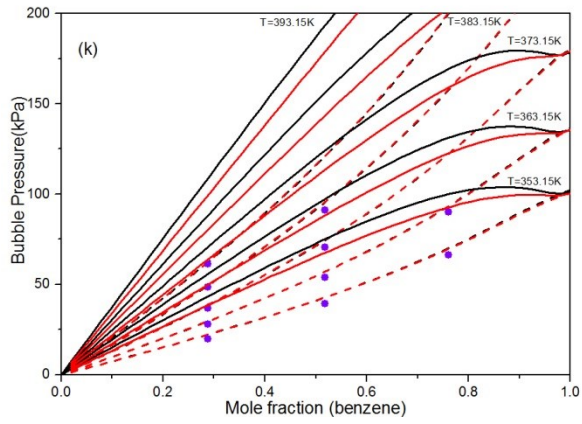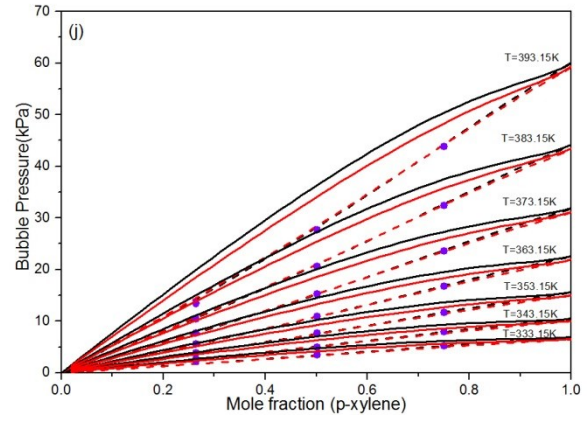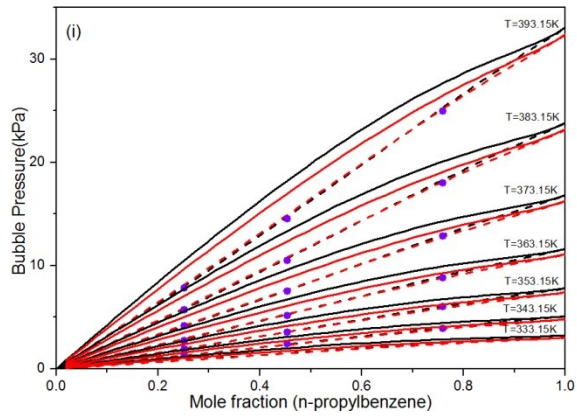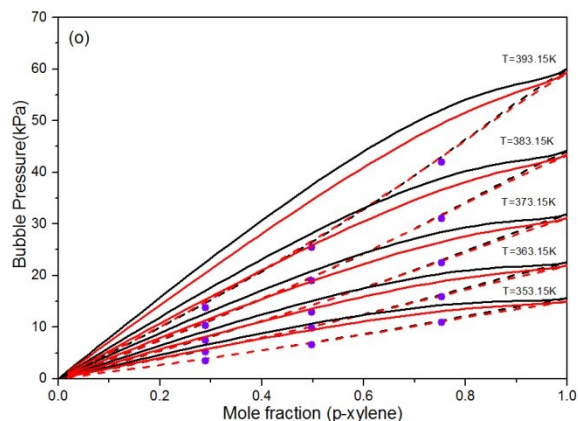
Figure 4.2 Bubble pressure–mole fraction diagram for: (a) benzene + n-C_{20}, (b) toluene + n-C_{20}, (c) ethylbenzene + n-C_{20}, (d) n-propylbenzene + n-C_{20}, (e) p-xylene + n-C_{20}, (f) benzene + n-C_{24}, (g) toluene + n-C_{24}, (h) ethylbenzene + n-C_{24}, (i) n-propylbenzene + n-C_{24}, (j) p-xylene + n-C_{24}, (k) benzene + n-C_{28}, (l) toluene + n-C_{28}, (m) ethylbenzene + n-C_{28}, (n) n-propylbenzene + n-C_{28}, (o) p-xylene + n-C_{28} using different k_{ij} values. Computed results from PR, SRK are shown in black and red lines. k_{ij} values used in calculation are: (—) standard k_{ij}, (---) fitted k_{ij}, represented by solid and dashed line. The purple dots (●) represent the experimental data from this work.

Table 4.8 Experimental data vs. calculated outcomes from PR EOS with fitted k_{ij}s.

Temperature (K) ±0.1K	Aromatic Mole Fraction $x \pm 0.0001$	Bubble Pressure(kPa)		Deviation	
		Experimental Uncertainty ± 1kPa	Calculated from PR EOS with fitted k_{ij}	Absolute Deviation (kPa)	Absolute Percent Deviation (%)
Benzene + n-C_{20}					
313.15		6.4	5.7	0.7	11.4
323.15		9.0	8.2	0.8	8.5
333.15		12.4	11.7	0.8	6.1
343.15	0.2555	16.8	16.1	0.7	4.0
353.15		22.4	21.8	0.6	2.8
363.15		29.2	28.9	0.3	1.0
313.15		12.8	11.9	0.9	7.2
323.15		18.1	17.3	0.8	4.2
333.15		25.4	24.6	0.9	3.4
343.15	0.5083	34.7	34.0	0.7	2.2
353.15		46.6	46.1	0.6	1.2

363.15		61.2	61.2	0.0	0.1
313.15		19.5	18.9	0.6	3.1
323.15		28.1	27.6	0.5	1.7
333.15		39.5	39.3	0.2	0.6
343.15	0.7593	54.4	54.6	0.1	0.2
353.15		73.6	74.2	0.6	0.8
363.15		97.4	98.9	1.6	1.6

Toluene + n-C$_{20}$

313.15		2.5	2.0	0.5	18.9
323.15		3.5	3.1	0.4	12.1
333.15		4.9	4.5	0.3	6.9
343.15		6.8	6.6	0.2	3.1
353.15	0.2514	9.3	9.2	0.1	0.6
363.15		12.4	12.7	0.3	2.2
373.15		16.5	17.1	0.6	3.7
383.15		21.3	22.6	1.3	6.2
393.15		27.6	29.3	1.7	6.2
313.15		4.6	4.1	0.4	9.4
323.15		6.7	6.3	0.4	5.4
333.15		9.7	9.4	0.3	2.6
343.15		13.6	13.6	0.0	0.2
353.15	0.5043	18.9	19.2	0.2	1.3
363.15		25.6	26.5	0.9	3.4
373.15		34.4	35.7	1.4	3.9
383.15		44.9	47.4	2.5	5.6
393.15		58.3	61.7	3.4	5.9
313.15		6.7	6.3	0.4	5.9
323.15		10.0	9.6	0.3	3.4
333.15		14.6	14.4	0.3	1.7
343.15		20.9	20.9	0.0	0.0
353.15	0.7526	29.3	29.6	0.3	0.9
363.15		40.1	40.9	0.8	2.0
373.15		54.2	55.6	1.3	2.4
383.15		71.5	74.0	2.5	3.4
393.15		93.5	96.9	3.4	3.6

Ethylbenzene + n-C$_{20}$

323.15		1.8	1.3	0.5	27.4
333.15		2.5	2.0	0.5	18.9
343.15		3.4	3.0	0.4	12.5
353.15		4.7	4.4	0.4	7.5
363.15	0.2511	6.5	6.2	0.3	4.2
373.15		8.8	8.7	0.1	1.7
383.15		11.7	11.8	0.1	0.6
393.15		15.5	15.8	0.3	1.9
323.15		3.1	2.6	0.5	15.5
333.15		4.5	4.0	0.5	10.4

343.15		6.4	6.1	0.4	6.0
353.15		9.1	8.9	0.3	3.0
363.15	0.5015	12.8	12.6	0.1	1.1
373.15		17.6	17.6	0.0	0.1
383.15		23.7	24.0	0.3	1.4
393.15		31.5	32.2	0.7	2.2
323.15		4.3	3.8	0.5	11.2
333.15		6.4	6.0	0.4	7.0
343.15		9.4	9.0	0.4	4.2
353.15		13.5	13.2	0.3	2.4
363.15	0.7502	19.1	18.9	0.2	0.9
373.15		26.4	26.5	0.0	0.2
383.15		36.0	36.3	0.3	0.7
393.15		48.2	48.8	0.6	1.3

n-Propylbenzene + n-C_{20}

333.15		1.4	0.9	0.5	35.4
343.15		1.9	1.4	0.5	26.1
353.15		2.6	2.1	0.5	18.6
363.15	0.2512	3.6	3.1	0.5	12.9
373.15		4.9	4.5	0.4	8.6
383.15		6.7	6.3	0.3	4.9
393.15		8.8	8.7	0.2	1.8
333.15		2.3	1.8	0.5	22.3
343.15		3.3	2.8	0.5	15.5
353.15	0.4999	4.7	4.2	0.5	10.2
363.15		6.6	6.2	0.5	6.9
373.15		9.3	8.9	0.4	4.3
383.15		12.8	12.5	0.3	2.3
393.15		17.3	17.2	0.1	0.4
333.15		3.1	2.6	0.5	16.7
343.15		4.5	4.0	0.5	10.9
353.15		6.6	6.1	0.5	7.3
363.15		9.5	9.0	0.5	4.8
373.15	0.7500	13.4	13.0	0.4	2.9
383.15		18.8	18.4	0.4	1.9
393.15		25.6	25.5	0.1	0.5

p-Xylene + n-C_{20}

323.15		1.6	1.1	0.5	33.1
333.15		2.3	1.7	0.6	25.1
343.15		3.1	2.6	0.6	17.7
353.15		4.3	3.8	0.5	12.2
363.15	0.2515	6.0	5.5	0.5	8.8
373.15		8.1	7.6	0.5	5.6
383.15		10.9	10.5	0.4	3.4
393.15		14.4	14.1	0.3	1.9
323.15		2.8	2.2	0.6	21.2

333.15		4.0	3.4	0.6	15.0
343.15		5.8	5.2	0.6	10.2
353.15	0.4991	8.3	7.7	0.6	7.5
363.15		11.6	11.1	0.5	4.5
373.15		16.1	15.6	0.5	3.1
383.15		21.7	21.4	0.3	1.5
393.15		29.0	28.9	0.1	0.4
323.15		3.9	3.3	0.6	14.8
333.15		5.8	5.2	0.6	9.8
343.15		8.5	7.9	0.5	6.4
353.15	0.7503	12.3	11.8	0.5	4.2
363.15		17.4	17.0	0.5	2.7
373.15		24.3	23.9	0.4	1.6
383.15		33.3	33.0	0.3	0.8
393.15		44.7	44.7	0.0	0.0

Benzene + n-C$_{24}$

333.15		10.7	11.5	0.8	7.8
343.15	0.2623	15.2	15.9	0.7	4.3
353.15		21.0	21.4	0.4	2.1
363.15		28.1	28.4	0.3	1.1
373.15		36.7	36.9	0.1	0.3
383.15		47.3	47.1	0.2	0.5
393.15		59.5	59.3	0.3	0.4
333.15	0.5212	24.0	24.4	0.4	1.6
343.15		33.8	33.8	0.0	0.0
353.15		45.9	45.7	0.2	0.5
363.15		61.3	60.6	0.7	1.1
373.15		79.7	79.0	0.8	1.0
333.15	0.7637	38.2	38.9	0.7	1.9
343.15		53.5	54.0	0.5	1.0
353.15		72.9	73.4	0.5	0.7

Toluene + n-C$_{24}$

333.15	0.2508	2.8	3.8	1.1	38.5
343.15		4.7	5.6	0.9	19.3
353.15		7.1	7.9	0.8	10.7
363.15		10.3	10.9	0.6	5.6
373.15		14.3	14.7	0.4	2.9
383.15		19.3	19.6	0.3	1.5
393.15		25.3	25.5	0.2	1.0
333.15	0.5008	8.4	8.2	0.3	3.2
343.15		12.3	11.9	0.5	3.9
353.15		16.6	16.8	0.2	1.1
363.15		23.4	23.3	0.2	0.8
373.15		32.1	31.6	0.5	1.6
383.15		42.6	42.0	0.6	1.5
393.15		55.9	54.9	1.0	1.8

333.15	0.7504	13.4	13.3	0.1	0.7
343.15		19.7	19.4	0.3	1.5
353.15		28.0	27.5	0.5	1.9
363.15		37.9	38.1	0.3	0.7
373.15		51.7	51.9	0.1	0.3
383.15		69.6	69.2	0.4	0.6
393.15		91.2	90.7	0.5	0.6

Ethylbenzene + n-C_{24}

333.15	0.2557	2.5	1.8	0.7	28.1
343.15		3.0	2.7	0.3	9.5
353.15		4.3	3.9	0.3	7.3
363.15		6.0	5.6	0.3	5.8
373.15		8.7	7.9	0.8	9.4
383.15		10.8	10.7	0.1	0.7
393.15		13.8	14.4	0.5	3.9
333.15		3.9	3.7	0.2	6.1
343.15		5.8	5.5	0.3	5.2
353.15		8.5	8.1	0.4	4.1
363.15	0.5051	11.7	11.6	0.1	0.8
373.15		16.6	16.3	0.3	2.1
383.15		22.1	22.3	0.1	0.6
393.15		30.5	29.9	0.6	1.9
333.15	0.7520	5.9	5.7	0.2	2.6
343.15		8.8	8.6	0.1	1.6
353.15		12.3	12.7	0.4	2.9
363.15		17.8	18.2	0.4	2.1
373.15		25.0	25.5	0.5	1.8
383.15		34.5	35.0	0.5	1.4
393.15		46.3	47.1	0.8	1.7

n-Propylbenzene + n-C_{24}

343.15	0.2519	1.4	1.3	0.2	11.9
353.15		2.0	1.9	0.1	5.1
363.15		2.8	2.8	0.0	0.1
373.15		4.2	4.1	0.2	3.6
383.15		5.7	5.7	0.0	0.4
393.15		7.9	7.9	0.0	0.4
343.15	0.4542	2.5	2.3	0.2	7.0
353.15		3.6	3.5	0.1	2.5
363.15		5.2	5.2	0.0	0.3
373.15		7.6	7.5	0.1	0.9
383.15		10.5	10.6	0.0	0.2
393.15		14.6	14.6	0.0	0.2
343.15	0.7593	4.0	3.9	0.0	0.8
353.15		6.1	6.0	0.1	1.8
363.15		8.9	8.9	0.0	0.5
373.15		12.9	12.9	0.0	0.4

383.15		18.0	18.2	0.1	0.7
393.15		25.0	25.2	0.2	0.7

		p-Xylene + n-C$_{24}$			
333.15	0.2648	2.3	1.7	0.7	28.7
343.15		2.7	2.5	0.2	7.5
353.15		3.9	3.7	0.2	5.8
363.15		5.6	5.3	0.3	4.9
373.15		7.7	7.5	0.2	3.1
383.15		10.5	10.3	0.2	1.9
393.15		13.5	13.9	0.4	2.8
333.15	0.5014	3.5	3.3	0.2	6.8
343.15		5.1	5.0	0.1	2.1
353.15		7.7	7.3	0.3	4.5
363.15		10.9	10.6	0.4	3.5
373.15		15.2	14.9	0.4	2.5
383.15		20.7	20.4	0.2	1.1
393.15		27.7	27.6	0.1	0.5
333.15	0.7509	5.3	5.1	0.2	3.7
343.15		8.0	7.8	0.2	2.6
353.15		11.8	11.5	0.2	2.0
363.15		16.8	16.6	0.2	1.2
373.15		23.6	23.4	0.2	0.7
383.15		32.3	32.3	0.0	0.0
393.15		43.7	43.8	0.0	0.1
		Benzene + n-C$_{28}$			
353.15	0.2885	19.7	21.3	1.6	8.2
363.15		27.9	28.3	0.4	1.5
373.15		36.7	37.0	0.3	0.7
383.15		48.4	47.4	1.0	2.0
393.15		61.1	59.9	1.1	1.8
353.15	0.5177	39.1	41.1	2.0	5.0
363.15		53.7	54.7	1.0	1.9
373.15		70.4	71.6	1.2	1.7
383.15		91.0	92.0	1.1	1.2
353.15	0.7614	66.3	68.3	2.0	3.0
363.15		90.0	91.1	1.1	1.3
		Toluene + n-C$_{28}$			
353.15	0.2981	8.5	8.8	0.3	3.0
363.15		12.1	12.2	0.1	1.2
373.15		16.6	16.6	0.0	0.2
383.15		22.0	22.1	0.1	0.5
393.15		28.7	28.9	0.2	0.7
353.15	0.5018	15.7	15.8	0.0	0.3
363.15		21.9	21.9	0.0	0.1
373.15		29.9	29.8	0.2	0.5
383.15		39.9	39.7	0.2	0.4

393.15		52.3	52.0	0.3	0.5
353.15	0.7598	26.5	26.8	0.3	1.0
363.15		36.9	37.2	0.3	0.9
373.15		50.4	50.7	0.3	0.6
383.15		67.4	67.7	0.3	0.4
393.15		88.6	88.9	0.2	0.3

<center>Ethylbenzene + n-C₂₈</center>

353.15	0.2584	3.4	3.5	0.1	3.7
363.15		4.9	5.0	0.1	2.4
373.15		7.1	7.1	0.0	0.1
383.15		9.7	9.7	0.0	0.2
393.15		13.0	13.0	0.1	0.5
353.15		7.4	7.3	0.1	1.1
363.15	0.5055	10.7	10.5	0.2	1.6
373.15		15.0	14.7	0.3	1.9
383.15		20.4	20.3	0.2	0.9
393.15		27.5	27.3	0.2	0.7
353.15	0.7510	11.8	11.9	0.1	0.5
363.15		17.1	17.1	0.1	0.3
373.15		24.1	24.0	0.1	0.5
383.15		33.0	33.0	0.0	0.1
393.15		44.5	44.6	0.1	0.2

<center>n-Propylbenzene + n-C₂₈</center>

363.15	0.2554	2.6	2.6	0.0	0.4
373.15		3.7	3.7	0.0	0.2
383.15		5.2	5.2	0.0	0.1
393.15		7.3	7.2	0.1	0.8
353.15	0.5127	3.7	3.6	0.1	2.3
363.15		5.5	5.4	0.1	1.2
373.15		7.9	7.8	0.1	1.5
383.15		11.2	11.1	0.2	1.3
393.15		15.4	15.3	0.1	0.7
353.15	0.7525	5.7	5.7	0.0	0.0
363.15		8.4	8.4	0.0	0.3
373.15		12.2	12.2	0.0	0.3
383.15		17.2	17.2	0.0	0.1
393.15		23.9	23.9	0.0	0.1

<center>p-Xylene + n-C₂₈</center>

353.15	0.2897	3.5	3.6	0.1	3.1
363.15		5.2	5.2	0.0	0.8
373.15		7.5	7.3	0.1	1.4
383.15		10.3	10.1	0.2	1.6
393.15		13.8	13.7	0.1	0.5
353.15	0.4985	6.7	6.5	0.1	1.5
363.15		9.8	9.5	0.3	3.2
373.15		12.9	13.4	0.5	3.8

Temperature (K)	Aromatic Mole Fraction	Experimental	Calculated	Absolute Deviation (kPa)	Absolute Percent Deviation (%)
383.15		19.0	18.5	0.5	2.4
393.15		25.4	25.1	0.4	1.4
353.15	0.7536	11.0	10.9	0.1	1.0
363.15		15.9	15.7	0.2	1.2
373.15		22.5	22.2	0.3	1.4
383.15		31.0	30.7	0.3	0.9
393.15		41.9	41.7	0.2	0.5
AAD (kPa)				0.41	
AAPD (%)					4.23

Table 4.9 Experimental data vs. calculated outcomes from SRK EOS with fitted k_{ij}s.

Temperature (K) ±0.1K	Aromatic Mole Fraction $x \pm 0.0001$	Bubble Pressure(kPa)		Deviation	
		Experimental Uncertainty ± 1kPa	Calculated from SRK EOS with fitted k_{ij}	Absolute Deviation (kPa)	Absolute Percent Deviation (%)
Benzene + n-C$_{20}$					
313.15		6.4	5.7	0.7	10.5
323.15		9.0	8.4	0.7	7.2
333.15		12.4	11.9	0.6	4.6
343.15	0.2555	16.8	16.4	0.4	2.2
353.15		22.4	22.2	0.2	0.9
363.15		29.2	29.5	0.3	1.2
313.15		12.8	11.9	0.9	7.3
323.15		18.1	17.4	0.7	3.8
333.15		25.4	24.7	0.7	2.7
343.15	0.5083	34.7	34.4	0.4	1.1
353.15		46.6	46.7	0.0	0.1
363.15		61.2	62.1	0.9	1.4
313.15		19.5	18.6	0.9	4.8
323.15		28.1	27.3	0.8	2.9
333.15		39.5	39.0	0.5	1.2
343.15	0.7593	54.4	54.5	0.0	0.0
353.15		73.6	74.3	0.7	1.0
363.15		97.4	99.4	2.0	2.1
Toluene + n-C$_{20}$					
313.15		2.5	1.8	0.6	25.9
323.15		3.5	2.8	0.7	18.7
333.15		4.9	4.2	0.6	13.1
343.15		6.8	6.2	0.6	8.8
353.15	0.2514	9.3	8.8	0.5	5.6

363.15		12.4	12.1	0.3	2.3
373.15		16.5	16.4	0.0	0.2
383.15		21.3	21.8	0.6	2.7
393.15		27.6	28.5	0.9	3.3
313.15		4.6	3.8	0.8	16.9
323.15		6.7	5.9	0.8	12.3
333.15		9.7	8.8	0.8	8.8
343.15		13.6	12.9	0.8	5.7
353.15	0.5043	18.9	18.3	0.7	3.6
363.15		25.6	25.4	0.2	0.8
373.15		34.4	34.5	0.1	0.3
383.15		44.9	46.0	1.1	2.4
393.15		58.3	60.2	1.9	3.3
313.15		6.7	5.8	0.9	12.8
323.15		10.0	9.0	1.0	9.6
333.15		14.6	13.6	1.0	7.1
343.15		20.9	19.9	1.0	4.8
353.15	0.7526	29.3	28.4	0.9	3.1
363.15		40.1	39.6	0.6	1.4
373.15		54.2	54.0	0.2	0.4
383.15		71.5	72.3	0.8	1.1
393.15		93.5	95.1	1.7	1.8

Ethylbenzene + n-C_{20}

323.15		1.8	1.2	0.6	32.2
333.15		2.5	1.9	0.6	23.5
343.15		3.4	2.9	0.6	16.7
353.15		4.7	4.2	0.5	11.4
363.15	0.2511	6.5	6.0	0.5	7.5
373.15		8.8	8.4	0.4	4.5
383.15		11.7	11.5	0.2	1.8
393.15		15.5	15.5	0.0	0.0
323.15		3.1	2.4	0.7	21.2
333.15		4.5	3.8	0.7	15.6
343.15		6.4	5.8	0.7	10.6
353.15		9.1	8.5	0.6	7.1
363.15	0.5015	12.8	12.2	0.6	4.6
373.15		17.6	17.1	0.5	2.8
383.15		23.7	23.5	0.2	1.0
393.15		31.5	31.6	0.1	0.3
323.15		4.3	3.6	0.7	17.1
333.15		6.4	5.6	0.8	12.3
343.15		9.4	8.6	0.8	8.8
353.15		13.5	12.7	0.9	6.4
363.15	0.7502	19.1	18.3	0.8	4.2
373.15		26.4	25.7	0.7	2.6
383.15		36.0	35.5	0.5	1.5

393.15		48.2	48.0	0.2	0.5

n-Propylbenzene + n-C_{20}

333.15		1.4	0.9	0.5	36.3
343.15		1.9	1.4	0.5	26.5
353.15		2.6	2.1	0.5	18.7
363.15	0.2512	3.6	3.2	0.5	12.5
373.15		4.9	4.5	0.4	7.9
383.15		6.7	6.4	0.3	3.8
393.15		8.8	8.8	0.0	0.3
333.15		2.3	1.7	0.6	24.6
343.15		3.3	2.7	0.6	17.3
353.15	0.4999	4.7	4.1	0.5	11.6
363.15		6.6	6.1	0.5	7.8
373.15		9.3	8.9	0.4	4.7
383.15		12.8	12.5	0.3	2.3
393.15		17.3	17.3	0.0	0.1
333.15		3.1	2.4	0.6	20.9
343.15		4.5	3.8	0.7	14.6
353.15		6.6	5.9	0.7	10.5
363.15		9.5	8.8	0.7	7.4
373.15	0.7500	13.4	12.8	0.7	4.9
383.15		18.8	18.1	0.6	3.3
393.15		25.6	25.2	0.4	1.4

p-Xylene + n-C_{20}

323.15		1.6	1.1	0.6	34.0
333.15		2.3	1.7	0.6	25.7
343.15		3.1	2.6	0.6	17.9
353.15		4.3	3.8	0.5	12.0
363.15	0.2515	6.0	5.5	0.5	8.2
373.15		8.1	7.7	0.4	4.6
383.15		10.9	10.6	0.2	2.2
393.15		14.4	14.4	0.0	0.3
323.15		2.8	2.1	0.7	23.4
333.15		4.0	3.4	0.7	16.8
343.15		5.8	5.1	0.7	11.5
353.15	0.4991	8.3	7.6	0.7	8.3
363.15		11.6	11.0	0.6	4.8
373.15		16.1	15.6	0.5	3.0
383.15		21.7	21.5	0.2	1.0
393.15		29.0	29.1	0.1	0.4
323.15		3.9	3.2	0.7	18.8
333.15		5.8	5.0	0.8	13.2
343.15		8.5	7.7	0.8	9.3
353.15	0.7503	12.3	11.5	0.8	6.5
363.15		17.4	16.7	0.8	4.4
373.15		24.3	23.6	0.7	2.8

383.15		33.3	32.8	0.5	1.5
393.15		44.7	44.6	0.1	0.2

Benzene + n-C$_{24}$					
333.15		10.7	11.5	0.8	7.6
343.15	0.2623	15.2	15.9	0.7	4.4
353.15		21.0	21.5	0.5	2.4
363.15		28.1	28.5	0.4	1.6
373.15		36.7	37.1	0.3	0.9
383.15		47.3	47.4	0.1	0.2
393.15		59.5	59.7	0.2	0.3
333.15	0.5212	24.0	24.3	0.2	0.9
343.15		33.8	33.7	0.1	0.3
353.15		45.9	45.7	0.3	0.6
363.15		61.3	60.7	0.6	0.9
373.15		79.7	79.2	0.5	0.6
333.15	0.7637	38.2	38.4	0.2	0.6
343.15		53.5	53.5	0.1	0.1
353.15		72.9	73.0	0.1	0.1

Toluene + n-C$_{24}$					
333.15	0.2508	2.8	3.8	1.0	37.9
343.15		4.7	5.6	0.9	19.3
353.15		7.1	7.9	0.8	11.1
363.15		10.3	10.9	0.6	6.2
373.15		14.3	14.9	0.5	3.7
383.15		19.3	19.8	0.5	2.5
393.15		25.3	25.8	0.5	2.1
333.15	0.5008	8.4	8.1	0.4	4.2
343.15		12.3	11.8	0.6	4.5
353.15		16.6	16.8	0.2	0.9
363.15		23.4	23.3	0.2	0.7
373.15		32.1	31.7	0.4	1.3
383.15		42.6	42.2	0.4	0.9
393.15		55.9	55.3	0.5	1.0
333.15	0.7504	13.4	13.0	0.4	2.8
343.15		19.7	19.1	0.6	3.1
353.15		28.0	27.2	0.8	3.0
363.15		37.9	37.9	0.0	0.0
373.15		51.7	51.7	0.0	0.0
383.15		69.6	69.2	0.4	0.6
393.15		91.2	91.0	0.2	0.3

Ethylbenzene + n-C$_{24}$					
333.15	0.2557	2.5	1.8	0.7	29.2
343.15		3.0	2.7	0.3	10.4
353.15		4.3	3.9	0.3	7.8
363.15		6.0	5.6	0.4	6.0
373.15		8.7	7.9	0.8	9.3

383.15		10.8	10.8	0.0	0.3
393.15		13.8	14.5	0.6	4.6
333.15		3.9	3.6	0.3	8.3
343.15		5.8	5.4	0.4	6.9
353.15		8.5	8.0	0.5	5.4
363.15	0.5051	11.7	11.5	0.2	1.6
373.15		16.6	16.2	0.4	2.5
383.15		22.1	22.2	0.1	0.6
393.15		30.5	29.9	0.5	1.7
333.15	0.7520	5.9	5.5	0.4	6.2
343.15		8.8	8.4	0.4	4.5
353.15		12.3	12.4	0.1	0.5
363.15		17.8	17.9	0.1	0.3
373.15		25.0	25.2	0.1	0.6
383.15		34.5	34.7	0.2	0.6
393.15		46.3	46.9	0.6	1.3

<div align="center">n-Propylbenzene + n-C_{24}</div>

343.15	0.2519	1.4	1.2	0.2	14.0
353.15		2.0	1.9	0.1	6.8
363.15		2.8	2.8	0.0	1.4
373.15		4.2	4.0	0.2	4.3
383.15		5.7	5.7	0.0	0.8
393.15		7.9	7.9	0.0	0.5
343.15	0.4542	2.5	2.3	0.2	9.9
353.15		3.6	3.4	0.2	4.9
363.15		5.2	5.1	0.1	2.1
373.15		7.6	7.4	0.2	2.2
383.15		10.5	10.5	0.1	0.6
393.15		14.6	14.5	0.1	0.6
343.15	0.7593	4.0	3.8	0.2	5.3
353.15		6.1	5.8	0.3	5.5
363.15		8.9	8.6	0.2	2.6
373.15		12.9	12.6	0.4	2.8
383.15		18.0	17.8	0.2	1.1
393.15		25.0	24.8	0.2	0.7

<div align="center">p-Xylene + n-C_{24}</div>

333.15	0.2648	2.3	1.6	0.7	30.6
343.15		2.7	2.5	0.3	9.4
353.15		3.9	3.7	0.3	7.2
363.15		5.6	5.3	0.3	5.9
373.15		7.7	7.4	0.3	3.8
383.15		10.5	10.3	0.2	2.2
393.15		13.5	13.9	0.4	2.8
333.15	0.5014	3.5	3.2	0.3	9.9
343.15		5.1	4.8	0.2	4.7
353.15		7.7	7.2	0.5	6.4

363.15		10.9	10.4	0.5	4.9
373.15		15.2	14.7	0.5	3.5
383.15		20.7	20.3	0.4	1.8
393.15		27.7	27.5	0.2	0.8
333.15	0.7509	5.3	4.9	0.4	7.8
343.15		8.0	7.5	0.5	6.0
353.15		11.8	11.2	0.6	4.8
363.15		16.8	16.3	0.6	3.4
373.15		23.6	23.0	0.6	2.4
383.15		32.3	32.0	0.4	1.2
393.15		43.7	43.4	0.3	0.7
Benzene + n-C$_{28}$					
353.15	0.2885	19.7	21.2	1.6	7.9
363.15		27.9	28.3	0.4	1.5
373.15		36.7	37.0	0.3	0.8
383.15		48.4	47.5	0.9	1.9
393.15		61.1	60.0	1.0	1.7
353.15	0.5177	39.1	40.9	1.8	4.6
363.15		53.7	54.6	0.9	1.7
373.15		70.4	71.5	1.1	1.6
383.15		91.0	92.1	1.1	1.2
353.15	0.7614	66.3	67.8	1.5	2.3
363.15		90.0	90.8	0.8	0.9
Toluene + n-C$_{28}$					
353.15	0.2981	8.5	8.8	0.2	2.5
363.15		12.1	12.2	0.1	1.0
373.15		16.6	16.6	0.0	0.3
383.15		22.0	22.2	0.2	0.7
393.15		28.7	29.0	0.3	1.0
353.15	0.5018	15.7	15.6	0.1	0.4
363.15		21.9	21.8	0.1	0.4
373.15		29.9	29.7	0.2	0.7
383.15		39.9	39.7	0.2	0.4
393.15		52.3	52.2	0.2	0.3
353.15	0.7598	26.5	26.4	0.1	0.3
363.15		36.9	36.9	0.0	0.1
373.15		50.4	50.4	0.0	0.0
383.15		67.4	67.5	0.1	0.1
393.15		88.6	88.9	0.2	0.3
Ethylbenzene + n-C$_{28}$					
353.15	0.2584	3.4	3.5	0.1	3.5
363.15		4.9	5.0	0.1	2.5
373.15		7.1	7.1	0.0	0.3
383.15		9.7	9.7	0.0	0.5
393.15		13.0	13.1	0.2	1.3
353.15		7.4	7.2	0.1	2.0

363.15	0.5055	10.7	10.4	0.2	2.1
373.15		15.0	14.7	0.3	2.0
383.15		20.4	20.3	0.1	0.7
393.15		27.5	27.4	0.1	0.3
353.15	0.7510	11.8	11.6	0.2	1.5
363.15		17.1	16.8	0.3	1.8
373.15		24.1	23.8	0.4	1.5
383.15		33.0	32.8	0.1	0.4
393.15		44.5	44.4	0.0	0.0
n-Propylbenzene + n-C_{28}					
363.15	0.2554	2.6	2.6	0.0	0.3
373.15		3.7	3.7	0.0	0.2
383.15		5.2	5.3	0.0	0.6
393.15		7.3	7.3	0.0	0.2
353.15	0.5127	3.7	3.6	0.1	3.7
363.15		5.5	5.4	0.1	2.1
373.15		7.9	7.8	0.2	1.9
383.15		11.2	11.1	0.2	1.4
393.15		15.4	15.3	0.1	0.5
353.15	0.7525	5.7	5.5	0.2	3.0
363.15		8.4	8.2	0.2	2.6
373.15		12.2	12.0	0.2	2.0
383.15		17.2	17.0	0.2	1.1
393.15		23.9	23.7	0.2	0.9
p-Xylene + n-C_{28}					
353.15	0.2897	3.5	3.6	0.1	1.8
363.15		5.2	5.2	0.1	1.6
373.15		7.5	7.3	0.1	1.9
383.15		10.3	10.1	0.2	1.8
393.15		13.8	13.7	0.1	0.4
353.15	0.4985	6.7	6.4	0.2	3.2
363.15		9.8	9.4	0.4	4.3
373.15		12.9	13.3	0.4	2.9
383.15		19.0	18.4	0.6	2.9
393.15		25.4	25.0	0.4	1.6
353.15	0.7536	11.0	10.6	0.4	3.5
363.15		15.9	15.4	0.5	3.2
373.15		22.5	21.9	0.6	2.8
383.15		31.0	30.4	0.6	1.9
393.15		41.9	41.4	0.5	1.1
AAD (kPa)				0.44	
AAPD (%)					5.17
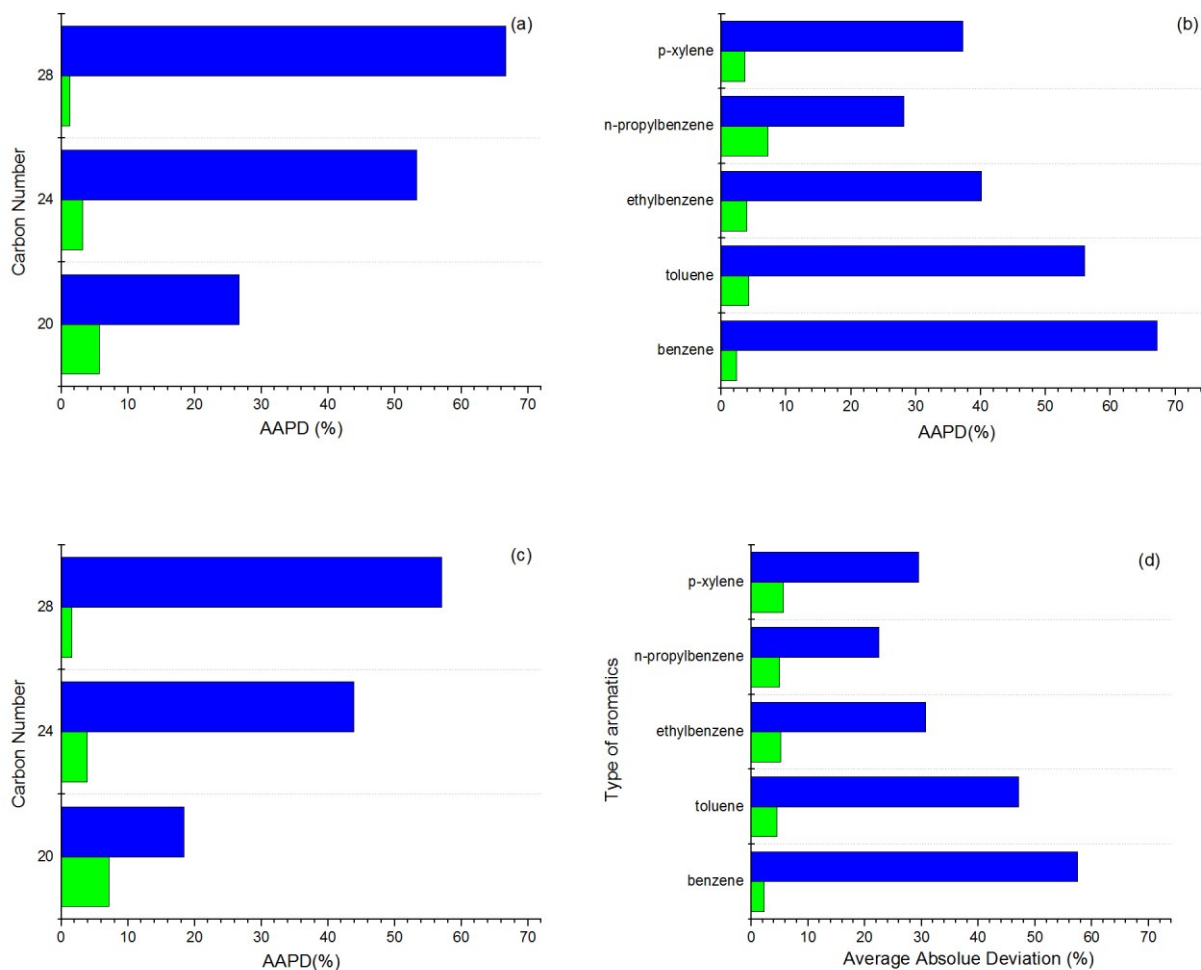
Figure 4.3 AAPD of predicted BPPs for aromatic + n-alkane binaries: (a) PR EOS with different carbon numbers of n-alkanes; (b) PR EOS with different aromatics; (c) SRK EOS with different carbon numbers of n-alkanes; (d) SRK EOS with different aromatics. (■) $k_{ij}=0$; (■) fitted k_{ij} values.

4.4 Uncertainty of regressed k_{ij} values

4.4.1 Uncertainties in regressed k_{ij} values introduced by BPP measurement uncertainty

A sensitivity analysis was performed to study the impact of experimental BPP measurement

uncertainty on regressed interaction parameters. Calculations were performed in VMGSim. As shown in Figure 3.3, corrected BPP values have an AAD of 0.5 kPa and are expected to fall within ± 1 kPa of measured values as demonstrated by the calibration. This uncertainty imposes bounds on the ranges of k_{ij} values. For each mixture, the widest range of k_{ij} values that fit the three experimental BPP points within ± 1 kPa determines the range of k_{ij} values at a single temperature. Two illustrative cases for the PR EOS are shown in Figure 4.4. For n-propylbenzene + n-C_{28} (Figure 4.4a), the upper bound k_{ij} value (k_{ij} = −0.033) is determined by calculated VLE outcomes (shown in green line) that fits the upper BPP bound of all three experimental points jointly. The lower bound k_{ij} value (k_{ij} = −0.078) fits the lower BPP values for all the experimental points jointly and is shown as the cyan line. The k_{ij} value for n-propylbenzene + n-C_{28} at 363.15K is the mean value of these two bounds and the uncertainty is half the span of these bounds (k_{ij} = −0.055 ± 0.023). Similarly, the k_{ij} value and limits for toluene + n-C_{28} is k_{ij} = −0.085 ± 0.005, shown in Figure 4.4b. These two examples illustrate that the range of possible k_{ij} values is larger for low BPPs and smaller for larger BPPs. Thus, for any given binary higher temperature BPP data impose narrower constraints on the possible range of k_{ij} values. k_{ij} values fit at each temperature and their uncertainties for each mixture are provided in Table 4.10. Regressing the BPP data in this way provides insights as to the "best-fit" k_{ij} value for a mixture over all and whether temperature–dependent k_{ij} values are warranted for a particular mixture. Two illustrative examples are provided in Figure 4.5 based on the PR EOS. For toluene + n-C_{20}, Figure 4.5a, there is a range of k_{ij} values, bounded by the horizontal dashed lines, that fit all of the BPP data. For toluene + n-C_{24}, fitted k_{ij} value at 333.15 K for the PR EOS fall outside the range of k_{ij} values at other temperatures. This case is exceptional, as is clear from Figure 4.5b, and such effects were ignored in determining the best-fit temperature– and

pressure–independent k_{ij} values and their uncertainty. Other cases include benzene + n-C_{20} and benzene + n-C_{28}. The extraordinary k_{ij} values, observed normally at boundary temperatures, are highlighted in Table 4.10. There is little or no justification for temperature– or composition–dependent k_{ij} values for any of the mixtures based on either cubic EOS.
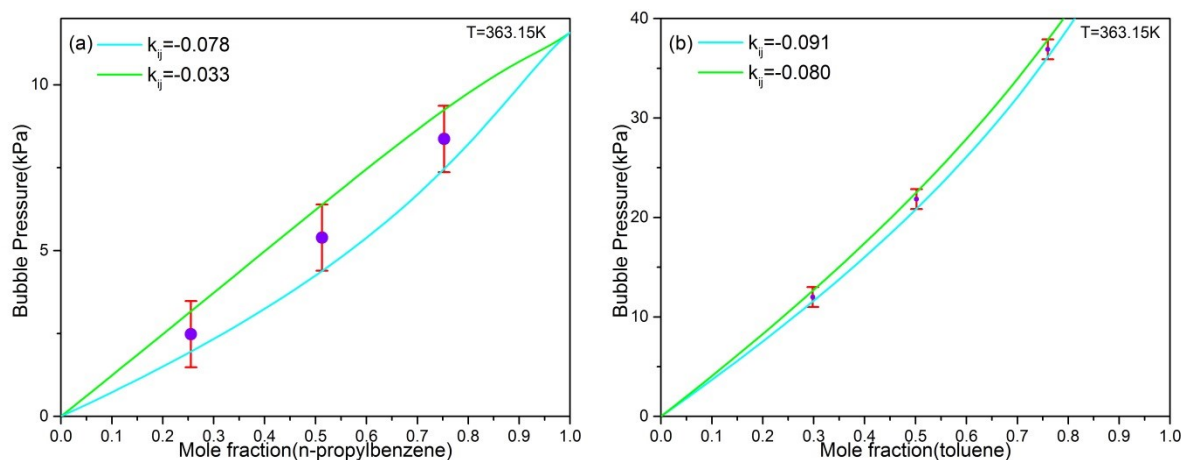
Figure 4.4 Uncertainty of regressed k_{ij} values caused by the BPP measurement uncertainty (±1 kPa) for a) n-propylbenzene + n-C_{28} at 363.15 K b) toluene + n-C_{28} at 363.15 K. The purple dots are experimental values obtained from this work. Computed results from PR EOS using k_{ij} values that fit the upper and lower BPP bounds are shown in green and cyan lines, respectively.

Table 4.10 Isothermal best-fit k_{ij} values for BPP (exceptional k_{ij}s are highlighted in bold fonts)

| Mixture | T (K) | Fitted k_{ij} values | | | |
		PR EOS	Uncertainty (±)	SRK EOS	Uncertainty (±)
	313.15	−0.058	0.010	−0.046	0.010
	323.15	−0.060	0.008	−0.050	0.007
n-C_{20}	333.15	−0.062	0.005	−0.051	0.006
+	343.15	−0.063	0.003	−0.054	0.004
Benzene	353.15	−0.065	0.002	−0.056	0.003
	363.15	−0.067	0.001	−0.059	0.001
n-C_{20}	313.15	−0.037	0.027	−0.026	0.026
+	323.15	−0.039	0.019	−0.028	0.018

Toluene	333.15	−0.042	0.014	−0.032	0.012
	343.15	−0.044	0.010	−0.035	0.009
	353.15	−0.046	0.007	−0.037	0.007
	363.15	−0.049	0.006	−0.041	0.005
	373.15	−0.050	0.005	−0.043	0.004
	383.15	−0.053	0.004	−0.046	0.003
	393.15	−0.054	0.003	−0.048	0.003
n-C$_{20}$ + Ethylbenzene	323.15	−0.020	0.040	−0.009	0.040
	333.15	−0.022	0.028	−0.012	0.028
	343.15	−0.025	0.021	−0.015	0.020
	353.15	−0.028	0.015	−0.018	0.014
	363.15	−0.030	0.011	−0.020	0.010
	373.15	−0.031	0.009	−0.023	0.008
	383.15	−0.033	0.007	−0.025	0.006
	393.15	−0.034	0.005	−0.027	0.005
n-C$_{20}$ + n-Propylbenzene	333.15	−0.012	0.052	−0.006	0.049
	343.15	−0.008	0.040	0.002	0.040
	353.15	−0.010	0.028	−0.002	0.028
	363.15	−0.013	0.020	−0.004	0.021
	373.15	−0.014	0.015	−0.006	0.015
	383.15	−0.017	0.012	−0.009	0.011
	393.15	−0.019	0.009	−0.012	0.009
n-C$_{20}$ + p-Xylene	323.15	−0.019	0.044	−0.010	0.043
	333.15	−0.021	0.031	−0.011	0.031
	343.15	−0.024	0.023	−0.014	0.022
	353.15	−0.026	0.016	−0.017	0.016
	363.15	−0.029	0.012	−0.021	0.012
	373.15	−0.030	0.009	−0.023	0.009
	383.15	−0.032	0.007	−0.025	0.007
	393.15	−0.034	0.006	−0.028	0.006
n-C$_{24}$ + Benzene	333.15	−0.089	0.005	−0.079	0.004
	343.15	−0.086	0.003	−0.077	0.003
	353.15	−0.085	0.002	−0.076	0.003
	363.15	−0.084	0.002	−0.075	0.002
	373.15	−0.083	0.002	−0.075	0.002
	383.15	−0.084	0.003	−0.076	0.003
	393.15	−0.084	0.003	−0.076	0.003
n-C$_{24}$ + Toluene	**333.15**	**−0.083**	**0.004**	**−0.075**	**0.004**
	343.15	−0.078	0.003	−0.069	0.003
	353.15	−0.076	0.003	−0.067	0.002
	363.15	−0.076	0.005	−0.068	0.004
	373.15	−0.074	0.003	−0.067	0.003
	383.15	−0.073	0.003	−0.066	0.002
	393.15	−0.073	0.002	−0.066	0.002
n-C$_{24}$ +	333.15	−0.050	0.027	−0.041	0.028
	343.15	−0.052	0.021	−0.043	0.022

Ethylbenzene	353.15	−0.056	0.011	−0.045	0.013
	363.15	−0.057	0.010	−0.048	0.012
	373.15	−0.054	0.005	−0.046	0.006
	383.15	−0.057	0.006	−0.049	0.007
	393.15	−0.055	0.002	−0.048	0.003
n-C$_{24}$ + n-Propylbenzene	343.15	−0.047	0.047	−0.038	0.048
	353.15	−0.046	0.033	−0.036	0.032
	363.15	−0.045	0.023	−0.037	0.023
	373.15	−0.042	0.017	−0.034	0.016
	383.15	−0.043	0.013	−0.036	0.013
	393.15	−0.042	0.009	−0.035	0.010
n-C$_{24}$ + p-Xylene	333.15	−0.050	0.031	−0.041	0.032
	343.15	−0.056	0.024	−0.044	0.022
	353.15	−0.050	0.017	−0.042	0.017
	363.15	−0.050	0.012	−0.043	0.013
	373.15	−0.051	0.009	−0.044	0.009
	383.15	−0.053	0.007	−0.046	0.007
	393.15	−0.054	0.005	−0.048	0.005
n-C$_{28}$ + Benzene	**353.15**	**−0.107**	**0.003**	**−0.098**	**0.003**
	363.15	−0.103	0.003	−0.094	0.002
	373.15	−0.103	0.002	−0.094	0.002
	383.15	−0.100	0.000	−0.092	0.000
	393.15	−0.097	0.003	−0.089	0.003
n-C$_{28}$ + Toluene	353.15	−0.086	0.008	−0.077	0.008
	363.15	−0.085	0.005	−0.077	0.006
	373.15	−0.084	0.004	−0.076	0.005
	383.15	−0.084	0.003	−0.077	0.004
	393.15	−0.084	0.002	−0.077	0.003
n-C$_{28}$ + Ethylbenzene	353.15	−0.070	0.016	−0.062	0.017
	363.15	−0.068	0.012	−0.060	0.012
	373.15	−0.067	0.009	−0.060	0.009
	383.15	−0.069	0.007	−0.061	0.007
	393.15	−0.069	0.005	−0.062	0.006
n-C$_{28}$ + n-Propylbenzene	353.15	−0.057	0.032	−0.049	0.033
	363.15	−0.055	0.023	−0.047	0.023
	373.15	−0.053	0.016	−0.046	0.017
	383.15	−0.053	0.012	−0.045	0.012
	393.15	−0.053	0.009	−0.046	0.009
n-C$_{28}$ + p-Xylene	353.15	−0.068	0.018	−0.059	0.017
	363.15	−0.065	0.013	−0.057	0.013
	373.15	−0.069	0.006	−0.061	0.005
	383.15	−0.065	0.007	−0.058	0.007
	393.15	−0.066	0.006	−0.059	0.006
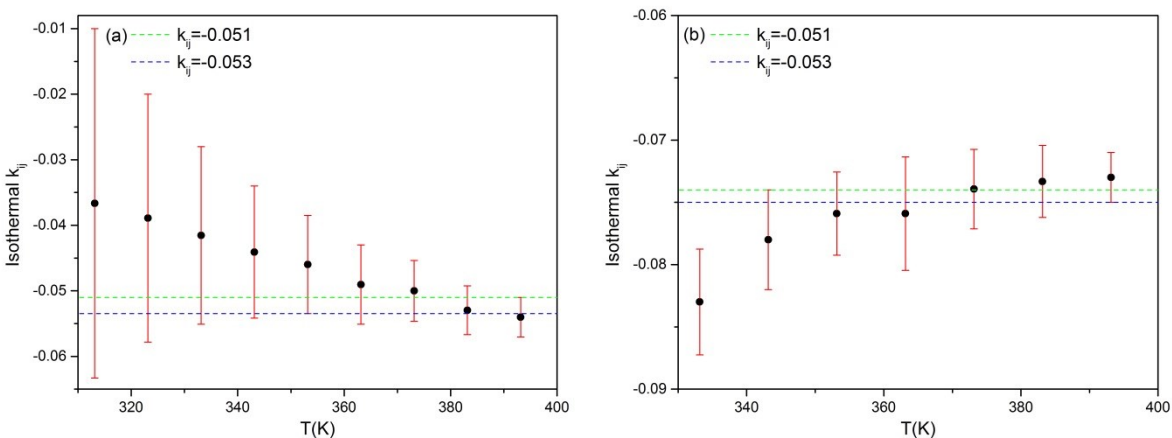
Figure 4.5 Uncertainty analysis of temperature–independent k_{ij} values for PR EOS for a) toluene + n-C_{20} b) toluene + n-C_{24}. The black dots are isothermal k_{ij} values regressed at different temperatures (shown in Table 4.10). Green and blue dash lines stand for the upper and lower bounds of temperature–independent k_{ij} values (reported in Table 4.7), respectively.

4.4.2 Impact of input parameter variability

4.4.2.1 Impact of critical properties for cubic EOS

For cubic EOS such as the PR and SRK EOS, using different sets of critical properties impacts calculated BPPs, and hence, regressed k_{ij} values. In this work, the critical properties used for calculation are from the NIST/TDE database and were used directly. The uncertainties associated with T_c, P_c from this database are shown previously in Table 4.2. For long chain n-alkanes, critical property uncertainty can be large relative to the uncertainty for aromatics, and this uncertainty propagates through to uncertainties of for regressed k_{ij} values. A case study of toluene + n-octacosane is presented here to show the impact of uncertainties in critical properties (T_c and P_c) on regressed k_{ij} values. Critical properties for these two compounds, retrieved from the NIST/TDE database, are summarized in Table 4.11.

Table 4.11 Critical properties for toluene and octacosane with reported uncertainties[1]

Compound	T_c (K)	P_c (kPa)
Toluene	591.89 ±0.02	4126 ± 66
Octacosane	824 ±8	750 ±137

To study the sensitivity of regressed k_{ij} values to variations of critical properties, three sets of critical temperatures combined with three sets of critical pressures for n-C$_{28}$, representing the upper, mean and lower bounds respectively, are used to regress the k_{ij} values based on the same set of experimental data (toluene + n-C$_{28}$ at 363.15 K). The mean T_c and P_c are used for toluene (T_c = 591.89 K, P_c = 4126 kPa). Results are shown in Table 4.12. Using a higher P_c or a higher T_c for n-C$_{28}$ leads to increased k_{ij} values. Conversely using lower T_c and P_c leads to lower regressed k_{ij} values. The large uncertainty of P_c for long chain n-alkanes has a significant impact on the uncertainty of regressed k_{ij}s for binaries containing these compounds, as demonstrated in Figure 4.6, where 3 sets of critical properties of n-C$_{28}$ (lower bound: T_c = 816 K, P_c = 613 kPa; mean: T_c = 824 K, P_c = 750 kPa; upper bound: T_c = 832 K, P_c = 888 kPa) are used to compute the BPPs for toluene + n-C$_{28}$ at 363.15 K. For k_{ij} = 0, the lower bound critical properties lead to the largest deviation between calculated and experimental data. Hence, the regressed k_{ij} value is the lowest. It is worth noting that the invariance of phase boundary pressure with composition in Figure 4.6 indicates liquid–liquid equilibria and illustrates incorrect prediction of the phase behavior type at k_{ij} = 0. By contrast, the uncertainties of critical properties for aromatic components impact the regressed k_{ij} values in a secondary manner. For toluene + n-C$_{28}$ at 363.15 K, with mean values

for n-C_{28} critical properties (T_c = 824 K, P_c = 750 kPa), k_{ij} values differ little as shown in Table 4.13.

Table 4.12 Regressed k_{ij} values based on input parameter uncertainty range for n-C_{28}

T_c (K) for n-C_{28}	P_c (kPa) for n-C_{28}	Regressed k_{ij} values at 363.15 K
816	613	−0.122
	750	−0.087
	888	−0.064
824	613	−0.120
	750	−0.085
	888	−0.063
832	613	−0.118
	750	−0.084
	888	−0.061
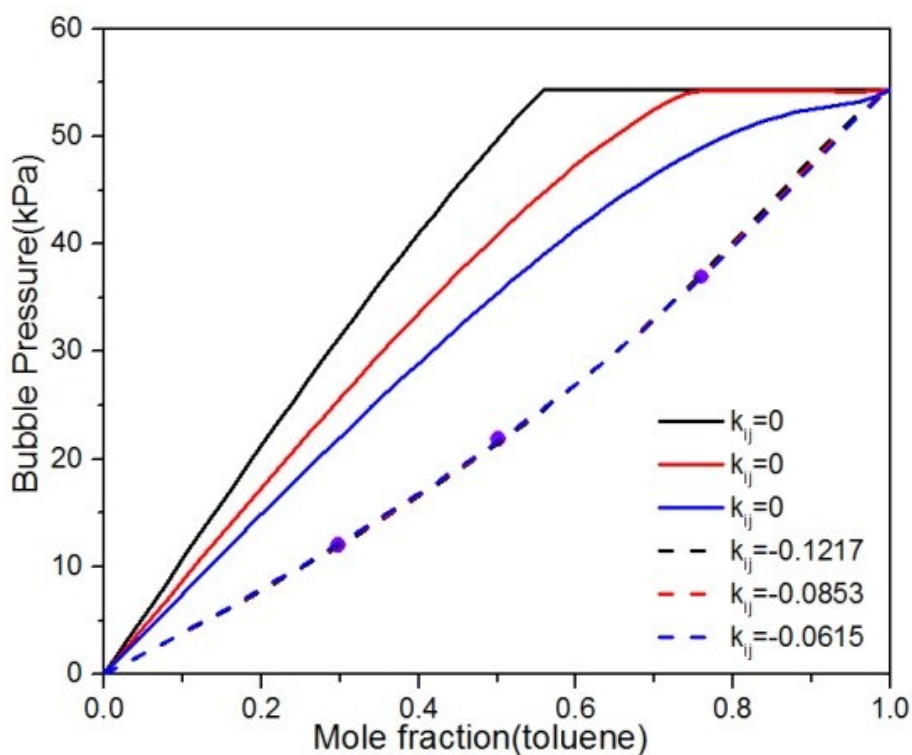
Figure 4.6 Computed VLE and regressed k_{ij} values for toluene + n-C_{28} mixture at 363.15 K based on 3 sets of critical properties of n-C_{28} (lower bound: T_c = 816 K, P_c = 613 kPa; mean: T_c = 824 K, P_c = 750 kPa; upper bound: T_c = 832 K, P_c = 888 kPa). Computed results from PR EOS using lower, mean and upper bound are shown in black, red and blue line, respectively. k_{ij} values used in calculation are: (—)k_{ij} = 0, (---) fitted k_{ij}, represented by solid and dashed line.

Table 4.13 Regressed k_{ij} values based on input parameter uncertainty for toluene

T_c (K) for toluene	P_c (kPa) for toluene	Regressed k_{ij}s at 363.15 K
	4059.7412	−0.080
591.87	4125.5165	−0.085
	4191.2918	−0.091
	4059.7412	−0.080
591.89	4125.5165	−0.085
	4191.2918	−0.090
	4059.7412	−0.080
591.91	4125.5165	−0.085
	4191.2918	−0.090

4.4.2.2 Impact of input parameters (PC-SAFT)

The impact of using different input parameters was also evaluated for PC–SAFT EOS. In the literature, multiple sets of segment number (m), segment diameter (σ) and segment–segment energy (ε/k) co-exist for long chain n-alkanes, as these parameters have been estimated using different methods[5]. For the toluene + octacosane binary, five sets of parameters for n-C_{28} retrieved from different references are shown in Table 4.14. Their impacts on predicted VLE data were evaluated. These sets of parameters have at best a secondary impact on calculated BPPs as shown in Figure 4.7. Only when rescaled parameters (Set 5) are used, do some discrepancies arise at high temperatures.

Table 4.14 PC–SAFT input parameters for n-C_{28} estimated by different methods[5]

n-C_{28}	m	σ (Å)	ε/k (K)	Reference
Set 1	11.083	3.9789	255.62	Tihic et al.[5]
Set 2	10.923	4.0069	261.6	von Solms et al.[6]
Set 3	10.8004	4.0019	255.67	Tihic et al.[5]
Set 4	10.3622	4.0217	252.0	Agarwal et al.[7]
Set 5	11.2201	4.1740	252.0119	Cismondi et al.[8]
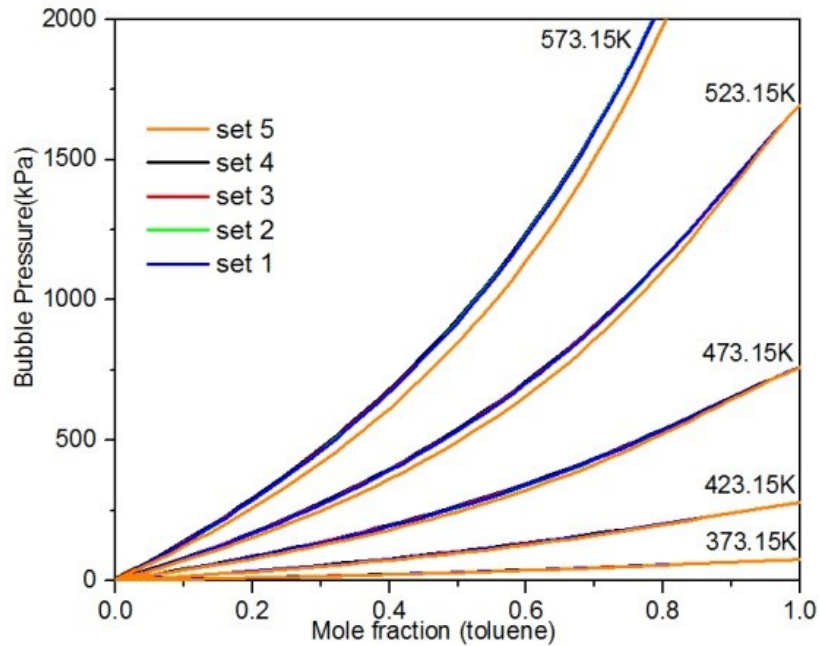
Figure 4.7 Impact of using different sets of pure component parameters on predicted VLE for PC–SAFT EOS for toluene + n-C_{28} mixture at different temperatures. Calculated outcomes using parameter sets 1–5 are represented by blue, green, red, black and orange line, respectively.

4.5 Impact of mixing rule selection on computed outcomes for cubic EOS

Computed results of PR EOS with Wong–Sandler mixing rule[9] (PRWS), PR EOS with Modified Huron–Vidal(2) mixing rule[10] (PRMHV2), and Predictive-SRK(PSRK)[11] EOS are compared with experimental data in Figure 4.8. For this comparison $k_{ij} = 0$. The performance of cubic EOS using these mixing rules is evaluated by the AAD of predicted VLE to experimental data. Results for 15 types binary mixtures listed in Table 1.1 at 353.15 K are presented as illustrative cases. Results for the PR and SRK EOS using classic vdW1f mixing rules with $k_{ij} = 0$ are presented as reference calculations.
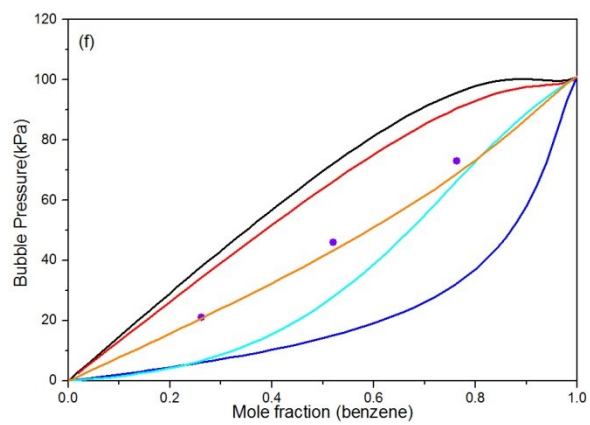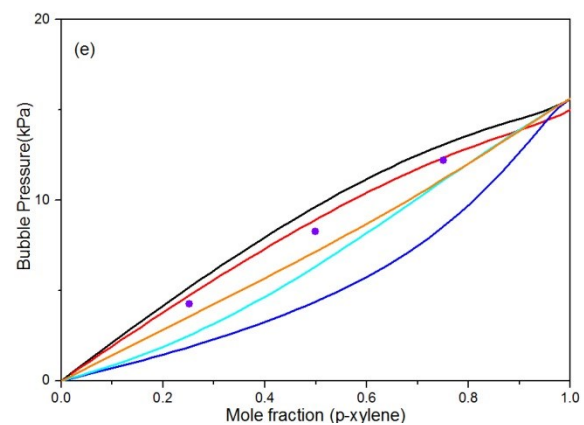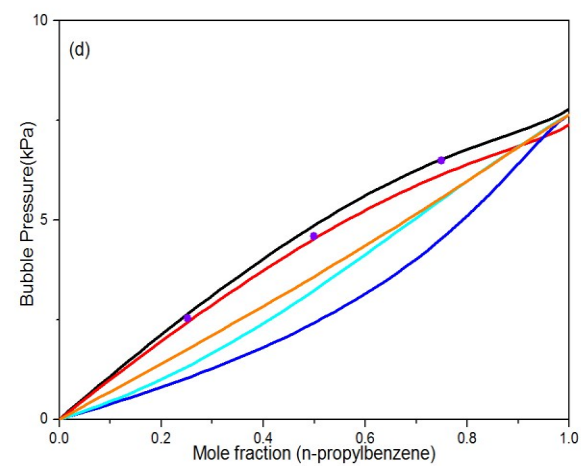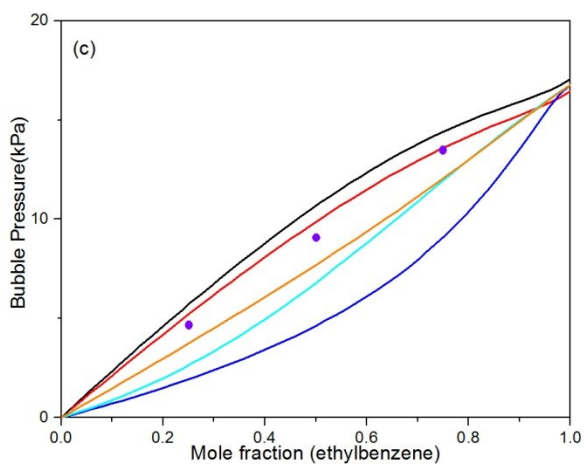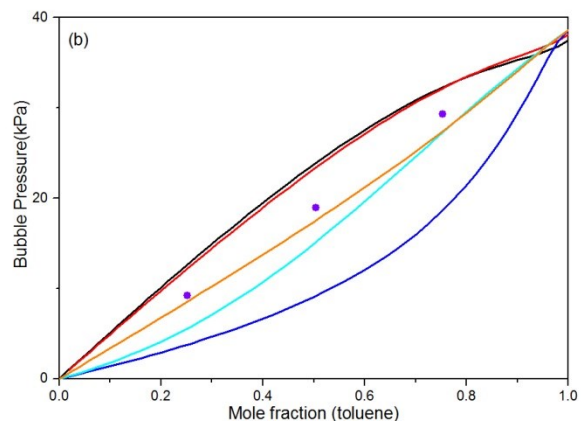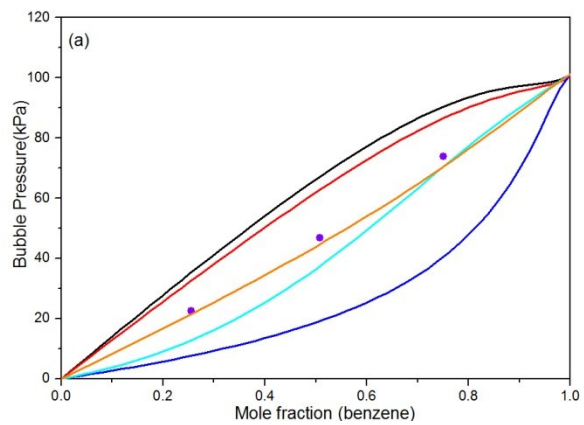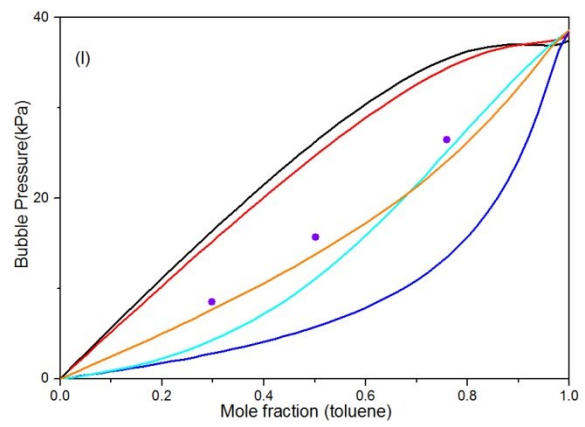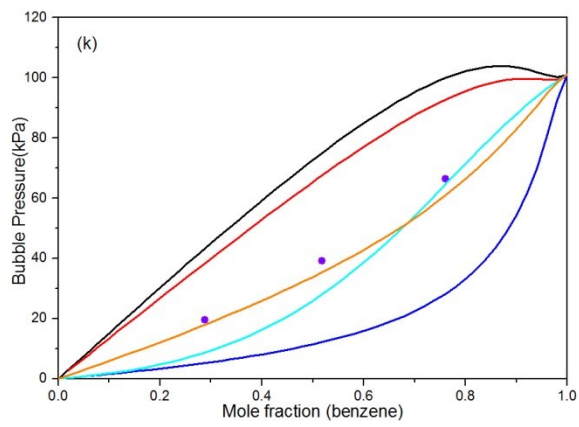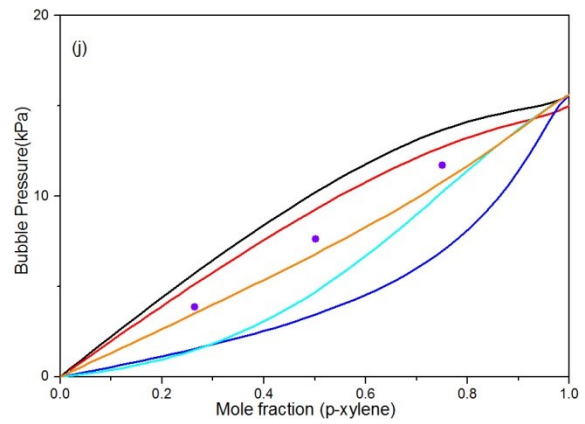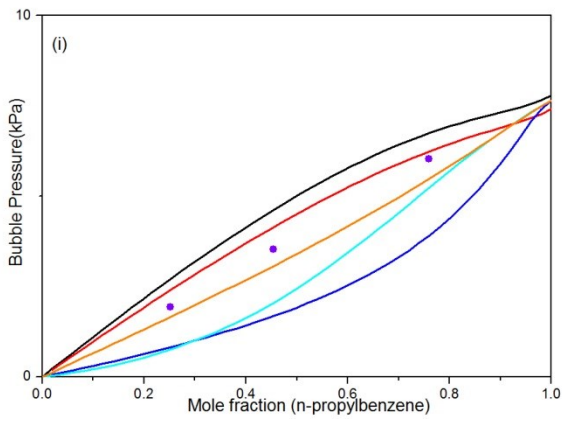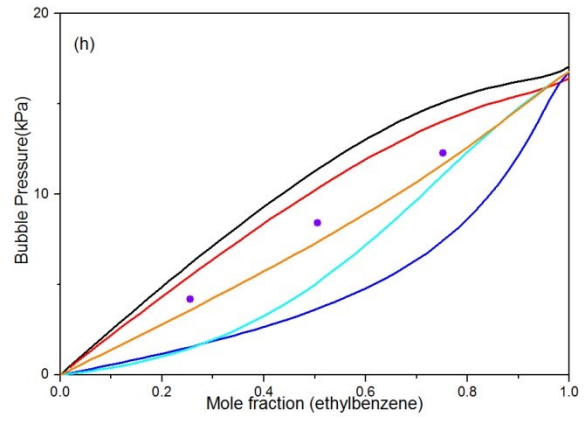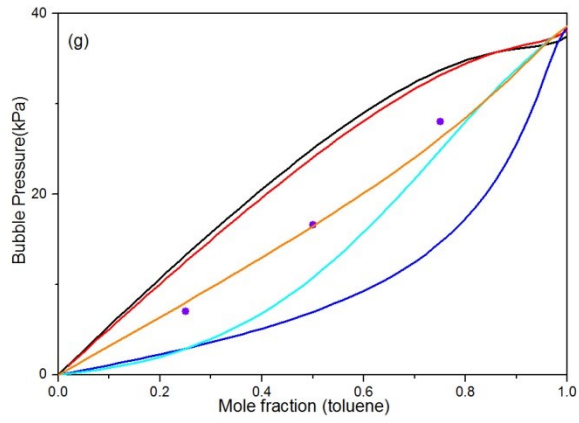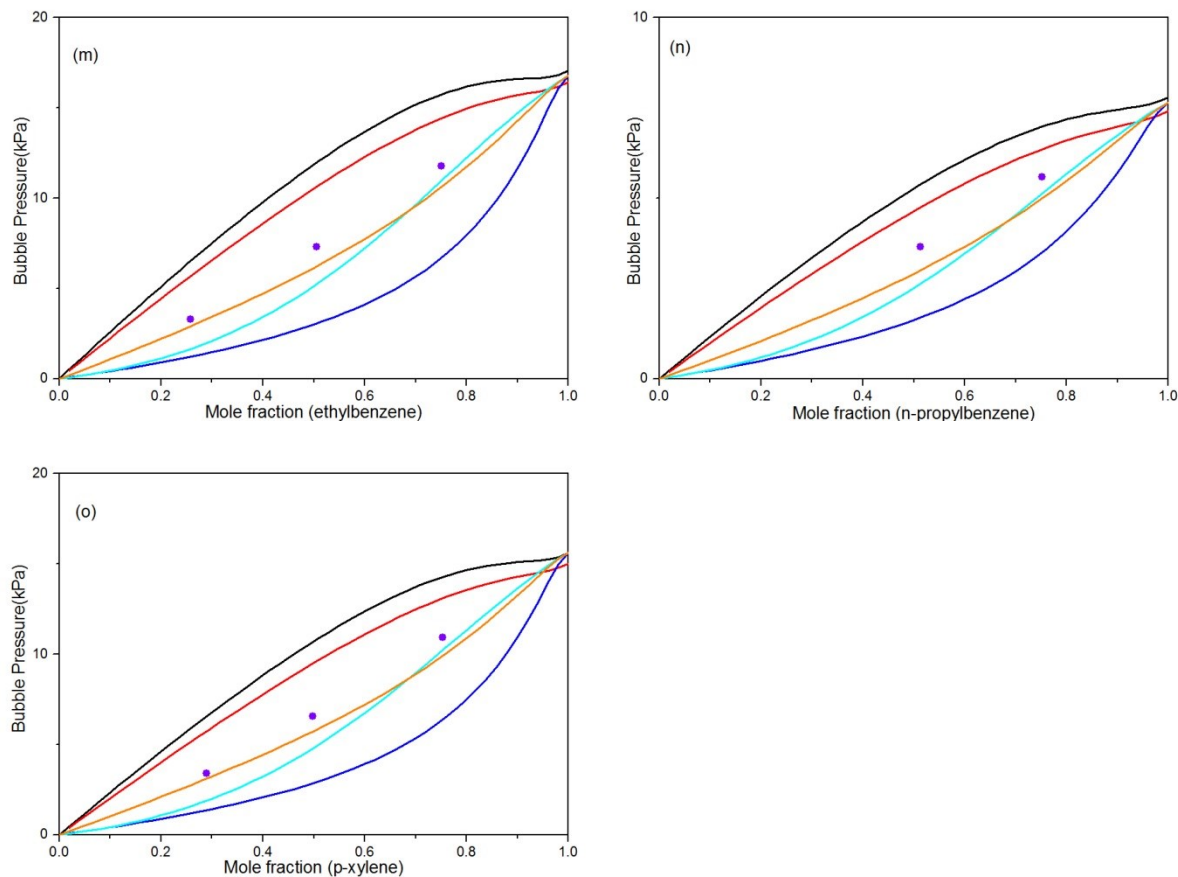
Figure 4.8 Computed VLE for binary mixtures at 353.15 K using cubic EOS with $k_{ij} = 0$ and diverse mixing rules: (——) PR EOS with classical mixing rule; (——) SRK EOS with classical mixing rule; (——) PR EOS with WS mixing rule; (——) PR with MHV2 mixing rule; (——) PSRK EOS. (a) benzene + n-C_{20}, (b) toluene + n-C_{20}, (c) ethylbenzene + n-C_{20}, (d) n-propylbenzene + n-C_{20}, (e) p-xylene + n-C_{20}, (f) benzene + n-C_{24}, (g) toluene + n-C_{24}, (h) ethylbenzene + n-C_{24}, (i) n-propylbenzene + n-C_{24}, (j) p-xylene + n-C_{24}, (k) benzene + n-C_{28}, (l) toluene + n-C_{28}, (m) ethylbenzene + n-C_{28}, (n) n-propylbenzene + n-C_{28}, (o) p-xylene + n-C_{28} using different k_{ij} values.

The PSRK mixing rule provides the closest match to experimental data, as illustrated in Figure 4.9. Using the MHV2 mixing rule for the PR EOS slightly increases the prediction accuracy for the PR EOS. PR with Wong–Sandler mixing rules significantly underestimates the BPPs for selected mixtures, and is not recommended. Overall alternative mixing rules tend to work better for mixtures with large size asymmetry. The over prediction of BPPs for cubic EOS with classical vdW1f mixing rule suggests that classical mixing rules do not account for the non-

randomness of mixing that arises in these mixtures. Alternative excess Gibbs energy mixing rules based on local composition can enhance the performance of traditional cubic EOS but they must be used with caution as this advantage is not universal. Adopting appropriate k_{ij} values and using classical mixing rules remains preferred.
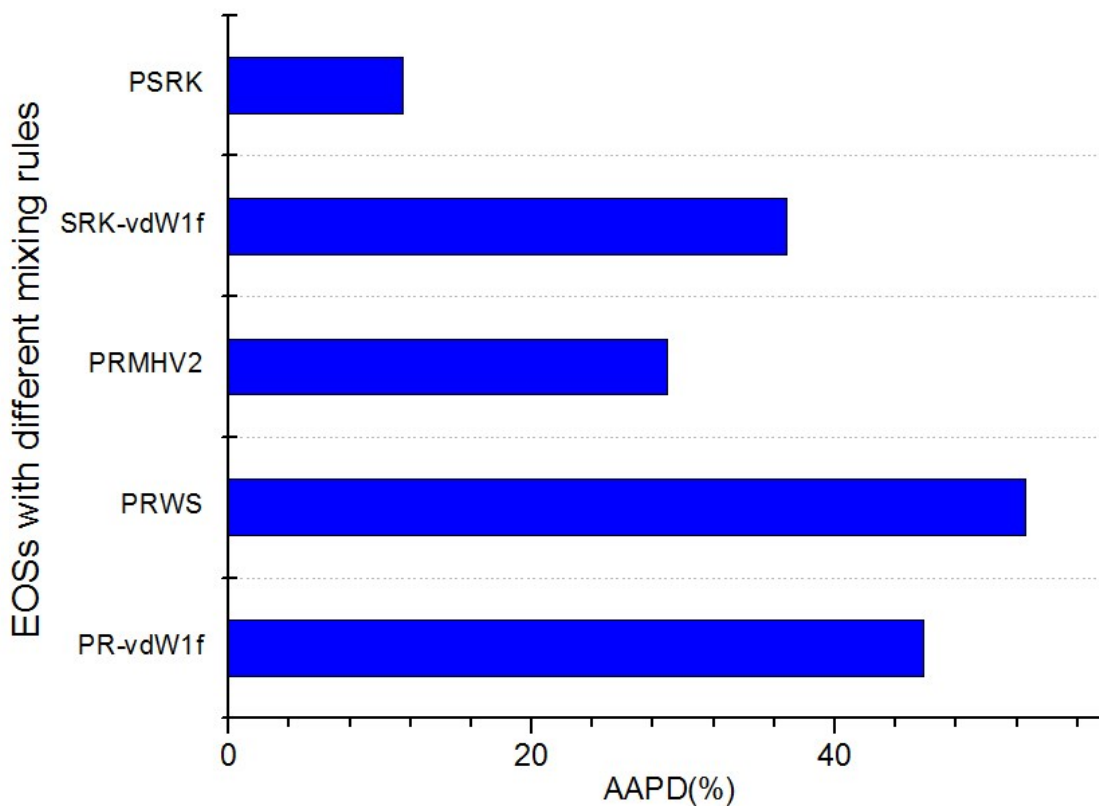
Figure 4.9 AAPD of predicted VLE for PR and SRK EOS variants (with $k_{ij} = 0$)

4.6 Performance of other EOS for predicting BPPs for aromatic + long chain alkane binaries at low pressure

The performance of activity coefficient models such as NRTL[12], UNIFAC[13] and COSMO-SAC[14] is evaluated and compared to the performance of cubic and PC–SAFT EOS results. An illustrative example is shown in Figure 4.10, where the calculated VLE for all binaries listed in Table 1.1 at 353.15 K is presented. Calculations were performed in Aspen Plus. For the n-C_{28} series, results for COSMO–SAC are not reported because the parameters required for n-C_{28} are not available. Activity coefficient models like UNIFAC have low deviations from experimental BPP data, and the deviations are not impacted significantly by size asymmetry. Models based on quantum chemistry such as COSMO–SAC also provide satisfactory results comparable to the PC–SAFT EOS. An overview of outcomes is provided in Figure 4.11. The PR and SRK cubic EOS with $k_{ij} = 0$ and vdW1f mixing rules give poor BPP predictions and fail to provide the correct phase behavior type for highly asymmetric binary mixtures. PC–SAFT provides correct phase behaviors consistently, even if the BPP estimates are not fully quantitative and it acts as threshold for successful methods. Neither the PSRK nor the NRTL meet this threshold. Only UNIFAC and COSMO–SAC do better than PC–SAFT without requiring data to fit outcomes. These methods can also be recommended in the absence of data for direct use or to fit k_{ij} values for cubic EOS in process simulators or in custom codes.
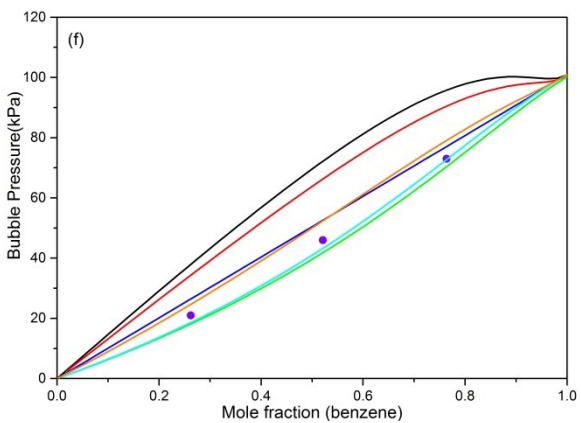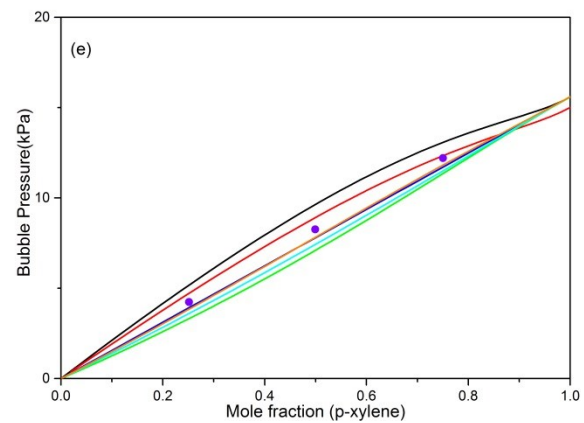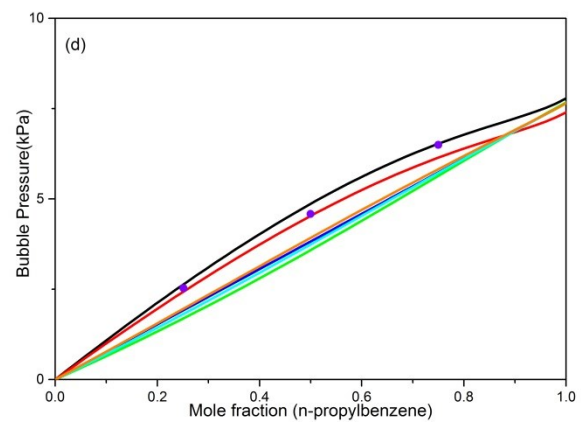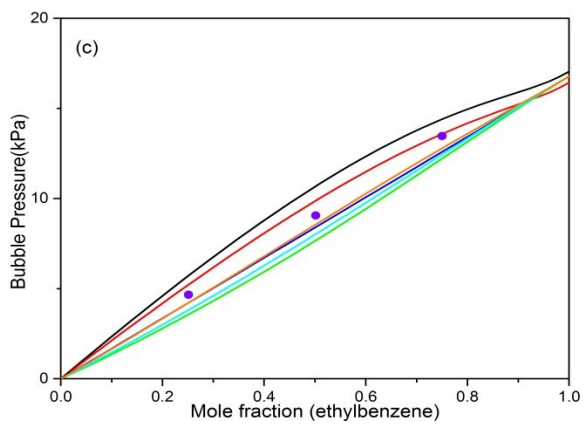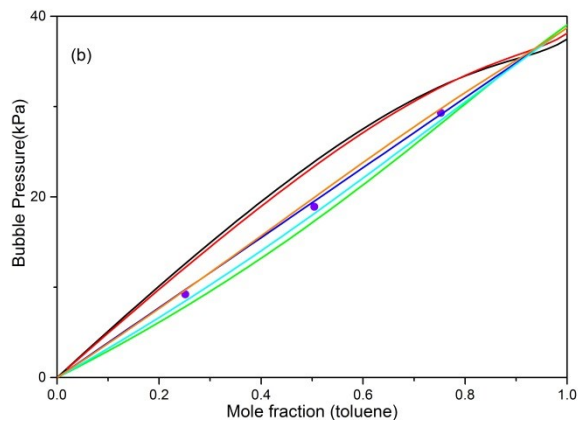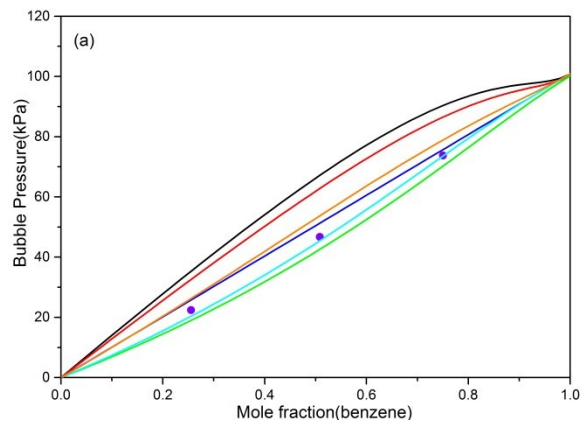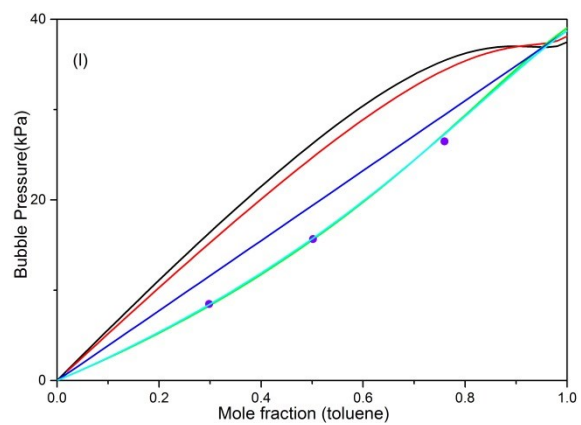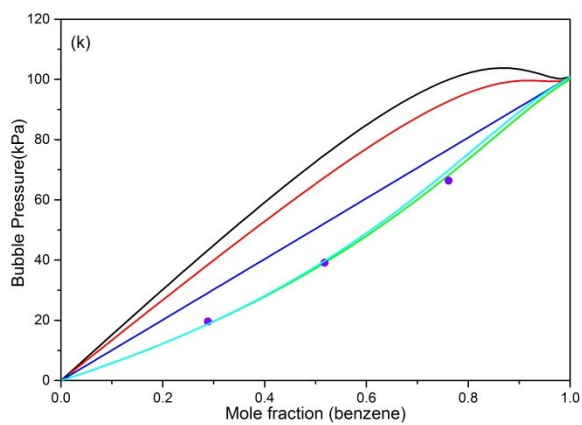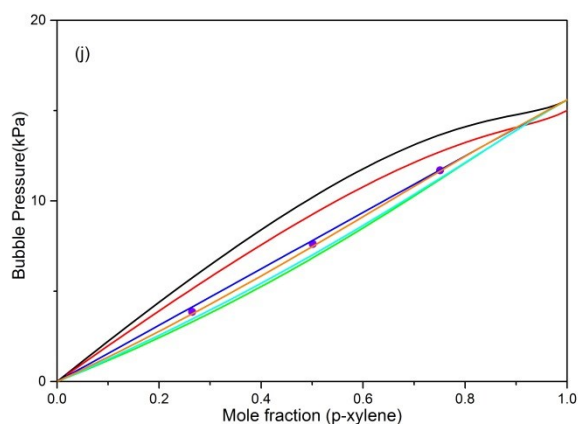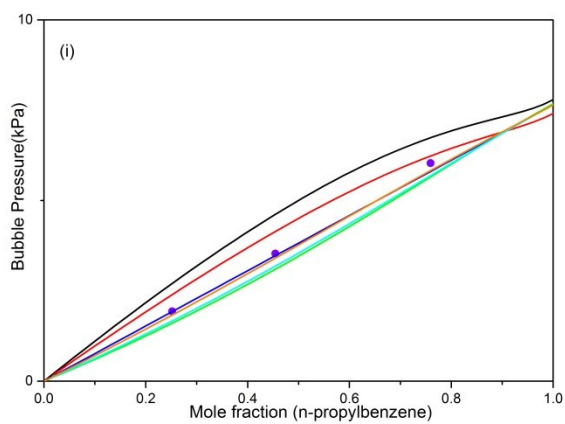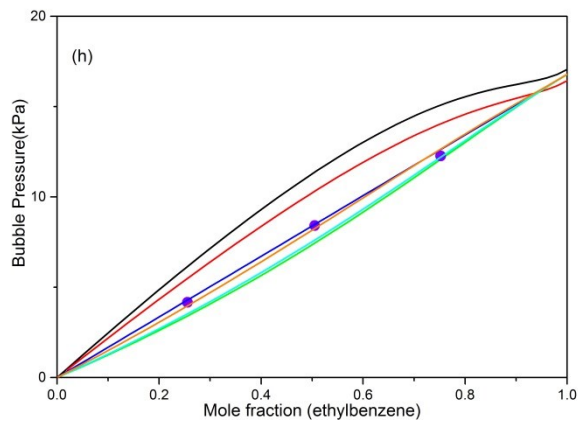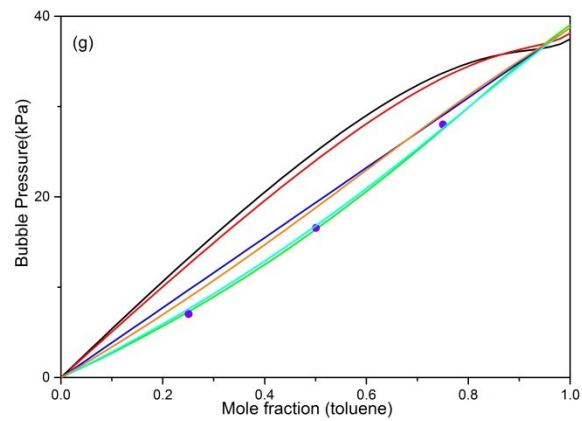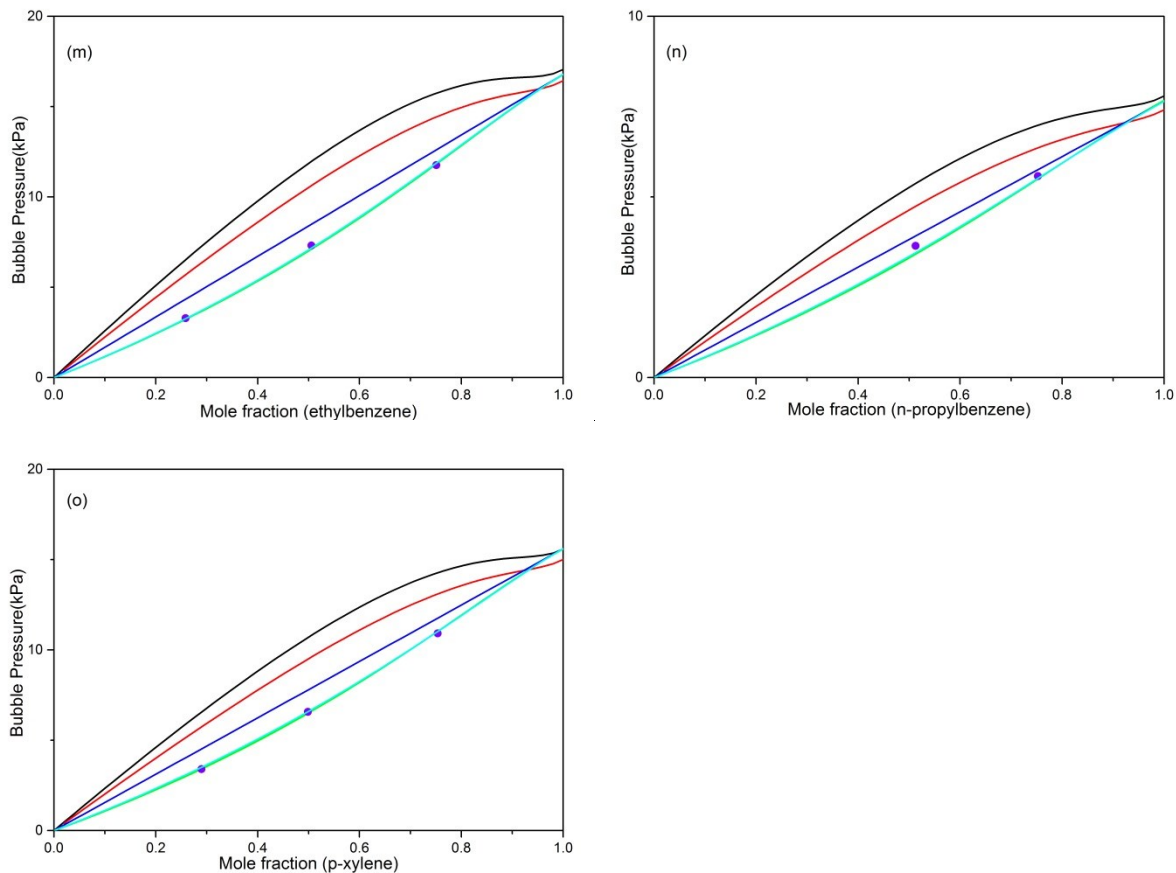
Figure 4.10 Computed VLE from different EOS for selected mixtures at 353.15 K. (——) PR EOS with classical mixing rule; (——) SRK EOS with classical mixing rule; (——) NRTL ; (——) UNIFAC; (——) COSMO–SAC;(——)PC–SAFT EOS. (a) benzene + n-C_{20}, (b) toluene + n-C_{20}, (c) ethylbenzene + n-C_{20}, (d) n-propylbenzene + n-C_{20}, (e) p-xylene + n-C_{20}, (f) benzene + n-C_{24}, (g) toluene + n-C_{24}, (h) ethylbenzene + n-C_{24}, (i) n-propylbenzene + n-C_{24}, (j) p-xylene + n-C_{24}, (k) benzene + n-C_{28}, (l) toluene + n-C_{28}, (m) ethylbenzene + n-C_{28}, (n) n-propylbenzene + n-C_{28}, (o) p-xylene + n-C_{28} using different k_{ij} values.
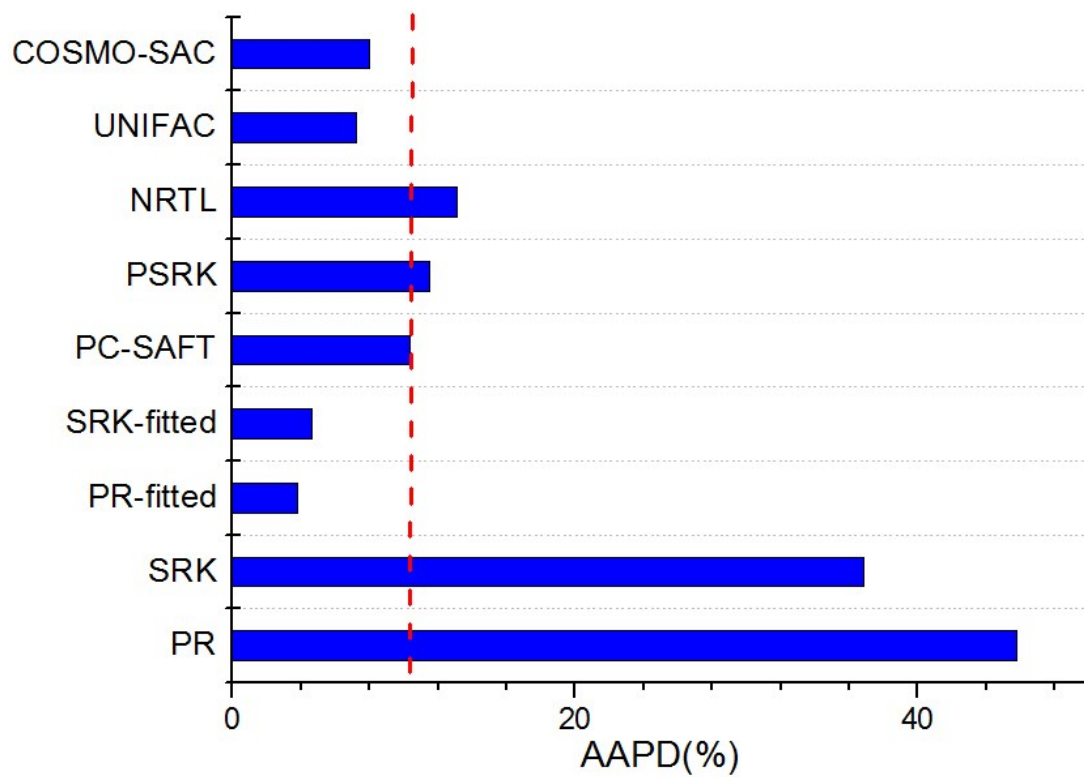
Figure 4.11 Summary of BPP predictions for aromatic + long chain binary mixtures using different thermodynamic models.

4.7 References

1. *NIST Standard Reference Database 103b*: NIST ThermoData Engine*, Version 7.1, accessed from Aspen Plus.

2. VMGSim Process Simulator, Version 9.5. Virtual Materials Group Inc.: Calgary, AB 2016

3. Aspen Plus, Version 8.8. Aspen Technology Inc.: Burlington, MA 2015

4. Gross, J.; Sadowski, G. Perturbed-chain SAFT: An equation of state based on a perturbation theory for chain molecules. *Ind Eng Chem Res* **2001***, 40*, 1244-1260.

5. Tihic, A.; Kontogeorgis, G. M.; von Solms, N.; Michelsen, M. L. Applications of the simplified perturbed-chain SAFT equation of state using an extended parameter table. *Fluid Phase Equilib.* **2006***, 248*, 29-43.

6. von Solms, N.; Michelsen, M. L.; Kontogeorgis, G. M. Computational and physical performance of a modified PC-SAFT equation of state for highly asymmetric and associating mixtures. *Ind Eng Chem Res* **2003***, 42*, 1098-1105.

7. Agarwal, R.; Prasad, D.; Maity, S.; Gayen, K.; Ganguly, S. Experimental measurement and model based inferencing of solubility of polyethylene in xylene. *J. Chem. Eng. Japan* **2004***, 37*, 1427-1435.

8. Cismondi, M.; Brignole, E. A.; Mollerup, J. Rescaling of three-parameter equations of state: PC-SAFT and SPHCT. *Fluid Phase Equilib.* **2005***, 234*, 108-121.

9. Wong, D. S. H.; Sandler, S. I. A theoretically correct mixing rule for cubic equations of state. *AIChE J.* **1992***, 38*, 671-680.

10. Dahl, S.; Fredenslund, A.; Rasmussen, P. The MHV2 model: a UNIFAC-based equation of state model for prediction of gas solubility and vapor-liquid equilibria at low and high pressures. *Ind Eng Chem Res* **1991***, 30*, 1936-1945.

11. Holderbaum, T.; Gmehling, J. PSRK: a group contribution equation of state based on UNIFAC. *Fluid Phase Equilib.* **1991***, 70*, 251-265.

12. Renon, H.; Prausnitz, J. M. Local compositions in thermodynamic excess functions for liquid mixtures. *AIChE J.* **1968***, 14*, 135-144.

13. Fredenslund, A.; Jones, R. L.; Prausnitz, J. M. Group-contribution estimation of activity coefficients in nonideal liquid mixtures. *AIChE J.* **1975***, 21*, 1086-1099.

14. Lin, S.; Sandler, S. I. A priori phase equilibrium prediction from a segment contribution solvation model. *Ind Eng Chem Res* **2002***, 41*, 899-913.

Chapter 5. Conclusions and Future Work

5.1 Conclusions

Bubble point pressures (BPPs) for 15 representative binary aromatic + n-alkane hydrocarbon mixtures were obtained in this work. The measurement method was validated and the quality of the experimental data was evaluated.

The experimental data were compared with computed outcomes for the Peng–Robinson (PR), Soave–Redlich–Kwong (SRK) and Perturbed–Chain Statistical Associating Fluid Theory (PC–SAFT) EOS, with $k_{ij} = 0$. The PC–SAFT EOS underestimates BPP values systematically but the outcomes are semi-quantitative. The cubic EOS systematically over-predict the BPPs for aromatic + long chain alkane binaries. They provide poor estimates for BPPs or indicated incorrect liquid–liquid phase behavior. Temperature–independent k_{ij} values were regressed from the experimental data. These k_{ij} values are negative and trend toward larger negative values with increased size asymmetry. These atypical k_{ij} values, the vdW1f mixing rules, and pure compound data from NIST are required for quantitative VLE estimation for aromatic + long chain n-alkane mixtures using either the PR or SRK EOS.

BPP data were also used to evaluate other computational approaches including the NRTL, UNIFAC and COSMO–SAC activity coefficient based models. These models provide good BPP prediction for aromatic + long chain n-alkane hydrocarbon mixtures at low pressure without modification. The UNIFAC and COSMO–SAC activity coefficient models are preferred over the PC–SAFT EOS and are recommended for quantitative BPP prediction, at low pressure, in the absence of experimental data if parameters for relevant compounds are available.

Alternative mixing rules for cubic EOS, including Wong–Sandler, Modified Huron–Vidal and PSRK mixing rules were tested. The PSRK mixing rules were found to be superior to the others. These mixing rules exhibit advantages for highly asymmetric mixtures over classical mixing rule, but must be used with caution as the advantages they convey are not universal. Overall, vdW1f mixing rules are preferred.

5.2 Future work

1. Perform BPP experiments for binary hydrocarbon mixtures such as naphthenic + large alkane, and alkane + polynuclear aromatic binaries, including branched alkanes.

2. Extend the temperature range for BPP data acquisition to higher temperatures to determine if k_{ij} values possess temperature dependence.

3. Measurement of other thermophysical properties, such as solubility, density and enthalpy of mixing for binary mixtures studied in this work, and examine whether regressed k_{ij} reported from this work would improve the prediction of other thermophysical properties.

4. Develop a correlation or a work flow for cubic EOS k_{ij} value calculation valid for aromatic and naphthenic + alkane mixtures including branched alkanes that combines BPP data with computed estimates based on the UNIFAC or COSMO–SAC models if parameters are available.

Bibliography

Agarwal, R.; Prasad, D.; Maity, S.; Gayen, K.; Ganguly, S. Experimental measurement and model based inferencing of solubility of polyethylene in xylene. *J. Chem. Eng. Japan* **2004**, *37*, 1427-1435.

Ahitan, S.; Satyro, M. A.; Shaw, J. M. Systematic misprediction of n-alkane + aromatic and naphthenic hydrocarbon phase behavior using common equations of state. *Journal of Chemical & Engineering Data* **2015**, *60*, 3300-3318.

Ahitan, S.; Shaw, J. M. Quantitative comparison between predicted and experimental binary n-alkane benzene phase behaviors using cubic and PC-SAFT EOS. *Fluid Phase Equilib.* **2016**, *428*, 4-17.

Aim, K. A modified ebulliometric method for high-boiling substances: vapour pressures of 2-chlorobenzonitrile and 4-chlorobenzonitrile at temperatures from 380 K to 490 K. *The Journal of Chemical Thermodynamics* **1994**, *26*, 977-986.

Aim, K. Measurement of vapor-liquid equilibrium in systems with components of very different volatility by the total pressure static method. *Fluid Phase Equilib.* **1978**, *2*, 119-142.

Altgelt, K. H. *Composition and analysis of heavy petroleum fractions;* CRC Press: 1993.

Ambrose, D.; Ewing, M. B.; Ghiassee, N. B.; Ochoa, J. S. The ebulliometric method of vapour-pressure measurement: vapour pressures of benzene, hexafluorobenzene, and naphthalene. *The Journal of Chemical Thermodynamics* **1990**, *22*, 589-605.

Anderko, A. Equation-of-state methods for the modelling of phase equilibria. *Fluid Phase Equilib.* **1990**, *61*, 145-225.

Aspen Plus, Version 8.8. Aspen Technology Inc.: Burlington, MA 2015.

Blas, F. J.; Vega, L. F. Prediction of binary and ternary diagrams using the statistical associating fluid theory (SAFT) equation of state. *Ind Eng Chem Res* **1998**, *37*, 660-674.

Boukouvalas, C.; Spiliotis, N.; Coutsikos, P.; Tzouvaras, N.; Tassios, D. Prediction of vapor-liquid equilibrium with the LCVM model: a linear combination of the Vidal and Michelsen mixing rules coupled with the original UNIF. *Fluid Phase Equilib.* **1994**, *92*, 75-106.

Chapman, W. G.; Gubbins, K. E.; Jackson, G.; Radosz, M. SAFT: equation-of-state solution model for associating fluids. *Fluid Phase Equilib.* **1989**, *52*, 31-38.

Christov, M.; Dohrn, R. High-pressure fluid phase equilibria: experimental methods and systems investigated (1994–1999). *Fluid Phase Equilib.* **2002**, *202*, 153-218.

Cismondi, M.; Brignole, E. A.; Mollerup, J. Rescaling of three-parameter equations of state: PC-SAFT and SPHCT. *Fluid Phase Equilib.* **2005***, 234*, 108-121.

Coutinho, J. A.; Kontogeorgis, G. M.; Stenby, E. H. Binary interaction parameters for nonpolar systems with cubic equations of state: a theoretical approach 1. CO_2/hydrocarbons using SRK equation of state. *Fluid Phase Equilib.* **1994***, 102*, 31-60.

Dahl, S.; Fredenslund, A.; Rasmussen, P. The MHV2 model: a UNIFAC-based equation of state model for prediction of gas solubility and vapor-liquid equilibria at low and high pressures. *Ind Eng Chem Res* **1991***, 30*, 1936-1945.

Dahl, S.; Michelsen, M. L. High-pressure vapor-liquid equilibrium with a UNIFAC-based equation of state. *AIChE J.* **1990***, 36*, 1829-1836.

de Loos, T. W.; Van der Kooi, Hedzer J; Ott, P. L. Vapor-liquid critical curve of the system ethane 2-methylpropane. *J. Chem. Eng. Data* **1986***, 31*, 166-168.

DECHEMA Gesellschaft für Chemische Technik und Biotechnologie e.V Website. http://dechema.de/ (accessed Dec 20, 2016).

Design Institute for Physical Property Data Website. https://www.aiche.org/dippr (accessed Dec 20, 2016).

Dohrn, R.; Brunner, G. High-pressure fluid-phase equilibria: experimental methods and systems investigated (1988–1993). *Fluid Phase Equilib.* **1995***, 106*, 213-282.

Dohrn, R.; Peper, S.; Fonseca, J. M. High-pressure fluid-phase equilibria: experimental methods and systems investigated (2000–2004). *Fluid Phase Equilib.* **2010***, 288*, 1-54.

Dohrn, R.; Pfohl, O. Thermophysical properties—industrial directions. *Fluid Phase Equilib.* **2002***, 194*, 15-29.

Duarte, M. C.; Galdo, M. V.; Gomez, M. J.; Tassin, N. G.; Yanes, M. High pressure phase behavior modeling of asymmetric alkane alkane binary systems with the RKPR EOS. *Fluid Phase Equilib.* **2014***, 362*, 125-135.

Economou, I. G. Statistical associating fluid theory: a successful model for the calculation of thermodynamic and phase equilibrium properties of complex fluid mixtures. *Ind Eng Chem Res* **2002***, 41*, 953-962.

Englezos, P.; Bygrave, G.; Kalogerakis, N. Interaction parameter estimation in cubic equations of state using binary phase equilibrium and critical point data. *Ind Eng Chem Res* **1998***, 37*, 1613-1618.

Fischer, K.; Gmehling, J. Further development, status and results of the PSRK method for the prediction of vapor-liquid equilibria and gas solubilities. *Fluid Phase Equilib.* **1995***, 112*, 1-22.

Fonseca, J. M.; Dohrn, R.; Peper, S. High-pressure fluid-phase equilibria: experimental methods and systems investigated (2005–2008). *Fluid Phase Equilib.* **2011***, 300*, 1-69.

Fornari, R. E.; Alessi, P.; Kikic, I. High pressure fluid phase equilibria: experimental methods and systems investigated (1978–1987). *Fluid Phase Equilib.* **1990***, 57*, 1-33.

Fredenslund, A.; Jones, R. L.; Prausnitz, J. M. Group-contribution estimation of activity coefficients in nonideal liquid mixtures. *AIChE J.* **1975***, 21*, 1086-1099.

Gao, G.; Daridon, J.; Saint-Guirons, H.; Xans, P.; Montel, F. A simple correlation to evaluate binary interaction parameters of the Peng-Robinson equation of state: binary light hydrocarbon systems. *Fluid Phase Equilib.* **1992***, 74*, 85-93.

Gibbs, R. E.; Van Ness, H. C. Vapor-liquid equilibria from total-pressure measurements. A new apparatus. *Industrial & Engineering Chemistry Fundamentals* **1972***, 11*, 410-413.

Gil-Villegas, A.; Galindo, A.; Whitehead, P. J.; Mills, S. J.; Jackson, G.; Burgess, A. N. Statistical associating fluid theory for chain molecules with attractive potentials of variable range. *J. Chem. Phys.* **1997***, 106*, 4168-4186.

Gmehling, J.; Li, J.; Fischer, K. Further development of the PSRK model for the prediction of gas solubilities and vapor-liquid-equilibria at low and high pressures II. *Fluid Phase Equilib.* **1997***, 141*, 113-127.

Goral, M. Vapour-liquid equilibria in non-polar mixtures. III. Binary mixtures of alkylbenzenes and n-alkanes at 313.15 K. *Fluid Phase Equilib.* **1994***, 102*, 275-286.

Gray, R. M. *Upgrading petroleum residues and heavy oils;* CRC press: 1994.

Gregorowicz, J.; de Loos, T. W. Prediction of Liquid−Liquid−Vapor Equilibria in asymmetric hydrocarbon mixtures. *Ind Eng Chem Res* **2001***, 40*, 444-451.

Gross, J.; Sadowski, G. Application of the perturbed-chain SAFT equation of state to associating systems. *Ind Eng Chem Res* **2002***, 41*, 5510-5515.

Gross, J.; Sadowski, G. Perturbed-chain SAFT: An equation of state based on a perturbation theory for chain molecules. *Ind Eng Chem Res* **2001***, 40*, 1244-1260.

Hay, G.; Loria, H.; Satyro, M. A. Thermodynamic modeling and process simulation through PIONA characterization. *Energy Fuels* **2013***, 27*, 3578-3584.

Hendriks, E.; Kontogeorgis, G. M.; Dohrn, R.; de Hemptinne, J.; Economou, I. G.; Zilnik, L. F.; Vesovic, V. Industrial requirements for thermodynamics and transport properties. *Ind Eng Chem Res.* **2010**, *49*, 11131-11141.

Holderbaum, T.; Gmehling, J. PSRK: a group contribution equation of state based on UNIFAC. *Fluid Phase Equilib.* **1991**, *70*, 251-265.

Horstmann, S.; Fischer, K.; Gmehling, J. PSRK group contribution equation of state: revision and extension III. *Fluid Phase Equilib.* **2000**, *167*, 173-186.

Horstmann, S.; Jabłoniec, A.; Krafczyk, J.; Fischer, K.; Gmehling, J. PSRK group contribution equation of state: comprehensive revision and extension IV, including critical constants and α-function parameters for 1000 components. *Fluid Phase Equilib.* **2005**, *227*, 157-164.

Huang, S. H.; Radosz, M. Equation of state for small, large, polydisperse, and associating molecules. *Ind Eng Chem Res* **1990**, *29*, 2284-2294.

Huron, M.; Vidal, J. New mixing rules in simple equations of state for representing vapour-liquid equilibria of strongly non-ideal mixtures. *Fluid Phase Equilib.* **1979**, *3*, 255-271.

Jaubert, J.; Mutelet, F. VLE predictions with the Peng–Robinson equation of state and temperature dependent kij calculated through a group contribution method. *Fluid Phase Equilib.* **2004**, *224*, 285-304.

Jaubert, J.; Vitu, S.; Mutelet, F.; Corriou, J. Extension of the PPR78 model (predictive 1978, Peng–Robinson EOS with temperature dependent k_{ij} calculated through a group contribution method) to systems containing aromatic compounds. *Fluid Phase Equilib.* **2005**, *237*, 193-211.

Kato, K.; Nagahama, K.; Hirata, M. Generalized interaction parameters for the Peng–Robinson equation of state: carbon dioxide—n-paraffin binary systems. *Fluid Phase Equilib.* **1981**, *7*, 219-231.

Klamt, A. Conductor-like screening model for real solvents: a new approach to the quantitative calculation of solvation phenomena. *J. Phys. Chem.* **1995**, *99*, 2224-2235.

Knudsen, M. Die Molekularströmung der Gase durch Offnungen und die Effusion. *Annalen der Physik* **1909**, *333*, 999-1016.

Kolbe, B.; Gmehling, J. Thermodynamic properties of ethanol water. I. Vapour-liquid equilibria measurements from 90 to 150 C by the static method. *Fluid Phase Equilib.* **1985**, *23*, 213-226.

Kontogeorgis, G. M.; Coutsikos, P.; Harismiadis, V. I.; Fredenslund, A.; Tassios, D. P. A novel method for investigating the repulsive and attractive parts of cubic equations of state and the

combining rules used with the vdW-1f theory. *Chemical engineering science* **1998***, 53*, 541-552.

Kontogeorgis, G. M.; Folas, G. K. *Thermodynamic models for industrial applications: from classical and advanced mixing rules to association theories;* John Wiley & Sons: 2009; .

Kordas, A.; Tsoutsouras, K.; Stamataki, S.; Tassios, D. A generalized correlation for the interaction coefficients of CO_2—hydrocarbon binary mixtures. *Fluid Phase Equilib.* **1994***, 93*, 141-166.

Lin, S.; Sandler, S. I. A priori phase equilibrium prediction from a segment contribution solvation model. *Ind Eng Chem Res* **2002***, 41*, 899-913.

Macknick, A. B.; Prausnitz, J. M. Vapor pressures of high-molecular-weight hydrocarbons. *J.Chem.Eng.Data;(United States)* **1979***, 24*.

Mathias, P. M. A versatile phase equilibrium equation of state. *Ind. Eng. Chem. Proc. Des. Dev.* **1983***, 22*, 385-391.

Mathias, P. M.; Copeman, T. W. Extension of the Peng-Robinson equation of state to complex mixtures: evaluation of the various forms of the local composition concept. *Fluid Phase Equilib.* **1983***, 13*, 91-108.

Melhem, G. A.; Saini, R.; Goodwin, B. M. A modified Peng-Robinson equation of state. *Fluid Phase Equilib.* **1989***, 47*, 189-237.

Messow, U.; Engel, I. Thermodynamic studies on solvent-paraffin systems. 7. Toluene (1)-dodecane (2) and toluene (1)-hexadecane (2). *ZEITSCHRIFT FUR PHYSIKALISCHE CHEMIE-LEIPZIG* **1977***, 258*, 798-800.

Messow, U.; Schuetze, D.; Hauthal, W. Thermodynamic studies on n-paraffin solvent systems. II. Benzene (1) n-tetradecane (2), benzene (1) n-hexadecane (2) and benzene (1) n-heptadecane (2). *Chemischer Informationsdienst* **1976***, 7*.

Molecule-based characterization methodology for correlation and prediction of properties for crude oil and petroleum fractions – an industry white paper, 2014. Aspen Technology Website. https://www.aspentech.com/Molecular_Characterization_White_Paper.pdf (accessed Dec 1, 2016)

Morgan, D. L.; Kobayashi, R. Direct vapor pressure measurements of ten n-alkanes m the 10-C28 range. *Fluid Phase Equilib.* **1994***, 97*, 211-242.

Mushrif, S. H.; Phoenix, A. V. Effect of Peng− Robinson binary interaction parameters on the predicted multiphase behavior of selected binary systems. *Ind Eng Chem Res* **2008***, 47*, 6280-6288.

Nishiumi, H.; Arai, T.; Takeuchi, K. Generalization of the binary interaction parameter of the Peng-Robinson equation of state by component family. *Fluid Phase Equilib.* **1988**, *42*, 43-62.

NIST Standard Reference Database 103b: NIST ThermoData Engine, Version 7.1, accessed from Aspen Plus.

NIST Thermodynamics Research Center Website. http://trc.nist.gov/ (accessed Dec 20, 2016).

Orbey, H.; Sandler, S. I. *Modeling vapor-liquid equilibria: cubic equations of state and their mixing rules;* Cambridge University Press: 1998; Vol. 1.

Paul, H.; Krug, J.; Knapp, H. Measurements of VLE, hE and vE for binary mixtures of n-alkanes with n-alkylbenzenes. *Thermochimica acta* **1986**, *108*, 9-27.

Péneloux, A.; Rauzy, E.; Frze, R. A consistent correction for Redlich-Kwong-Soave volumes. *Fluid Phase Equilib.* **1982**, *8*, 7-23.

Peng, D.; Robinson, D. B. A new two-constant equation of state. *Ind.Eng.Chem.Fundam* **1976**, *15*, 59-64.

Peng, D.; Robinson, D. B. Two and three phase equilibrium calculations for systems containing water. *The Canadian Journal of Chemical Engineering* **1976**, *54*, 595-599.

Peridis, S.; Magoulas, K.; Tassios, D. Sensitivity of distillation column design to uncertainties in vapor–liquid equilibrium information. *Sep. Sci. Technol.* **1993**, *28*, 1753-1767.

Rahman, S.; Barrufet, M. A. A new technique for simultaneous measurement of PVT and phase equilibria properties of fluids at high temperatures and pressures. *Journal of Petroleum Science and Engineering* **1995**, *14*, 25-34.

Redlich, O.; Kwong, J. N. On the thermodynamics of solutions. V. An equation of state. Fugacities of gaseous solutions. *Chem. Rev.* **1949**, *44*, 233-244.

Renon, H.; Prausnitz, J. M. Local compositions in thermodynamic excess functions for liquid mixtures. *AIChE J.* **1968**, *14*, 135-144.

Rogalski, M.; Malanowski, S. Ebulliometers modified for the accurate determination of vapour—liquid equilibrium. *Fluid Phase Equilib.* **1980**, *5*, 97-112.

Růžička, K.; Fulem, M.; Růžička, V. Vapor pressure of organic compounds. Measurement and correlation, 2008. http://old.vscht.cz/fch/Kvetoslav.Ruzicka/ICTP_VaporPressureGroup.pdf. (accessed January 15, 2017)

Saber, N.; Shaw, J. M. Toward multiphase equilibrium prediction for ill-defined asymmetric hydrocarbon mixtures. *Fluid Phase Equilib.* **2009**, *285*, 73-82.

Sako, T.; Sugeta, T.; Nakazawa, N.; Okubo, T.; Sato, M.; Taguchi, T.; Hiaki, T. Phase equilibrium study of extraction and concentration of furfural produced in reactor using supercritical carbon dioxide. *J. Chem. Eng. Japan* **1991**, *24*, 449-455.

Sako, T.; Wu, A. H.; Prausnitz, J. M. A cubic equation of state for high-pressure phase equilibria of mixtures containing polymers and volatile fluids. *J Appl Polym Sci* **1989**, *38*, 1839-1858.

Sengers, J. V.; Kayser, R. F.; Peters, C. J.; White, H. J. *Equations of state for fluids and fluid mixtures;* Elsevier: 2000; Vol. 5.

Slot-Petersen, C. A systematic and consistent approach to determine binary interaction coefficients for the Peng-Robinson Equation of State (includes associated papers 20308 and 20393). *SPE Reservoir Engineering* **1989**, *4*, 488-494.

Soave, G. Equilibrium constants from a modified Redlich-Kwong equation of state. *Chemical Engineering Science* **1972**, *27*, 1197-1203.

Speight, J. G. *Introduction to enhanced recovery methods for heavy oil and tar sands;* Gulf Professional Publishing: 2016.

Speight, J. G. *The chemistry and technology of petroleum;* CRC press: 2014 .

Stamataki, S.; Magoulas, K. Prediction of phase equilibria and volumetric behavior of fluids with high concentration of hydrogen sulfide. *Oil & Gas Science and Technology* **2000**, *55*, 511-522.

Stamataki, S.; Tassios, D. Performance of cubic EOS at high pressures. *Revue de l'Institut Franais du Ptrole* **1998**, *53*, 367-377.

Stevens, R.; Shen, X. M.; De Loos, T. W.; de Swaan Arons, J. A new apparatus to measure the vapour-liquid equilibria of low-volatility compounds with near-critical carbon dioxide. Experimental and modelling results for carbon dioxide n-butanol, 2-butanol, 2-butyl acetate and vinyl acetate systems. *The Journal of Supercritical Fluids* **1997**, *11*, 1-14.

Tihic, A.; Kontogeorgis, G. M.; von Solms, N.; Michelsen, M. L. Applications of the simplified perturbed-chain SAFT equation of state using an extended parameter table. *Fluid Phase Equilib.* **2006**, *248*, 29-43.

Towler, B. F. Fundamental principles of reservoir engineering, vol 8, SPE textbook series. Henry L. Doherty Memorial Fund of AIME. *Society of Petroleum Engineers, Richardson* 2002.

Tsonopoulos, C.; Tan, Z. The critical constants of normal alkanes from methane to polyethylene: II. Application of the Flory theory. *Fluid Phase Equilib.* **1993**, *83*, 127-138.

Twu, C. H.; Bluck, D.; Cunningham, J. R.; Coon, J. E. A cubic equation of state with a new alpha function and a new mixing rule. *Fluid Phase Equilib.* **1991***, 69*, 33-50.

Van Konynenburg, P. H.; Scott, R. L. Critical lines and phase equilibria in binary van der Waals mixtures. *Philosophical Transactions of the Royal Society of London A: Mathematical, Physical and Engineering Sciences* **1980***, 298*, 495-540.

Vapor Pressure Tester MINIVAP VPXpert/-L Operation Manual, 2015. Grabner Instruments.

VMGSim Process Simulator, Version 9.5. Virtual Materials Group Inc.: Calgary, AB 2016.

von Solms, N.; Michelsen, M. L.; Kontogeorgis, G. M. Computational and physical performance of a modified PC-SAFT equation of state for highly asymmetric and associating mixtures. *Ind Eng Chem Res* **2003***, 42*, 1098-1105.

Voutsas, E. C.; Boukouvalas, C. J.; Kalospiros, N. S.; Tassios, D. P. The performance of EoS/G E models in the prediction of vapor-liquid equilibria in asymmetric systems. *Fluid Phase Equilib.* **1996***, 116*, 480-487.

Waals, J. D.; Rowlinson, J. S. *JD van der Waals: On the continuity of the gaseous and liquid states;* North Holland: 1988; Vol. 14.

Wei, Y. S.; Sadus, R. J. Equations of state for the calculation of fluid-phase equilibria. *AIChE J.* **2000***, 46*, 169-196.

Weir, R. D.; de Loos, T. W. *Measurement of the thermodynamic properties of multiple phases;* Gulf Professional Publishing: 2005.

Wertheim, M. S. Fluids with highly directional attractive forces. I. Statistical thermodynamics. *Journal of statistical physics* **1984***, 35*, 19-34.

Wertheim, M. S. Fluids with highly directional attractive forces. II. Thermodynamic perturbation theory and integral equations. *Journal of statistical physics* **1984***, 35*, 35-47.

Wertheim, M. S. Fluids with highly directional attractive forces. III. Multiple attraction sites. *Journal of statistical physics* **1986***, 42*, 459-476.

Wertheim, M. S. Fluids with highly directional attractive forces. IV. Equilibrium polymerization. *Journal of statistical physics* **1986***, 42*, 477-492.

Wong, D. S. H.; Sandler, S. I. A theoretically correct mixing rule for cubic equations of state. *AIChE J.* **1992***, 38*, 671-680.